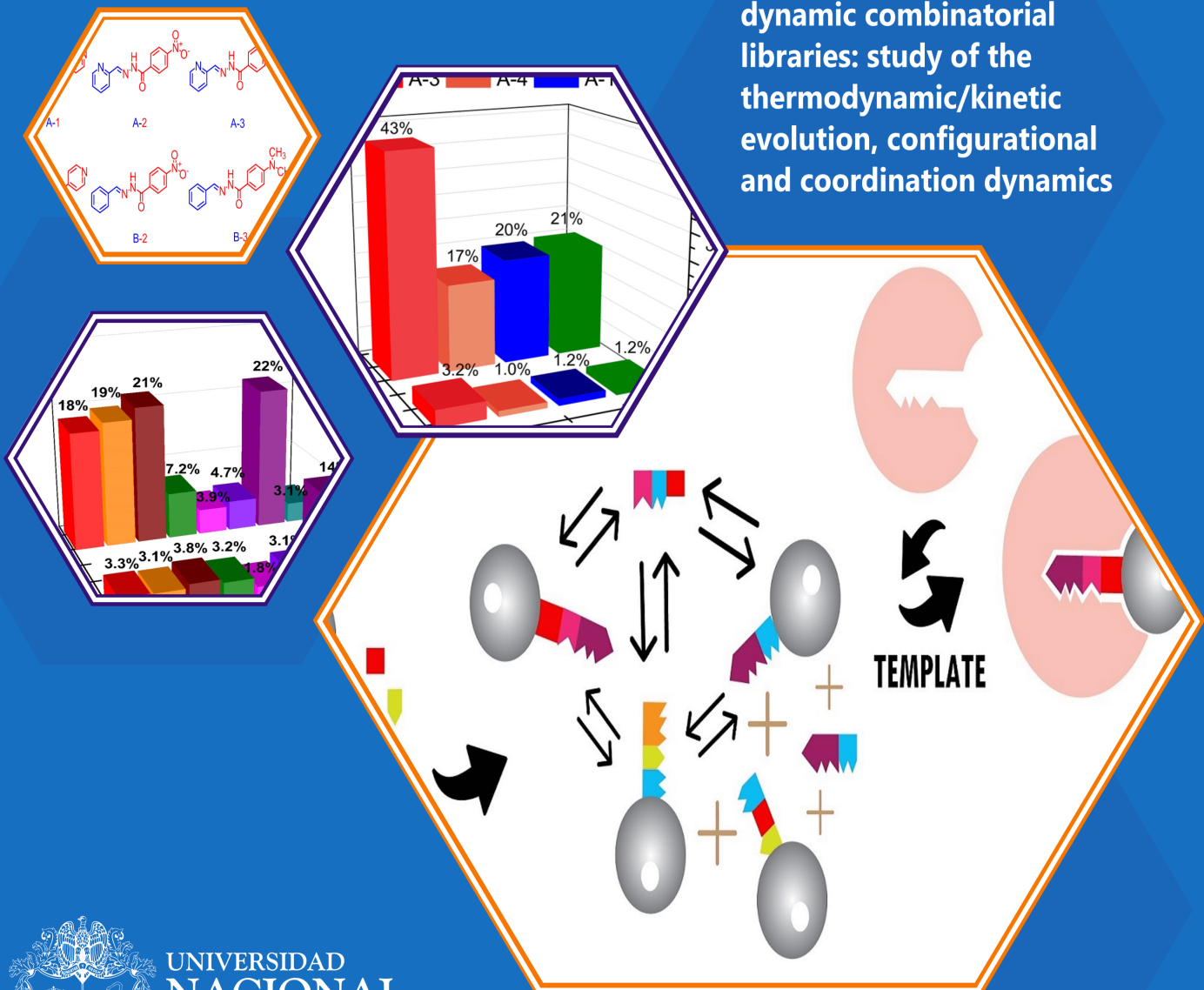
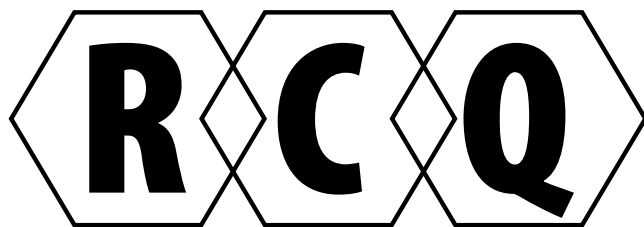


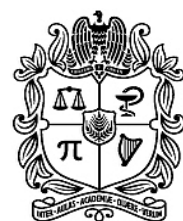
Acylydrazone-based dynamic combinatorial libraries: study of the thermodynamic/kinetic evolution, configurational and coordination dynamics





Revista Colombiana de Química

Volumen 45, No. 3, septiembre - diciembre de 2016



UNIVERSIDAD
NACIONAL
DE COLOMBIA

SEDE BOGOTÁ
FACULTAD DE CIENCIAS
DEPARTAMENTO DE QUÍMICA

Edición

© Universidad Nacional de Colombia
Facultad de Ciencias - Departamento de Química
Sede Bogotá
ISBN versión impresa: 0120-2804
ISBN versión electrónica: 2357-3791
DOI de la publicación by CrossRef.org:
<http://dx.doi.org/10.15446/rev.colomb.quim>

Indizada en

Publindex- Índice Bibliográfico Nacional (categoría A2)
Chemical Abstracts
SciELO Colombia
Scopus Q4 (SJR/2013: 0,112)
Latindex
Redalyc
REDIB
Directory of Open Access Journals (DOAJ)

Periodicidad

Cuatrimestral

Contacto

Departamento de Química
Universidad Nacional de Colombia
Apartado Aéreo 5997
Bogotá, D.C., Colombia
Fax: 571- 3165220
Correo electrónico: rcolquim_fcbog@unal.edu.co

Consulta Open Access

<http://www.revistas.unal.edu.co/index.php/rcolquim>
http://www.scielo.org.co/scielo.php?script=sci_serial&pid=0120-2804&lng=es&nrm=iso

Director Revista

Carlos Eduardo Narváez Cuenca, Ph. D., Universidad Nacional de Colombia.

Comité Editorial

Cristian Blanco Tirado, Ph. D., Universidad Industrial de Santander, Colombia.
Francisco Carrasco Marín, Dr. Sc., Universidad de Granada, España.
Leonardo Castellanos Hernández, Dr. Sc., Universidad Nacional de Colombia
Pedro Joseph-Nathan, Dr. Sc., Instituto Politécnico Nacional, México.
Sonia Moreno Guáqueta, Dr. Sc., Universidad Nacional de Colombia.
Cristian Ochoa Puentes, Dr. rer. nat., Universidad Nacional de Colombia.
Luz Patricia Restrepo Sánchez, M. Sc., Universidad Nacional de Colombia.
Juscelino Tovar, Dr. Sc., Universidad de Lund, Suecia.

Comité Científico

Gustavo Adolfo González Aguilar, Dr. Sc., Centro de investigación en Alimentación y Desarrollo, México.
Ljubisa R. Radovic, Dr. Sc., Pensilvania State University, USA.
Augusto Rivera Umaña, Dr. Sc., Universidad Nacional de Colombia.
Fabio Zuluaga Corrales, Dr. Sc., Universidad del Valle, Colombia.
Kushalappa Ajjamada, Ph. D., McGill University, Canadá.

Suscripciones y canje

Valor del ejemplar \$10.000; suscripción anual \$30.000 y USD \$30 para el exterior, incluyendo en ambos casos el envío. Los pagos en Colombia deben realizarse mediante consignación en la cuenta de ahorros N° 220012720017 del Banco Popular, a nombre de Fondo Especial, Facultad de Ciencias U.N. Desde el exterior los pagos deben hacerse mediante cheque de un banco de Estados Unidos girado a nombre de Fondo Especial, Facultad de Ciencias U.N o mediante transferencia electrónica a la cuenta citada anteriormente. Por favor enviar cheques y fotocopias de giros o consignaciones a la dirección de la Revista Colombiana de Química.

Para canjes dirigirse al SINAB: biblioteca_bog@unal.edu.co ó cevelascozaza@unal.edu.co.

Propósito y alcance

La Revista Colombiana de Química es publicada cuatrimestralmente por el Departamento de Química de la Universidad Nacional de Colombia. Publica contribuciones provenientes de la investigación en las diversas áreas de la química. El contenido de los artículos debe ser original, inédito y no debe haber sido enviado, total o parcialmente, para publicación a otra revista. La redacción asume el derecho de reproducción de los trabajos aceptados. Su publicación en otro medio requiere permiso del editor. La revista es dirigida a estudiantes y profesionales relacionados con cualquier área de la química.

Preparación editorial

Camila Alejandra Rincón Carrillo, asistente editorial.
Sindy Tatiana Bedoya Mesa, asistente editorial.
Coordinación de Publicaciones.
Facultad de Ciencias, Universidad Nacional de Colombia, Sede Bogotá.
Cuidado editorial: Camila Alejandra Rincón Carrillo, Sindy Tatiana Bedoya Mesa.
Diseño y maquetación: Camila Alejandra Rincón Carrillo, Sindy Tatiana Bedoya Mesa.
Impresión y encuadernación: Proceditor Ltda.

Tabla de contenido

Carta del editor
Editor's letter

1-4

Química Orgánica y Bioquímica

Anti-pepsin activity of silicon dioxide nanoparticles
Actividad antipepsina de nanopartículas de dióxido de silicio
Atividade antipepsina de nanopartículas de dióxido de silício
Hussein Kadhem Al-Hakeim, Khlowd Mohammed Jasem, Shatha Rouf Moustafa

5-11

Química Aplicada y Analítica

Comparison between extraction methods to obtain volatiles from lulo (*Solanum quitoense*) pulp
Comparación entre métodos de extracción para la obtención de volátiles a partir de pulpa de lulo (*Solanum quitoense*)
Comparação entre métodos de extração para a obtenção de voláteis a partir da polpa de lulo (*Solanum quitoense*)
Eduardo J. Corpas, Gonzalo Taborda, Omar A. Tapasco, Aristófeles Ortiz

12-21

Analytical method validation of GC-FID for the simultaneous measurement of hydrocarbons (C₂-C₄) in their gas mixture
Validación de un método analítico GC-FID para la medida simultánea de hidrocarburos (C₂-C₄) en una mezcla gaseosa
Validação de uma metodologia analítica GC-FID para a medida simultânea de hidrocarbonetos (C₂-C₄) em uma mistura gasosa
Oman Zuas, Muhammad R. Mulyana, Harry Budiman

22-27

Fisicoquímica y Química Inorgánica

A DFT study on Dichloro {(E)-4-dimethylamino-N'-[(pyridin-2 yl)methylidene-κN]benzohydrazide-κO}M²⁺ (M=Zn, Cu, Ni, Fe, Mn, Ca and Co) complexes: Effect of the metal over association energy and complex geometry
Un estudio DFT en complejos Dicloro {(E)-4-dimetilamino-N'-[(piridin-2 il)metylideno-κN] benzohidrazida-κO} M²⁺ (M = Zn, Cu, Ni, Fe, Mn, Ca y Co): efecto del metal sobre la energía de asociación y la geometría del complejo
Um estudo DFT nos complexos Dicloro {(E)-4-dimetilamino-N'-[(piridin-2 il) metilideno-κN] benzohidrazida-κO} M²⁺ (M = Zn, Cu, Ni, Fe, Mn, Ca y Co): efeito do metal sobre a energia de associação e a geometria do complexo
Gustavo Gutiérrez, Mónica A. Gordillo, Manuel N. Chaur

28-32

Síntesis y caracterización estructural de hidrotalcitas de Cu-Zn-Al
Synthesis and structural characterization of Zn-Al-Cu hydroxylates
Síntese e caracterização estrutural de hidrotalcitas de Cu-Zn-Al
Johana Rodríguez Ruiz, Adolfo Pájaro Payares, Edgardo Meza Fuentes

33-38

Acylhydrazone-based dynamic combinatorial libraries: study of the thermodynamic/kinetic evolution, configurational and coordination dynamics
Librerías combinatorias dinámicas basadas en acil-hidrazone: estudio del desarrollo termodinámico/cinético, dinámicas de configuración y de coordinación
Livrarias combinatórias dinâmicas baseadas na acil-hidrazone: estudo da evolução cinética/termodinâmica, dinâmicas de configuração e da coordenação
Mónica A. Gordillo, Fabio Zuluaga, Manuel N. Chaur

39-50

Guía para autores
Guide for authors

51-60

El tercer número del volumen 45 del año 2016 de la Revista Colombiana de Química cuenta con la participación de distintos autores nacionales e internacionales. Las contribuciones provienen de autores de Indonesia e Iraq; Manizales, Cali y Cartagena (Colombia). A continuación se presenta el contenido del número.

La sección de Química Orgánica y Bioquímica cuenta con un artículo en el que se utilizaron nanopartículas de dióxido de silicio para reducir la actividad enzimática de la pepsina, una de las causas principales del reflujo gastroesofágico (GERD). Se encontró que con el uso de estas nanopartículas sumado a cierta fuerza iónica, la actividad enzimática se reduce significativamente.

La sección de Química Aplicada y Analítica cuenta con dos artículos. En el primero de ellos, se utilizaron dos metodologías distintas para la obtención de volátiles a partir de la pulpa de lulo (*Solanum quitoense*), por un lado, extracción y destilación simultánea (SDE) y por el otro, microextracción en fase sólida con espacio de cabeza (HS-SPME). Se encontró que las dos metodologías se complementan, pues arrojan información diferente sobre la composición de volátiles. En el segundo artículo se validó la técnica de cromatografía de gases con detector de ionización de llama para analizar hidrocarburos ligeros de manera simultánea. Se encontró que dicha metodología es exacta y precisa, ya que separaron dichos analitos de manera confiable de acuerdo a los estándares de la ISO/IEC 17025.

La sección de Fisicoquímica y Química Inorgánica cuenta con tres artículos. El primero de ellos es un estudio computacional basado en la teoría del funcional de densidad (DFT), en el cual se evalúa la geometría molecular de un derivado de hidrazone [(E)-4-dimetilamino-N'-(piridin-2-il)metilideno- κ N]benzohidrazida] formando complejos con diversos cationes divalentes. Se encontró que los cálculos realizados concuerdan con los datos cristalográficos reportados, la formación más favorable del complejo ocurre con Mn^{2+} , mientras que con Ca^{2+} y Cu^{2+} es menos favorable.

El segundo artículo de esta sección trata de la síntesis y caracterización de hidrocalcitas a base de Cu-Zn-Al y sus derivados calcinados, ambos moléculas de interés por sus propiedades catalíticas. Los resultados señalan que un alto contenido de cobre induce a la formación de hidróxido, que limita la formación de estructuras tipo hidrocalcitas laminares y disminuye su estabilidad térmica. De igual modo, en todos los sólidos sintetizados se produjeron óxidos metálicos y descomposición de carbonatos.

Finalmente, el último artículo describe un estudio cinético y termodinámico de la formación de determinadas especies derivadas de acil-hidrazonas y aldehídos mediante librerías combinatorias dinámicas (DLC) en reacciones evaluadas por medio de 1H -RMN. Logró encontrarse cuál es el producto cinético y termodinámico bajo las condiciones de estudio, de igual modo logró establecerse cómo amplificar los productos de interés mediante el uso de luz UV o de iones metálicos.

The third issue of volume 45 of 2016 of Revista Colombiana de Química counts with the participation of different national and international authors. Contributions come from the authors of Indonesia and Iraq; Manizales, Cali, and Cartagena (Colombia). Here are the contents of the issue, published according to their subject.

The section of Organic Chemistry and Biochemistry has an article in which silicon dioxide nanoparticles were used to reduce the enzymatic activity of pepsin, a major cause of gastroesophageal reflux (GERD). By using these nanoparticles, at a certain ionic strength, the enzymatic activity was significantly reduced.

The section of Applied and Analytical Chemistry has two articles. In the first one two different extraction techniques were used to obtain volatile compounds from lulo (*Solanum quitoense*) pulp: on the one hand, simultaneous extraction and distillation (SDE) and on the other hand, solid phase microextraction with head space (HS-SPME). It was found that the two methodologies complement each other, since they yielded different data in the extraction process. In the second article gas chromatography with flame ionization detector was validated to simultaneously analyze light hydrocarbons. The methodology was accurate and precise, since the analytes were well separated according to the standards of ISO/IEC 17025.

The section of Physical Chemistry and Inorganic Chemistry has three articles. The first of these is a computational study based on density functional theory (DFT), in which the molecular geometry of a hydrazone derivative [(E)-4-dimethylamino-N'-(pyridine-2-yl)methylidene- κ N]benzohydrazide] forming complexes with various divalent cations was studied. It was found that calculations correspond well with the previously reported crystallographic data, the most favorable formation of the complex occurs with Mn^{2+} , whereas with Ca^{2+} and Cu^{2+} is less favorable.

The second article of this section studies the synthesis and characterization of Cu-Zn-Al-based hydrocalcites and their calcined derivatives, both of which are of interest because of their catalytic properties. Results indicate that a high copper content induces a hydroxide formation, which limits the formation of lamellar hydrocalcite type structures and decreases the thermal stability of the products. Likewise, in all synthesized solids, metal oxides and carbonate decomposition were produced.

Finally, the last article describes a kinetic and thermodynamic study on the formation of derivative species of acylhydrazones and aldehydes by using dynamic combinatorial libraries (DLC) in reactions evaluated by means of 1H -NMR. The kinetic and thermodynamic product was found under the studied conditions, as well as how to amplify the products of interest by using UV light or metal ions.



Hussein Kadhem Al-Hakeim^{1,*}, Khlowd Mohammed Jasem², Shatha Rouf Moustafa³

¹Department of Chemistry, Faculty of Science, Kufa University, Kufa, Iraq.

²Department of Chemistry, College of Science, Kerbala University, Kerbala, Iraq.

³Clinical Analysis Department, College of Pharmacy, Hawler Medical University, Havalan City, Erbil, Iraq.

*Corresponding author: headm2010@yahoo.com

Recibido: 30 de Junio de 2016. Aceptado: 9 de Septiembre de 2016.

Anti-pepsin activity of silicon dioxide nanoparticles

Abstract

SiO_2NPs as an inhibitor of pepsin enzyme for treatment of gastro-esophageal reflux disease (GERD) were investigated. Silicon dioxide nanoparticles (pepsin coated SiO_2NPs) are among the safest nanoparticles that can be used inside the human body. The activity of pepsin before and after the addition of certain amounts of the NPs to the reaction mixture was measured spectrophotometrically. Furthermore, these experiments were repeated at different temperatures, different weights of NPs, and different ionic strengths. The kinetic parameters (K_m & V_{max}) of the pepsin-catalyzed reactions were calculated from the Lineweaver-Burk plots. The results showed that there is a significant reduction of pepsin activity by SiO_2NPs (V_{max} of free pepsin = 4.82 U and V_{max} of the immobilized pepsin = 2.90 U). The results also indicated that the presence of ionic strength causes remarkable reduction of pepsin activity. It can be concluded the best condition for inhibition of pepsin activity is by using a combination of SiO_2NPs and high concentration NaCl at 37 °C.

Keywords: GERD, SiO_2 nanoparticles, pepsin, enzyme inhibition.

Actividad antipepsina de nanopartículas de dióxido de silicio

Resumen

Se usaron nanopartículas de dióxido de silicio como inhibidores de la pepsina para el tratamiento del reflujo gastroesofágico (GERD). Estas nanopartículas (SiO_2NPs recubiertas de pepsina) son unas de las más seguras y pueden usarse en el cuerpo humano. Se midió a través de espectrofotometría la actividad de la pepsina antes y después de añadir cierta cantidad de NPs a la mezcla reactante. Adicionalmente, se repitieron estas pruebas a diferentes temperaturas, variando el peso de las NPs y la fuerza iónica. Se calcularon los parámetros cinéticos (K_m y V_{max}) de las reacciones catalizadas con pepsina a través de las gráficas de Lineweaver-Burk. Los resultados mostraron que, usando SiO_2NPs (V_{max} de pepsina libre = 4.82 U y V_{max} de pepsina inmovilizada = 2.90 U) y a través de la presencia de fuerza iónica, la actividad enzimática se reduce significativamente. Se concluye que la mejor condición para inhibir la actividad enzimática es usando una combinación de SiO_2NPs y una alta concentración de NaCl a 37 °C.

Palabras clave: GERD, nanopartículas de SiO_2 , pepsina, inhibición enzimática.

Atividade antipepsina de nanopartículas de dióxido de silício

Resumo

Foram usadas nanopartículas de dióxido de silício como inibidores da pepsina para o tratamento do refluxo gastroesofágico (GERD). Estas nanopartículas (SiO_2NPs cobertas de pepsina) são uma das mais seguras e podem usar-se no corpo humano. Foi medida a atividade da pepsina mediante espectrofotometria antes e depois de agregar certa quantidade de NPs à mistura de reação. Adicionalmente, repetiram-se estas provas a diferentes temperaturas, variando o peso das NPs e a força iônica. Foram calculados os parâmetros cinéticos (K_m e V_{max}) das reações catalisadas com pepsina a través das gráficas de Lineweaver-Burk. Os resultados mostraram que, usando SiO_2NPs (V_{max} de pepsina livre = 4.82 U e V_{max} de pepsina imobilizada = 2.90 U) e a través da presença de força iônica, a atividade enzimática se reduz significativamente. Foi concluído que a melhor condição para inibir a atividade enzimática é usando uma combinação de SiO_2NPs e uma alta concentração de NaCl a 37 °C.

Palavras-Chave: GERD, nanopartículas de SiO_2 , pepsina, inibição enzimática.

Introduction

Gastro-esophageal reflux disease (GERD) evolves when reflux of stomach contents causes complications into the esophagus (1). GERD is a popular disease with a prevalence of 10% - 20% in the western countries (2) and some researchers reported up to 35.9% (3), but its risk factors and causes are not clearly known (4). The disease causes various symptoms, among which are heartburn and regurgitation, which affect up to 30% of the population and continue to increase (5-7). Pepsin, which is the most important substance in the gastric contents for the necrosis of the mucosal tissues, plays the main role in the formation of GERD and associated diseases (8).

Although proton-pump inhibitors are known to alleviate symptoms in most patients, a significant portion of patients continue to present GERD (9). There is a wide range of specific inhibitors that can bind to the active site and effectively remove the activity of pepsin, one of the best known ones is pepstatin, a specific pepsin inhibitor, which at acidic pH, tightly binds to the catalytic site of both pepsin and its precursor pepsinogen (10). The best way to determine K_m (the concentration of substrate at $V_{max}/2$) and V_{max} (Maximum velocity of an enzyme-catalyzed reaction at definite conditions) values of the basic Michaelis-Menten equation is by taking the reciprocal of both sides of equation to give the double reciprocal equation or Lineweaver-Burk's equation.

$$\frac{1}{V_0} = \frac{K_m}{V_{max}[S]} + \frac{1}{V_{max}}$$

Where V_0 represents the initial velocity or the activity of the enzyme-catalyzed reaction. A plot of $1/V_0$ versus $1/[S]$ yields a straight line with an intercept of $1/V_{max}$ and a slope of K_m/V_{max} (11).

Use of NPs to inhibit the activity of pepsin *in vitro* as a model for the treatment of GERD was performed and published previously (12). Silicon dioxide nanoparticles (SiO_2NPs), also known as silica NPs or nanosilica, are the basis for a great deal of biomedical research due to their stability, low toxicity, and ability to be functionalized with a range of molecules and polymers (13). SiO_2NPs have received an intensive attention by scientific community due to its broad applications in biomedical and biotechnological fields such as drug delivery, gene therapy and molecular imaging, cancer therapy, and enzyme immobilization (14). In addition, it is widely used in cosmetics, food, varnishes, papermaking, and drugs (15). Fruijtier-Polloth *et al.* (16) evaluated the toxic effects and safety of SiO_2NPs and concluded that they are as safe as conventional SiO_2 . Amorphous SiO_2NPs are widely used in food products, for example, as thickeners, anticaking agents, carriers of fragrances and flavors, and additives (17). The aim of the present study is to optimize the process of pepsin inhibition by SiO_2NPs as a possible new treatment for GERD.

Materials and methods

Reagents

Pepsin (EC 3.4.23.1), MWt = 36,450 D, 99.5% purity, was supplied from BDH, England. Spherical Silicon dioxide nanoparticles (SiO_2NPs), particle diameter = 39.644 nm, 99.5% purity, was supplied from Nanjing nanotechnology, China. Lyophilized Hemoglobin (human red blood cells), 96% purity, was supplied from Lee Biosolutions, Missouri, USA. Trichloroacetic acid (TCA), 98% purity from Alpha Chemika, India. Hydrochloric acid (HCl, Analytical Grade, 35.4%) was supplied from Central Drug House, New Delhi, India.

Characterization of NPs

The SiO_2NPs used in the present study were visualized using SEM and TEM techniques to further confirmation for their shape and size. The TEM studies were performed by using a JEM-2010 instrument working with an acceleration voltage of 200 kV. SEM images were carried out by using a Hitachi S-4800 SEM at 20 kV.

Estimation of pepsin activity

The enzyme activity was determined by a kinetic method (18). The principle depends on the fact that pepsin cleaves peptides from hemoglobin which are soluble in trichloroacetic acid (TCA). The tyrosine and tryptophan content of these TCA-soluble peptides is determined by the measurement of the extinction at 280 nm. Briefly, pepsin is dissolved in 0.01 N HCl to obtain a concentration of 0.5 mg/mL. Just prior to assay there is another dilution in 0.01 N HCl to a concentration of 5-20 µg/mL.

The steps of the method were as follows: 1 mL of hemoglobin substrate was pipetted into test tubes containing 0.2 mL of the diluted pepsin at 37 °C. After 10 min, the reaction was stopped by adding 2 mL of 5% TCA. The tubes containing the reaction mixture were removed from water bath after 5 min and clarified (filtrates should be clear).

E280 nm was read of filtrate and subtract E280 nm of the appropriate blank using spectrophotometer (Model 721-Taiwan) set at 280 nm and 37 °C. The method of estimation of pepsin activity was repeated at different temperatures (22, 27, 32 and 42 °C). A unit of pepsin enzyme was defined as an amount of enzyme which renders TCA soluble 0.001 E280 nm per minute at 37 °C, using a denatured hemoglobin substrate.

Inhibition of pepsin activity by SiO_2NPs

To study the inhibition of pepsin by SiO_2NPs , a weight of 19.8 mg of SiO_2NPs was weighed by Sartorius balance (Model A200) dissolved in 10 mL of 0.01N HCl, and agitated by ultrasonic water bath (IsoLab, Germany) at 37 °C for 20 min. Five mg of pepsin were added to the SiO_2NPs -containing tubes and incubated at 37 °C for 30 min. These amounts of pepsin and NPs were calculated to produce pepsin monolayer on the SiO_2NPs . SiO_2NPs and pepsin surface areas were calculated in order to estimate theoretically the enough number of pepsin to cover the surface of one spherical SiO_2NP in one layer manner.

The calculations describe the pepsin and SiO₂NPs properties (radius, density, mass of one NP, and the volume of one NP) to calculate the surface areas of pepsin and SiO₂NPs which were $1.50 \times 10^{-13} \text{ cm}^2$ and $4.94 \times 10^{-11} \text{ cm}^2$, respectively. The number of pepsin molecules that can cover one SiO₂NP in a monolayer manner was obtained from the division of one SiO₂NPs surface area on one pepsin surface area ≈ 329 molecules of pepsin per SiO₂NP. This means that a 5 mg of pepsin were required to cover 19.8 mg of SiO₂NPs to obtain a monolayer of the adsorbed pepsin.

The method of pepsin activity estimation was repeated and the activity of the immobilized pepsin was estimated. To study the effect of weight on the pepsin activity the same method was repeated using different weights of SiO₂NPs (39.6 mg, 59.4 mg, 79.2 mg and 99.0 mg).

Effect of temperature on the inhibition of pepsin activity by SiO₂NPs

To study the temperature effect in the presence of SiO₂NPs, 19.8 mg of SiO₂NPs was dissolved in 10 mL of 0.01 N HCl, and agitated by ultrasonic water bath at different temperatures (22, 27, 32, 37 and 42 °C) for 20 min. Five milligrams of pepsin were added to each tube and incubated at 42 °C for 30 min. The method of estimation of pepsin activity was repeated and the pepsin activity was estimated after adding the SiO₂NPs.

Effect of a combination of ionic strength and SiO₂NPs on the inhibition of pepsin activity

To study the effect of the ionic strength in the presence of SiO₂NPs, 15 mg of SiO₂NPs and 1.3 mg of NaCl were dissolved in 10 mL of 0.01 N HCl, and agitated by ultrasonic water bath at 37 °C for 20 min. Five mg of pepsin were added to the tubes and incubated at 37 °C for 30 min. The method of estimation of pepsin activity was repeated and the pepsin activity was calculated. The protocol of the research is presented in Figure 1.

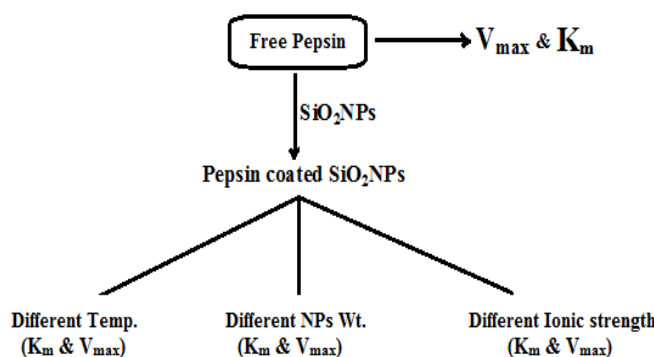


Figure 1. Workflow of the protocol of the research.

Results and discussion

The images of SiO₂NPs taken by SEM and TEM are presented in Figure 2. It is clear that the shape of SiO₂NPs is spherical with a particle size around 39 nm.

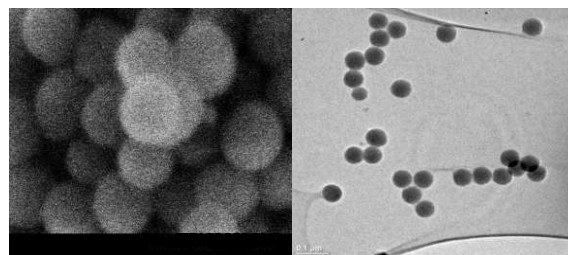


Figure 2. SEM (left) and TEM (right) images of the SiO₂NPs.

Effect of SiO₂NPs weight on the pepsin catalyzed reaction

The activity of the enzyme was measured by using seven different concentrations of hemoglobin ($3.01, 6.21, 9.31, 12.41, 15.52, 18.62$, and $21.72 \times 10^{-5} \text{ M}$) and five different weights of added SiO₂NPs (19.8, 39.6, 59.4, 79.2 and 99 mg) to the 10 mL of the 0.01 N HCl to prepare SiO₂NPs solution. These experiments were used to examine the effect of SiO₂NPs weights on the activity of pepsin catalyzed reaction. The Lineweaver-Burk plots of the five experiments, were plotted in Figure 3.

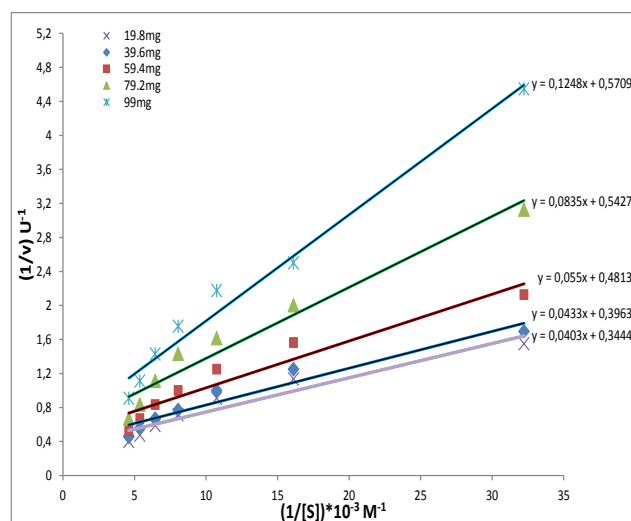


Figure 3. Lineweaver-Burke lines of pepsin catalyzed reaction after adding different amounts of SiO₂NPs.

The results in Figure 3 revealed that the presence of SiO₂NPs causes reduction in the V_{\max} of pepsin catalyzed reaction. The values of V_{\max} and K_m are shown in Table 1.

Table 1. Effect of weight of SiO₂NPs at 37 °C on the activity of pepsin coated SiO₂NPs.

Wt. of SiO ₂ NPs (mg)	Slope	Intercept	V_{\max} (U)	$K_m \times 10^{-5}$ (M)
0	0.034	0.208	4.82	19.210
19.8	0.040	0.344	2.90	11.702
39.6	0.040	0.396	2.52	10.177
59.4	0.055	0.481	2.08	11.427
79.2	0.083	0.543	1.84	15.202
99.0	0.125	0.571	1.75	21.860

The data in Table 1 demonstrate the effect of weight of SiO₂NPs on pepsin activity. These weights were selected from the calculations of the amount of SiO₂NPs needed to be coated with a monolayer of pepsin molecules. The first weight (19.8 mg) of SiO₂NPs in the reaction mixture represents a NPs coated with a monolayer of pepsin molecules. The results showed that V_{\max} of free pepsin (4.82 U) decreases to 2.90 U when the enzyme was immobilized on the surface of SiO₂NPs. The activity continued to decrease as the weight of the added NPs increases until becoming 1.75 U when the weight added is 99 mg. It is clear that the SiO₂NPs has remarkable inhibitory effect on pepsin activity. Most of the reduction in the pepsin enzyme activity is due to the change in the secondary structures of the whole enzyme and particularly in the active site structure. These changes are caused by the adsorption forces between the surface of the NPs and various chemical groups of the pepsin molecules. The attractive forces are strong enough to hold molecules on the NPs surface and modify the H-bonding that constitute the secondary structure of the pepsin molecules. Therefore, the change in the secondary structure is the most probable cause for the decrease in the activity of the immobilized forces.

Studies indicate that the activity of lysozyme adsorbed onto SiO₂NPs is lower than that of the free protein, and the fraction of activity lost correlates well with the decrease in α -helix content (19). Binding of proteins on planar surfaces often induces significant changes in the secondary structure (20). However, a study of a variety of nanoparticle surfaces and proteins indicates that perturbation of protein structure still occurs to varying extents. The proteins show a rapid conformational change at both secondary and tertiary structure levels (20, 21). Numerous studies have found that activity reduction is related to the loss of α -helical content when proteins are adsorbed onto NPs regardless of an increase in the β -sheet (20). Binding of proteins to planar surfaces often induces significant changes in secondary structure; the high curvature of NPs can help proteins to retain their original structure (22). Several *in vivo* and *in vitro* studies of the toxicity of SiO₂NPs have been performed and found that they are safe and can be employed in food production (23). These findings and the findings of the present research encourages the use of SiO₂NPs as an inhibitor of pepsin for the treatment of GERD *in vivo*.

Effect of temperature on the interaction of SiO₂NPs with pepsin

The activity of the immobilized enzyme was measured at different temperatures (22, 27, 32, 37, and 42 °C) by using 19.8 mg of SiO₂NPs and the same concentrations of hemoglobin. These experiments were used to examine the effect of temperature on the activity of pepsin catalyzed reaction in the presence of SiO₂NPs. The Lineweaver-Burk lines of the immobilized pepsin activity at five different temperatures are presented in Figure 4.

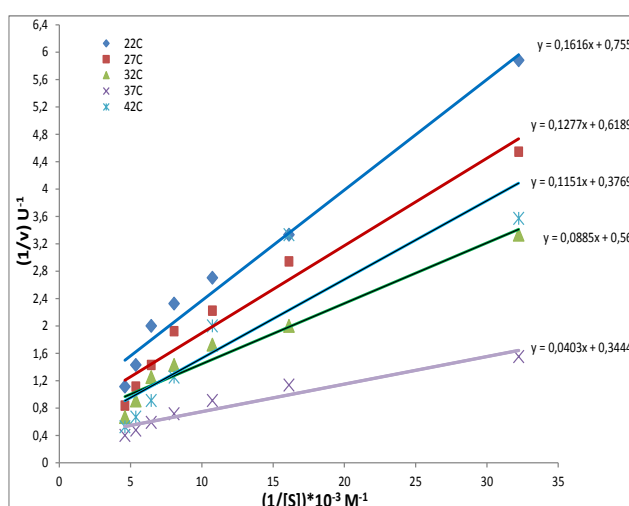


Figure 4. Lineweaver-Burk lines of the SiO₂-immobilized pepsin catalyzed reaction at (22, 27, 32, 37, and 42 °C).

The values of V_{\max} and K_m of the pepsin catalyzed reaction at different temperatures in the presence of SiO₂NPs are listed in Table 2. The results revealed that the V_{\max} at 37 °C is 2.91 U and then is reduced as temperature decreases. Whereas the K_m at 37 °C equal to 11.72×10^{-5} M then increases as temperature decreases. It means that the change in temperature may cause a change in the form of active site and thus change V_{\max} .

Table 2. Maximum velocities and Michaelis constants of the SiO₂NPs-immobilized pepsin at different temperatures.

Temp. (°C)	Equation	V_{\max} (U)	$K_m \times 10^{-5}$ (M)
22	$y = 0.162x + 0.755$	1.33	21.40
27	$y = 0.128x + 0.620$	1.62	20.63
32	$y = 0.089x + 0.560$	1.79	15.80
37	$y = 0.040x + 0.344$	2.91	11.72
42	$y = 0.115x + 0.380$	2.65	30.54

The results in Table 2 revealed that K_m and V_{max} change when the temperature changes. V_{max} increases as the temperature increases until reaching the optimum temperature and then tends to decrease when the temperature reaches 42 °C, while K_m decreases as temperature increases. However, at 42 °C, the K_m increases again indicating that there are conformational changes in the immobilized pepsin or changes in the interaction between the pepsin molecules and the SiO₂NPs.

In a previous study, it is found that the interaction between SiO₂NPs and three different enzymes are dependent on the functional groups on the surface of NPs (24). These findings indicated the presence of weak electrostatic interactions between the protein molecules and the surface of NPs. When nanomaterials are in contact with a biological environment, the proteins can immediately bind to the surface of the NPs, which creates protein coronas (25).

The bio-distribution of the nanomaterial is affected by this protein coating, which aids in understanding the mechanisms of protein coronas formations on nanomaterial surfaces including the effect of the nanomaterial surface properties (26). Weak protein-NPs interactions were studied previously in a low binding regime as a model for the soft protein corona around NPs in complex biological fluids. Noncovalent and reversible interactions between protein and SiO₂NPs showed significant alteration in conformation and enzymatic activity in a NP-size dependent manner. These facts indicated the presence of very weak interactions between protein and SiO₂NPs (27). Changes of environment temperature can alter the intramolecular attractive forces (hydrogen bonding, dipole-dipole interaction, hydrophobic interaction etc.) of the protein (e.g. enzyme). This can alter the active site of the enzyme rendering it inactive (28).

Effect of SiO₂NPs and ionic strength

The pepsin activity was measured at various conditions, i.e., free pepsin, in the presence of 130 mg of NaCl, immobilized pepsin on SiO₂NPs, and immobilized pepsin in the presence of 130 mg NaCl. All experiments were carried out at 37 °C. These experiments were carried out to explore the effect of the combination of ionic strength and SiO₂NPs on the activity of pepsin. The Lineweaver-Burk plots of the four experiments were plotted in Figure 5.

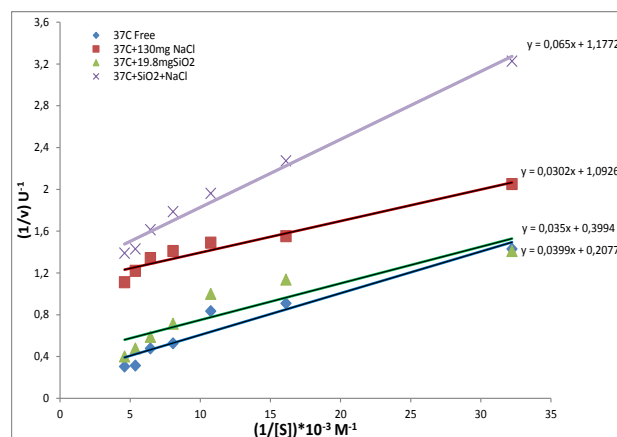


Figure 5. Lineweaver-Burke lines of pepsin catalyzed reaction at 37 °C after adding 130 mg NaCl, 19.8 mg SiO₂NPs and in the presence of both (130 mg NaCl and 19.8 mg SiO₂NPs).

Table 3. Comparison of free pepsin, pepsin with 130 mg NaCl, 19.8 mg SiO₂NPs, and both (19.8 mg SiO₂NPs + 130 mg NaCl).

Wt (mg)	Slope	Intercept	V _{max} (U)	K _m x 10 ⁻⁵ (M)
Free	0.040	0.208	4.82	19.21
19.8 mg SiO ₂ NPs	0.035	0.399	2.50	8.76
130 mg NaCl	0.030	1.093	0.92	2.76
19.8mg SiO ₂ +130 mg NaCl	0.065	1.177	0.85	5.52

In Table 3, the comparison of free pepsin activity, immobilized pepsin on SiO₂NPs, and immobilized pepsin in the presence of 130 mg NaCl is shown. The results showed the V_{max} of free enzyme equal to 4.82 U and then became 2.50 U when 19.8 gm of SiO₂NPs were added. Then V_{max} decreased and became 0.92 U when 130 mg of NaCl were added to the enzyme reaction mixture, and then it became equal to 0.85 U when NaCl and SiO₂NPs were added together to the reaction mixture. It can be easily noticed that the effect of the combination of the ionic strength and SiO₂NPs causes high reduction of pepsin activity.

Most of the reduction in the enzyme activity is due to the changes in the secondary structures of the whole enzyme and particularly in the three dimensional structure of the active site, as previously mentioned in the Effect of SiO₂NPs weight on the pepsin catalyzed reaction section. Furthermore, a study by Wu *et al.* (20) showed that both β-lactoglobulin and lysozyme unfolded to a greater extent at lower surface concentration on SiO₂NPs. The proteolytic activity of pepsin is affected by the conditions of the dissolution medium. There is a significant reduction in the activity of pepsin after adding different concentrations of surfactants salts (29). Salts can form weak bonds with the charged functional groups on the protein surface.

Depending on the nature of ions, the balance among the forces are changed. However, higher concentration of salt can lead to salting out effect or decreased solubility of protein (30). There have been many interesting studies done about the inhibition of various enzyme activities upon adsorption on the surface of different nanoparticles (31, 32). Using advanced techniques such as circular dichroism and fluoroscopy, it is found that the most affective factors responsible for the reduction in the enzyme activity, after adsorption on the nanoparticle surface, is the change in the secondary and tertiary structures of the enzyme especially around 18 the active site (32, 33). The same explanation can be generalized for the pepsin-SiO₂NPs system and it can be concluded that the reduction in the pepsin activity is due to the perturbation in the secondary and tertiary protein structures.

Conclusions

The results of the present study revealed that the SiO₂NPs has an ability to inhibit the pepsin activity. The results also indicates that the presence of high ionic strength causes remarkable reduction of pepsin activity. The increase in the amount of SiO₂NPs in the reaction medium leads to more reduction in the pepsin activity. Furthermore, the optimum temperature for the NPs to inhibit the reaction is 37 °C. Therefore, the best conditions of inhibition of pepsin enzyme is by using higher amounts of SiO₂NPs in the presence of NaCl at 37 °C.

References

1. Herbella, F. A.; Patti, M. G. Gastroesophageal reflux disease: From pathophysiology to treatment. *World. J. Gastroenterol.* **2010**, *16* (30), 3745-3749. DOI: <https://doi.org/10.3748/wjg.v16.i30.3745>.
2. Badillo, R.; Francis D. Diagnosis and treatment of gastroesophageal reflux disease. *World. J. Gastrointest. Pharmacol. Ther.* **2014**, *5* (3), 105-112. DOI: <https://doi.org/10.4292/wjgpt.v5.i3.105>.
3. Ha, J.O.; Lee, T.H.; Lee, C.W.; Park, J.Y.; Choi, S.H.; Park, H.S.; et al. Prevalence and risk factors of gastroesophageal reflux disease in patients with type 2 diabetes Mellitus. *Diabetes. Metab. J.* **2016**, *40* (4), 297-307. DOI: <https://doi.org/10.4093/dmj.2016.40.4.297>.
4. Kim, J.; Oh, S.W.; Myung, S.K.; Kwon, H.; Lee, C.; Yun, J. M.; et al. Association between coffee intake and gastroesophageal reflux disease: a meta-analysis. *Dis. Esophagus.* **2014**, *27* (4), 311-317. DOI: <http://dx.doi.org/10.1111/dote.12099>.
5. Katz, P. O.; Gerson, L. B.; Vela, M. F. Guidelines for the diagnosis and management of gastroesophageal reflux disease. *Am. J. Gastroenterol.* **2013**, *108*, 308-328. DOI: <https://doi.org/10.1038/ajg.2012.444>.
6. Zajac, P.; Holbrook, A.; Super, M. E.; Vogt, M. An overview: Current clinical guidelines for the evaluation, diagnosis, treatment, and management of dyspepsia. *Osteopathic Family Physician.* **2013**, *5* (2), 79-85. DOI: <https://doi.org/10.1016/j.osfp.2012.10.005>.
7. El-Serag, H.B.; Sweet, S.; Winchester, C.C.; Dent, J. Update on the epidemiology of gastro-oesophageal reflux disease: A systematic review. *Gut.* **2014**, *63* (6), 871-880. DOI: <http://dx.doi.org/10.1136/gutjnl-2012-304269>.
8. Samuels, T. L.; Johnston N. Pepsin as a causal agent of inflammation during nonacidic reflux. *Otolaryngol. Head. Neck. Surg.* **2009**, *141*, 559-563. DOI: <http://dx.doi.org/10.1016/j.otohns.2009.06.555>.
9. Ho, C. E.; Goh, Y.; Zhao, X. X.; Yu, C.Y.; Zhang, C. GERD: An Alternative Perspective. *Psychosomatics.* **2016**, *57*(2), 142-151. DOI: <https://doi.org/10.1016/j.psym.2015.10.007>.
10. Nagahama, K.; Nishio, H.; Yamato, M.; Takeuchi, K. Orally administered l-arginine and glycine are highly effective against acid reflux esophagitis in rats. *Med. Sci. Monitor.* **2012**, *18* (1), BR9-BR15. DOI: <https://doi.org/10.12659/msm.882190>.
11. Berg JM, Tymoczko JL, Stryer L. *Biochemistry*. 5th Edition. W H Freeman, New York: 2002.
12. Al-Hakeim, H.K.; Jasem, K.M. High ionic strength enhances the anti-pepsin activity of titanium dioxide nanoparticles. *Nano. Biomed. Eng.* **2016**, *8* (3), 136-143. DOI: <https://doi.org/10.5101/nbe.v8i3.p136-143>.
13. Dubey, R.S.; Rajesh, Y.B.; More, M.A. Synthesis and characterization of SiO₂ nanoparticles via sol-gel method for industrial applications. *Mater. Today* **2015**, *2* (4-5), 3575-3579. DOI: <http://dx.doi.org/10.1016/j.matpr.2015.07.098>.
14. Liu, T.; Liu H.; Fu C.; Li, L.; Chen, D.; Zhang, Y.; et al. Silica nano rattle with enhanced protein loading: a potential vaccine adjuvant. *J. Colloid. Interface. Sci.* **2013**, *400*, 168-174. DOI: <https://doi.org/10.1016/j.jcis.2013.03.005>.
15. Chen, Z.; Meng, H.; Xing, G.M.; Yuan, H.; Zhao, F.; Liu, R. Age-related differences in pulmonary and cardiovascular responses to SiO₂ nanoparticle inhalation: nanotoxicity has susceptible population. *Environ. Sci. Technol.* **2008**, *42*, 8985-8992. DOI: <http://dx.doi.org/10.1021/es800975u>.
16. Fruijtier-Polloth, C. The toxicological mode of action and the safety of synthetic amorphous silica-a nanostructured. *Toxicology* **2012**, *294* (2-3), 61-79. DOI: <https://doi.org/10.1016/j.tox.2012.02.001>.
17. Wang, H.; Du, L. J.; Song, Z. M.; Chen, X. X. Progress in the characterization and safety evaluation of engineered inorganic nanomaterials in food. *Nanomedicine (London, U. K.)* **2013**, *8* (12), 2007-2025. DOI: <http://dx.doi.org/10.2217/nmm.13.176>.
18. Knight, J.; Lively M.; Johnston, N.; Dettmar, P. W.; Koufman, J. A. Sensitive pepsin immunoassay for detection of laryngopharyngeal reflux. *Laryngoscope* **2005**, *115* (8), 1473-1478. DOI: <https://doi.org/10.1097/01.mlg.0000172043.51871.d9>.
19. Vertegel, A. A.; Siegel, R. W.; Dordick, J. S. Silica nanoparticle size influences the structure and enzymatic activity of adsorbed lysozyme. *Langmuir* **2004**, *20*, 6800-6807. DOI: <https://doi.org/10.1021/la0497200>.
20. Wu, X.; Narsimhan, G. Characterization of secondary and tertiary conformational changes of beta-lactoglobulin adsorbed on silica nanoparticle surfaces. *Langmuir* **2008**, *24*, 4989-4998. DOI: <https://doi.org/10.1021/la703349c>.
21. Shang, W.; Nuffer, J. H.; Dordick, J. S.; Siegel, R. W. Unfolding of ribonuclease A on silica nanoparticle surfaces. *Nano. Lett.* **2007**, *7*, 1991-1995. DOI: <http://dx.doi.org/10.1021/nl070777r>.
22. Fei, L.; Perrett, S. Effect of nanoparticles on protein folding and fibrillogenesis. *Int. J. Mol. Sci.* **2009**, *10*, 646-655. DOI: <http://dx.doi.org/10.3390/ijms10020646>.
23. Yoshida, T.; Yoshioka, Y.; Takahashi, H.; Misato, K.; Mori, T.; Hirai, T. et al. Intestinal absorption and biological effects of orally administered amorphous silica particles. *Nanoscale. Res. Lett.* **2014**, *9*, 1-7. DOI: <https://doi.org/10.1186/1556-276X-9-532>.
24. Sun, X.; Feng, Z.; Zhang, L.; Hou, T.; Li, Y. The selective interaction between silica nanoparticles and enzymes from molecular dynamics simulations, *PLoS one* **2014**, *9* (9), e107696. DOI: <http://dx.doi.org/10.1371/journal.pone.0107696>.
25. Lynch, I.; Dawson, K.A. Protein-nanoparticle interactions. *Nano. Today* **2008**, *3*, 40-47. DOI: [http://dx.doi.org/10.1016/s1748-0132\(08\)70014-8](http://dx.doi.org/10.1016/s1748-0132(08)70014-8).
26. Wang, B.; Peng, R.; Grulke, E.A. Influence of surface charge on lysozyme adsorption to ceria nanoparticles. *Appl. Surf. Sci.* **2012**, *258*, 5332-5341. DOI: <https://doi.org/10.1016/j.apsusc.2012.01.142>.
27. Wang, J.; Jensen, U. B.; Jensen, G. V.; Shipovskov, S.; Vijay, S. Soft interactions at nanoparticles alter protein function and conformation in a size dependent manner. *Nano. Lett.* **2011**, *11* (11), 4985-4991. DOI: <https://doi.org/10.1021/nl202940k>.
28. Banga, A.K. *Therapeutic Peptides and Proteins formulation, processing and Delivery Systems*. 2nd ed. New York: Taylor & Francis, 2006.

29. Guzman, M. L.; Marques, M. R.; Olivera, M. E.; Stippler, E. S. Enzymatic activity in the presence of surfactants commonly used in dissolution media, Part 1: Pepsin. *Pharma. Sci.* **2016**, *2* (6), 15-19. DOI: <https://doi.org/10.1016/j.rinphs.2016.02.002>.
30. Shamim, N.; Hong, L.; Hidajat, K.; Uddin, M. S. Thermosensitive-polymer-coated magnetic nanoparticles: Adsorption and desorption of bovine serum albumin. *J. Colloid. Interface. Sci.* **2006**, *304*, 1-8. DOI: <http://dx.doi.org/10.1016/j.jcis.2006.08.047>.
31. Middaugh, C.R.; Volkin, D.B. Protein solubility. In Ahren T.J. and Manning M.C. (eds), *Pharmaceutical Biotechnology. Stability of protein Pharmaceuticals. Part A: Chemical and physical pathways of protein degradation*. New York: Plenum Press, 1992 (2); pp 109-134.
32. Al-Hakeim, H.K.; Kareem, M.M.; Grulke, E.A. Synthesis a new magnetic nanoparticles and study the interaction with xanthine oxidase. *Am. J. Nanomaterials* **2014**, *2* (2), 13-20. DOI: <http://dx.doi.org/10.12691/ajnn-2-2-1>.
33. Al-Hakeim, H.K.; Khudhair, M.K.; Grulke, E.A. Immobilization of urease enzyme on nanoceria modifies secondary and tertiary protein structures. *Acta. Chim. Slovaca.* **2016**, *9* (1), 44-53. DOI: <https://doi.org/10.1515/acs-2016-0008>.

Article citation:

Al-Hakeim, H. K.; Jasem, K. M.; Moustafa, S. R. Anti-pepsin activity of silicon dioxide nanoparticles. *Rev. Colomb. Quim.* **2016**, *45* (3), 5-11. DOI: <http://dx.doi.org/10.15446/rev.colomb.quim.v45n3.58760>.



Eduardo J. Corpas^{1*}, Gonzalo Taborda², Omar A. Tapasco², Aristófeles Ortiz³

¹Universidad Católica de Manizales, Instituto de Investigación en Microbiología y Biotecnología Agroindustrial, Carrera 23 # 60-63, Manizales, Caldas, Colombia.

²Universidad de Caldas, Facultad de Ciencias Exactas y naturales, Calle 65 # 26-10, Manizales, Caldas, Colombia.

³Centro Nacional de Investigaciones de Café CENICAFÉ, Área de Calidad y Producción, Km 4 vía Manizales Chinchiná, Caldas, Colombia.

*Corresponding author: ecorpas@ucm.edu.co

Recibido: 26 de Agosto de 2016. Aceptado: 1 de Octubre de 2016.

Comparison between extraction methods to obtain volatiles from lulo (*Solanum quitoense*) pulp

Abstract

Simultaneous Distillation-Solvent Extraction (SDE) and Headspace Solid Phase Micro-extraction (HS-SPME), coupled to Gas Chromatography-Mass Spectrometry (GC-MS), for recovery of volatiles from lulo pulp (*Solanum quitoense*) were compared. A completely randomized SDE/GC-MS design was applied to establish differences between the areas obtained with different solvents, whereas a two-way HS-SPME/GC-MS indicated the most appropriate extraction conditions of volatiles, having the type of fiber and the adsorption temperature as factors. SDE/GC-MS mainly promoted the extraction of hydrocarbons, aldehydes, and esters; whereas esters and aldehydes had higher areas using HS-SPME/GC-MS. Furthermore, the variance analysis showed a significant interaction among the type of fiber, the adsorption temperature, and the functional groups.

Comparación entre métodos de extracción para la obtención de volátiles a partir de pulpa de lulo (*Solanum quitoense*)

Resumen

Se compararon los métodos de extracción y destilación simultánea (SDE) y microextracción en fase sólida con espacio de cabeza (HS-SPME), acoplados a cromatografía de gases con detector de espectrometría de masas (GC-MS), para la recuperación de volátiles a partir de pulpa de lulo (*Solanum quitoense*). Se realizó un diseño completamente al azar aplicado al tipo de solvente para SDE/GC-MS, mientras que para HS-SPME/GC-MS se ejecutó un diseño a dos vías, teniendo como factores el tipo de fibra y la temperatura de adsorción. En el primer caso se obtuvieron principalmente hidrocarburos, aldehídos y ésteres; en el segundo, se recuperaron ésteres y aldehídos. El análisis de varianza mostró una interacción significativa entre el tipo de fibra, la temperatura de adsorción y los grupos funcionales.

Comparação entre métodos de extração para a obtenção de voláteis a partir da polpa de lulo (*Solanum quitoense*)

Resumo

Foram comparados os métodos de extração e destilação simultânea (SDE) e microextração em fase sólida com espaço de cabeça (HS-SPME), acopladas à cromatografia gasospectrometria de massa (GC-MS), para à recuperação de voláteis a partir da polpa de lulo (*Solanum quitoense*). Foi realizado um delineamento completamente casualizado aplicado ao tipo de solvente para à SDE/GC-MS, enquanto à HS-SPME/GC-MS foi executado um desenho de duas vias, tendo como fatores o tipo de fibra e a temperatura de adsorção. No primeiro caso foram obtidos sobretudo hidrocarbonetos, aldeídos e ésteres; no segundo foram obtidos ésteres e aldeídos. A análise de variância mostrou uma interação significativa entre o tipo de fibra, a temperatura de adsorção e os grupos funcionais.

Keywords: Chemical analysis, *Solanum quitoense*, metabolite profile, HS-SPME, SDE, volatile organic compounds.

Palabras clave: análisis químico, *Solanum quitoense*, perfil de metabolitos, HS-SPME, SDE, compuestos orgánicos volátiles.

Palavras-Chave: análise química, *Solanum quitoense*, perfil de metabolitos, HS-SPME, SDE, compostos orgânicos voláteis.

Introduction

Volatile organic compounds (VOC) are responsible for the distinctive flavor in each fruit, even though some of these components are not able to interact with the human olfactory receptors for triggering the subsequent sensory impact (1). Obtaining a complete volatile profile from a ripe fruit constitutes a relevant evidence regarding its sensorial quality features (2). A predominance of esters, alcohols, and aldehydes has been denoted in several types of fruit, mostly climacteric (3-7). On the contrary, in other climacteric fruits the hydrocarbons were the outstanding group (8-10).

The diverse chemical nature of volatile compounds arises due to the different metabolic pathways that exist in fruits (11, 12). The metabolites obtained depend on the extraction method employed. The Simultaneous Distillation-Solvent Extraction (SDE) method, based on the recovery of compounds by polar affinity to a simultaneously distilled organic solvent, promotes the extraction of diverse chemical classes (13). Nevertheless, SDE is a sensitive method for obtaining compounds at trace concentrations (14). It requires great amount of sample, has a prolonged extraction time (2), and promotes the loss of highly volatile metabolites (15). On the other hand, Solid Phase Micro-extraction (SPME), supported on the partition equilibrium of the metabolites between both fiber and matrix analyzed (16) is fast, easy, sensitive, solventless, and avoids loss of volatiles with low boiling point (17, 18).

Previous studies have demonstrated the complementarity between SDE and HS-SPME to obtain more complete volatile profiles in several fruits (15, 17, 19, 20). The increase in the compounds using SDE and HS-SPME methods occurs due to the affinity of each method for compounds with a specific polarity and molecular weight. The extracts from SDE contain high molecular weight compounds and are poor in highly volatile metabolites (21), but using HS-SPME the obtaining of heavy volatile compounds is lower (2). In addition, each fruit has a volatile profile with different characteristics, which justifies in some cases the extraction with nonpolar solvents such as diethyl ether (1, 22, 23), or solvents of intermediate polarity such as dichloromethane (17, 18, 22, 24, 25). In addition to SDE, the extraction with HS-SPME has been carried out in several fruits using fibers with a specific polarity (2, 15, 18, 20), after the selection of this as the higher performance fiber in the extraction of volatile metabolites.

Lulo (*Solanum quitoense* Lam.) is a *Solanaceae* species native to South America, whose pulp has potential for both processing and marketing at industrial scale (26). A comparative referent between the volatile profiles of frozen lulo pulp cultivated in Colombia and Costa Rica, obtained by extraction with pentane and ether (2:1), showed differences attributed to the different environmental conditions in each country (27). Moreover, supercritical CO₂ enabled to recover the volatile profiling from the lulo pulp and to identify 52 compounds, mainly alcohols and esters (among which, decane, methyl benzoate, acetic acid, hexadecane, and methyl hexanoate had the highest concentrations (28)).

In addition, 65 compounds from *S. vestissimum*, another lulo species, were identified with SDE/GC-MS, using diethyl ether and pentane (1:1). Among the volatiles obtained, those of highest concentration were methyl propionate, methyl butanoate, butyl acetate, 3-methylbutyl acetate, methyl hexanoate, methyl (E)-2-methyl-2-butenoate, (Z)-3-hexenylacetate, methyl benzoate, (Z)-3-hexenol, linalool, α -terpineol, and geraniol (29).

This study aimed to obtain volatile profiles from lulo pulp, using two extraction methods: SDE with solvents of different polarity and HS-SPME by using several fibers. The extracts were analyzed by GC-MS. In both experiments, the comparison of total volatile areas and those of the functional groups allowed to establish which treatment was the most efficient for the extraction of volatiles from lulo pulp.

Materials and methods

Fruit selection

Lulo fruit, harvested in stage five (30), came from seedlings which were generated through *in vitro* propagation by the company Agro in-vitro S.A.S. (Manizales, Colombia) and harvested at the Villa Malicia farm, placed at 1 km from Manizales. In addition, the fruit grew from a developed crop in controlled conditions with Green Seal fungicides and had the following features as a selection criteria: diameter of 5-6 cm, orange skin, and brix degrees of 10.3 ± 0.2 (30). Moreover, fruit with spoilage signs, triggered by insects or molds, was discarded.

Reagents and materials

Sodium chloride was acquired from Carlo Erba Reagents® (Barcelona, Spain). The solvents hexane, dichloromethane, and ethyl acetate were provided by Sigma-Aldrich® (Saint Louis, USA). The SPME holder and the fibers used in the adsorption of volatile metabolites were obtained from Supelco® (Bellenfonte, PA, USA). Four fibers for were employed: polydimethylsiloxane (PDMS, 100 μ m), carboxen/polydimethylsiloxane (CAR/PDMS, 75 μ m), polydimethylsiloxane/divinylbenzene (PDMS/DVB, 65 μ m), divinylbenzene/carboxen/polydimethylsiloxane (DVB/CAR/PDMS, 50/30 μ m), which were conditioned prior to their use as indicated by the manufacturer. The alkane standard solution C7-C40 was provided by Sigma-Aldrich Chemical S.A.

SDE procedure

The fruit was washed with distilled water for 20 s and cut for separating the peel and obtaining the pulp. 200 g of pulp were weighed in a sample flask with 500 mL capacity. The extraction was conducted in a modified Likens-Nickerson apparatus. In the first one side, the flask containing the sample was adapted, and in the second one, another flask with 50 mL of the respective solvent was installed. The flasks underwent the boiling temperature of each solvent and SDE extraction was carried out for 1 h. Thereafter, an extracted volume of approximately 20 mL was collected and completed to a fixed volume of 50 mL with each solvent. Subsequently, 1 mL of this sample was added on a vial with capacity of 2 mL. Finally, 1 μ L of extract was inserted to desorb in the injection port of the gas chromatograph.

HS-SPME procedure

Each fruit was washed with distilled water for 20 s and 10 g of the pulp were added into a vial with 20 mL of capacity. Subsequently, the vial was closed with a rubber cap and placed on a water bath. Thereafter, the respective SPME fiber was manually inserted into the headspace (HS) of the pulp and exposed at temperature of 40 or 60 °C for 30 min, according to the experimental design proposed. After removing, the fiber was inserted into the injection port of the gas chromatograph to desorb the extracted compounds at 230 °C in splitless mode for 2 min.

Analysis of volatile compounds

In order to analyze the volatile compounds from lulo pulp, a gas chromatograph Shimadzu GCMS-QP2010 Plus coupled to a mass spectrometry detector was used. Regarding the samples extracted by HS-SPME, a liner of 0.75 mm I.D. (Supelco, Bellefonte, PA) was used to conduct the metabolites to the column, whereas for the extracts obtained by SDE, a 3.4 mm I.D. liner (Shimadzu) was used. As a carrier gas, helium at a constant flow rate of 4 mL/min was used. A Shimadzu 5% polysiloxane (30 m x 0.25 mm ID x 1.4 µm DF) semi-polar analytical column with a temperature range of -40 °C to 260 °C was used. Flow control worked at a linear velocity of 36 cm/s, the pressure was 55.2 kPa and the column flow was 0.98 mL/min. The temperature ramp program was as follows: one min at 50 °C, increasing at 2.5 °C/min up to 150 °C, in which remained for seven min; subsequently, it was increased at 15 °C/min up to 220 °C, remaining in this state for three min; and finally, the temperature was increased at 15 °C/min up to 230 °C and maintained for two min.

On the other side, the mass spectrometer was operated with ionization energy (IE) 70 eV, ion source temperature 235 °C, time of solvent cut-off 3 min, threshold of 1000, and mass range between 33-350 Da. The detector operated was operated at 1.0 kV and the mass spectrum had a scan speed of 666 Hz. The analyses of volatiles from extractions by HS-SPME were carried out for 50 min, whereas each assay of the SDE treatments lasted 60 min. The identification of each peak was based on the comparison between the mass spectrum of each compound and generated compounds from the NIST library version 8, having as an identification criteria a concordance equal or superior to 93%. In addition, a verification of the Kovats retention index was made from the analysis of a mixture of alkanes (C7-C24) under the same conditions used with the samples.

Statistical analysis

In relation to SDE experiments, a completely randomized design was performed having the type of solvent with three treatments (hexane, dichloromethane, and ethyl acetate) as a factor, and the total area of volatiles and functional groups areas as a response variable. Six replicates per treatment were carried out. After evaluating the statistical assumptions, an analysis of variance (ANOVA) was performed to establish differences between treatments and the Tukey test to define for which of the treatments there were differences.

Regarding the SPME fiber treatments, a two-way design was performed: the first factor was the type of fiber with four levels (PDMS, CAR/PDMS, PDMS/DVB, and DVB/CAR/PDMS), and the second factor was the adsorption temperature with two levels (40 °C and 60 °C). The response variable was the total area of volatile compounds. Five repetitions were carried out for each treatment. Moreover, the areas of the functional groups in each treatment were analyzed.

Volatiles data were submitted to an ANOVA to establish differences between both the total areas and the functional groups areas. The relative standard deviation (RSD) of the functional groups areas was lower than 12% in all experiments. Finally, a t-test for the areas of the functional groups of the most efficient treatments from each experiment was made. Using the SPSS software version 22, the obtained data from the treatments were analyzed.

Results and discussion

Volatile compounds from lulo pulp by SDE/GC-MS using different solvents

Total area

Through SDE/GC-MS, 47 volatile compounds with molecular weights ranging from 60 to 282 Da were obtained, mainly hydrocarbons (42.55%), followed by aldehydes (17.02%), esters (17.02%), alcohols (10.63%), ketones (6.38%), and acids (4.25%). Furthermore, 34 of these compounds were identified as well. In addition, there was a higher percentage of the area obtained from compounds such as decanal, furfural, benzeneacetaldehyde, methylbutanoate, (Z)-3-hexen-1-ol acetate, and hexadecane (Table 1).

The assumptions of normality were confirmed through the Shapiro-Wilk from the SDE data with the solvents hexane ($P = 0.369$), dichloromethane ($P = 0.496$), and ethyl acetate ($P = 0.914$), as well as through the homogeneity of the variances of these datasets from Levene test statistic ($P = 0.566$).

Firstly, a lower total area of volatiles was presented from the hexane extraction, whereas ethyl acetate enabled to recover a mean area higher than that obtained with the other solvents. Secondly, the ANOVA showed statistically significant differences among the treatments considering the type of solvent ($P = 0.00$), whereas the Tukey test showed that extraction using hexane (mean area: 2.2×10^8) was less effective than those obtained with dichloromethane (mean area: 3.7×10^8) and ethyl acetate (mean area: 1.12×10^9). However, there were no statistical differences between the mean areas using the last two mentioned solvents.

Area of the functional groups

When comparing the areas, a predominance of hydrocarbons in the treatments using hexane and dichloromethane was observed, but through ethyl acetate the aldehydes predominated and the hydrocarbons were not recovered due to its nonpolar nature (Figure 1).

Table 1. Volatile compounds obtained by SDE/GC-MS from lulo pulp with different solvents.

Name of the compound	Hexane			Dichloromethane			Ethyl acetate		
	MA	%MA	RSD	MA	% MA	RSD	MA	% MA	RSD
Acetic acid, 1-methylethyl ester	-	-	-	-	-	-	8349569	0.7	9.1
Acetic acid	-	-	-	-	-	-	711173709	63.5	12.2
n-Propyl acetate	-	-	-	-	-	-	3325308	0.3	10.7
Butanoic acid methyl ester	13700138	6.2	12.3	30231061	8.0	9.2	12751611	1.1	7.6
2,3-Pentanedione	-	-	-	-	-	-	3560892	0.3	11.7
(E)-2-Pentenal	-	-	-	3211431	0.9	8.1	-	-	-
(E)-2-Butenoic acid methyl ester	-	-	-	1977985	0.5	15.5	3319264	0.3	12.3
2,4-Dimethyl-1-heptene	8830760	4.0	8.8	8535166	2.3	10.1	-	-	-
Butanoic acid	-	-	-	2350855	0.6	11.5	9328692	0.8	13.1
(Z)-3-Hexen-1-ol	-	-	-	-	-	-	9680148	0.9	10.8
Furfural	-	-	-	12087306	3.2	9.0	100354393	9.0	12.2
(E)-2-Hexenal	-	-	-	4522348	1.2	12.9	6357839	0.6	10.9
2,4-Hexadiene-1-ol	-	-	-	-	-	-	4760558	0.4	8.8
Hexanoic acid methyl ester	-	-	-	12840318	3.4	13.3	-	-	-
5-Methyl-2(3H)-furanone	-	-	-	-	-	-	8646088	0.8	9.2
Decane	8592208	3.9	12.6	7840464	2.1	12.7	-	-	-
Octanal	8700512	3.9	11.2	8467739	2.2	10.1	-	-	-
Undecane	-	-	-	4170176	1.1	6.2	-	-	-
Unidentified 1	3313142	1.5	7.0	3818386	1.0	6.1	-	-	-
(Z)-3-Hexen-1-ol acetate	-	-	-	-	-	-	44026559	3.9	10.2
Acetic acid hexyl ester	-	-	-	-	-	-	16183208	1.4	10.3
Unidentified 2	8977702	4.0	12.3	7430529	2.0	7.8	-	-	-
Unidentified 3	9002962	4.0	10.7	8388167	2.2	11.2	-	-	-
5-Methyl-2-furancarboxaldehyde	-	-	-	-	-	-	7957055	0.7	9.1
Benzeneacetaldehyde	9221058	4.1	13.8	2726208	0.7	9.8	74545677	6.7	12.7
3,7-Dimethyl-1,6-octadien-3-ol	-	-	-	-	-	-	7697874	0.7	12.4
Methyl benzoate	-	-	-	7296803	1.9	11.3	-	-	-
Nonanal	1628773	0.7	8.3	48365026	12.8	11.9	-	-	-
Unidentified 4	-	-	-	3709879	1.0	12.5	-	-	-
4,6-Dimethyl-undecane	6087865	2.7	9.1	7167158	1.9	11.8	-	-	-
Unidentified 5	-	-	-	-	-	-	3567490	0.3	9.9
Unidentified 6	6544510	2.9	11.7	4775928	1.3	12.2	-	-	-
3-Cyclohexene-1-methanol	-	-	-	-	-	-	6984032	0.6	10.9
Unidentified 7	2993714	1.3	9.8	3582355	1.0	10.7	-	-	-
Decanal	25733315	11.6	9.3	37443212	9.9	9.2	-	-	-
4,6-Dimethyl-dodecane	13243309	6.0	11.4	17255615	4.6	13.9	-	-	-
Hexadecane	19228523	8.6	12.2	27105021	7.2	10.0	-	-	-
Heptadecane	13375019	6.0	8.0	18284273	4.9	8.7	-	-	-
2-Methoxy-4-vinylphenol	-	-	-	-	-	-	78240184	7.0	13.2
Octadecane	6573614	3.0	12.8	8604822	2.3	11.5	-	-	-
Eicosane	5020961	2.3	12.9	8283655	2.2	12.9	-	-	-
Unidentified 8	7562784	3.4	8.3	7906485	2.1	10.7	-	-	-
Unidentified 9	11795471	5.3	10.2	8948913	2.4	11.0	-	-	-
Unidentified 10	11519071	5.2	5.6	14333226	3.8	10.2	-	-	-
Unidentified 11	13065763	5.9	8.6	11436293	3.0	10.9	-	-	-
Unidentified 12	7662815	3.4	10.6	14376827	3.8	10.6	-	-	-
Unidentified 13	-	-	-	9024703	2.4	9.0	-	-	-

MA: Mean Area; %MA: Percentage Mean Area; RSD: Relative Standard Deviation.

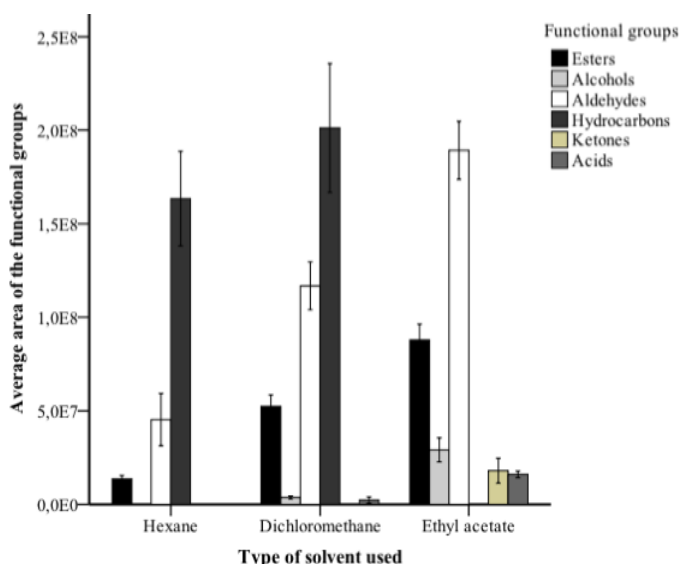


Figure 1. Lineweaver-Burk lines of the SiO_2 -immobilized pepsin catalyzed reaction at (22, 27, 32, 37, and 42 °C).

Furthermore, a higher area of esters, alcohols, and aldehydes was observed when increasing the polarity of the solvent. However, when hexane was used, neither alcohols nor ketones were extracted. The compounds of higher area extracted with ethyl acetate were furfural and benzeneacetaldehyde. Nonanal had the highest extraction with dichloromethane, followed by decanal, which was the compound with the highest mean area using hexane.

The ANOVA indicated statistical differences among the areas of the functional groups obtained with different extraction solvents ($P = 0.00$), whereas the Tukey multiple comparison test showed that esters (mean area: 8.7×10^7), alcohols (mean area: 3.7×10^7), aldehydes (mean area: 1.8×10^8), ketones (mean area: 1.8×10^7), and acids (mean area: 7.2×10^8) extracted with ethyl acetate belong to a different subset with means statistically higher than those obtained with dichloromethane and hexane. Besides, the hydrocarbons recovered with dichloromethane belong to a different subset of higher area (mean area: 2.0×10^8) in relation to the areas obtained using other solvents.

Volatile compounds from lulo pulp by HS-SPME/GC-MS

Total area

A number of 63 volatiles were obtained and 55 were identified, among them, 28.8% were esters and 23.1% were aldehydes. The identified metabolites had molecular weights ranging from 60 to 198 Da (C_3 to C_{12}). Moreover, by using the fiber CAR/PDMS, a larger number of compounds (42 at both temperatures) was obtained, whereas with the fiber of PDMS less than 15 compounds were recovered. The compounds with the highest abundance were (*Z*)-3-hexen-1-ol acetate, (*Z*)-3-hexen-1-ol, and (*E*)-2-hexenal (Table 2).

In order to establish differences among the areas of volatiles, the data normality of the total areas from different fibers was verified through Shapiro-Wilk test ($P = 0.243$), the homogeneity of variances via the Levene statistic ($P = 0.082$), and the absence of correlation among the residuals of the data by the Durbin-Watson test ($P = 0.141$). When performing the ANOVA from the total areas, an interaction between the type of fiber and the adsorption temperature ($P = 0.00$) was found. Using the fiber coated of CAR/PDMS, a higher total area of volatiles at 40 °C and 60 °C was obtained, as compared to those produced by PDMS/DVB and CAR/PDMS/DVB fibers; nevertheless, the last two mentioned fibers promoted higher total areas at 40 °C than at 60 °C, in contrast to the fiber coated with CAR/PDMS, which was more efficient at 60 °C.

Area of the functional groups

The ANOVA applied to the areas of the functional groups showed a significant interaction among the factors: type of fiber, adsorption temperature, and functional groups ($P = 0.00$). At 40 °C, the fiber made of CAR/PDMS had greater affinity than the other fibers for the extraction of alcohols (mean area: 1.3×10^8), esters (mean area: 1.3×10^8), and aldehydes (mean area: 8.7×10^7). The fiber coated of CAR/PDMS/DVB yielded the second highest level of extraction, having a higher area of alcohols (mean area: 6.6×10^7) and aldehydes (mean area: 5.0×10^7), and a lower area of esters (mean area: 1.0×10^8) as compared to the fiber coated with PDMS/DVB (Figure 2).

Moreover, the groups of ketones, hydrocarbons, and acids behaved similarly in terms of extraction using different fibers at 40 °C. The extraction at 60 °C also showed a better performance with the fiber made of CAR/PDMS for the alcohols extraction (mean area: 1.8×10^8), esters (mean area: 1.5×10^8), and aldehydes (mean area: 1.1×10^8). Finally, in both temperatures the fiber coated with PDMS showed the lowest extraction to the different functional groups.

Comparison between SDE/GC-MS and HS-SPME/GC-MS

A t-test to establish differences between the means of the functional groups obtained with the most efficient treatments of HS-SPME (CAR/PDMS) and SDE (ethyl acetate) was performed (Table 3).

Differences between the mean area ($P = 0.00$) of the functional groups acids, aldehydes, and ketones were found by SDE/GC-MS. For the areas of the esters, alcohols, and hydrocarbons, statistical differences were obtained, suggesting higher extraction by HS-SPME/GC-MS.

The current study constitutes not only the first comparative antecedent among SPME fibers to obtain volatile compounds from lulo, but it is also the first work in which SDE/GC-MS and HS-SPME/GC-MS are contrasted in this fruit. Regarding the HS-SPME method, the denoted differences are attributable to the polarity and molecular weight of the volatiles in each fruit. The fibers CAR/PDMS, PDMS/DVB, and DVB/CAR/PDMS have affinity for low molecular weight volatile (C_3 - C_{12}), polar and nonpolar, whereas the fiber coated of PDMS mainly promotes the recovery of nonpolar volatile compounds. In regard to the SDE method, the polarity of the solvent used influences the extraction of volatile compounds.

Table 2. Volatile compounds obtained by HS-SPME/GC-MS from lulo pulp with different fibers.

Compound Name	CAR/PDMS				DVB/CAR/PDMS				PDMS/DVB				PDMS										
	40 °C		60 °C		40 °C		60 °C		40 °C		60 °C		40 °C		60 °C								
	MA	RSD	MA	RSD	MA	RS D	MA	RS D	MA	RS D	MA	RS D	MA	RS D	MA	RS D							
Acetic acid methyl ester	14654011	9.3	8439839	5.7	2680994	11.5	1740335	9.3	370398	13.3	-	-	43164	11.6	32337	10.5							
2-Methyl propanal	113237	9.3	-	-	-	-	-	-	-	-	-	-	-	-	-	-							
Ethyl acetate	3483665	8.4	2213864	8.0	230605	12.2	147980	13.8	131318	11.9	-	-	-	-	-	-							
Methyl propionate	937759	9.7	565121	4.6	210817	12.1	-	-	-	-	-	-	-	-	-	-							
Unidentified 1	772475	7.6	1310856	12.0	974278	9.5	1354106	11.9	346396	10.6	1094440	11.7	-	-	-	-							
Acetic acid methylethyl ester	392981	9.1	162496	12.9	-	-	-	-	-	-	-	-	-	-	-	-							
Acetic acid	341335	12.5	284000	12.1	-	-	123695	12.3	-	-	-	-	-	-	-	-							
(E)-2-butenal	293031	5.4	-	-	191814	8.4	134018	11.1	-	-	-	-	-	-	-	-							
1-Penten-3-ol	1779914	11.1	1427206	5.6	247712	11.9	113388	12.1	177441	13.9	-	-	-	-	-	-							
1-Penten-3-one	418922	9.0	452101	11.6	124701	9.0	56551	7.5	-	-	-	-	-	-	-	-							
3-Pentanol	133130	15.0	-	-	-	-	-	-	-	-	-	-	-	-	-	-							
Pentanal	710511	6.7	552868	5.7	120465	4.6	-	-	-	-	-	-	-	-	-	-							
Butanoic acid methyl ester	4199820	12.8	3043884	3.4	614693	8.7	269839	11.0	494419	12.4	-	-	-	-	-	-							
Propanoic acid 2-methyl-2-propenyl ester	-	-	177414	11.3	-	-	-	-	-	-	-	-	15213	11.7	-	-							
Toluene	3300707	6.4	7328125	11.1	1440403	10.8	442537	10.2	861033	11.5	-	-	29644	8.2	-	-							
2-Butenoic acid methyl ester	1414531	8.0	1689797	13.7	688254	11.6	772184	7.6	123761	13.2	-	-	-	-	-	-							
Acetic acid 2-methylpropyl ester	472544	14.2	361165	8.6	148490	7.9	-	-	76260	13.7	-	-	-	-	-	-							
(E)-2-Pentenal	712128	9.2	904742	7.8	236984	12.0	291748	10.2	-	-	-	-	-	-	-	-							
(Z)-2-Penten-1-ol	1039871	12.6	1319366	5.9	182524	13.1	-	-	-	-	-	-	-	-	-	-							
2-Methyl-1-penten-1-one	538814	11.8	864111	7.0	345539	10.4	164207	10.5	156315	7.8	-	-	-	-	-	-							
Hexanal	8501900	7.5	9478684	5.0	3271647	14.6	1034491	5.4	1871099	10.7	917465	7.5	56450	7.9	31605	13.7							
o-Xylene	557634	12.7	-	-	-	-	-	-	-	-	-	-	-	-	-	-							
(E)-3-Hexen-1-ol	1397845	10.0	1759317	9.5	451444	13.2	278086	8.7	391627	13.6	206856	11.0	-	-	-	-							
(Z)-3-Hexen-1-ol	81002246	5.2	1096606	32	6.2	3861282	8	3.9	2737868	9.9	2924282	9	1801810	3	10.3	902630	8.1	780396	12.3				
1-Hexanol	45799929	6.7	6078846	0	8.2	2423138	5	9.7	1613536	2	1960528	5	9.3	1057032	4	10.8	639148	8.1	385630	8.5			
(E)-2-Hexenal	72391001	5.0	9668317	1	5.6	4273000	2	10.2	3214509	1	4.7	1652239	9	10.2	1134314	9	7.6	707404	14.3	610967	8.0		
(Z)-2-Penten-1-ol acetate	1557557	9.8	1912917	10.4	1147564	13.7	477474	9.2	1154536	8.6	319905	10.8	-	-	-	-	-	-	-	-			
Acetic acid pentyl ester	250300	13.4	291244	11.8	-	-	-	-	144714	11.3	-	-	-	-	-	-	-	-	-	-			
Unidentified 2	-	-	-	-	166055	11.3	-	-	-	-	-	-	-	-	-	-	-	-	-	-			
Unidentified 3	204190	9.3	279861	10.5	-	-	-	-	-	-	-	-	-	-	-	-	-	-	-	-			
Decane	297568	4.9	683908	11.9	177368	8.6	-	-	-	-	-	-	-	-	-	-	-	-	-	-			
(E,E)-2,4-Hexadienal	1582894	11.8	2378771	14.4	270957	7.9	478276	13.7	-	-	-	-	-	-	-	-	-	-	-	-			
1-Octen-3-ol	255063	8.7	-	-	281234	8.7	-	-	-	-	-	-	-	-	-	-	-	-	-	-			
1-Octen-3-one	430436	12.4	-	-	640250	14.1	302217	11.6	424617	7.6	395507	6.4	-	-	-	-	-	-	-	-			
(Z)-2-Heptenal	1642947	9.4	1494823	11.7	1474597	8.0	678900	12.7	1058918	11.2	-	-	-	-	-	-	-	-	-	-			
(Z)-3-Hexen-1-ol acetate	82733792	4.4	1068693	29	4.3	7890395	6	5.0	4172198	8	12.0	8734512	3	8.0	3603198	2	11.7	508506	4	8.5	187748	11.2	
Acetic acid hexyl ester	20892974	8.3	2726049	4	8.1	1793356	5	7.8	9846636	8.2	1852669	5	7.7	7677780	6.9	942637	10.1	236380	10.6	-	-		
Octanal	576087	12.4	418084	11.6	395528	12.0	192202	11.3	403631	10.4	137240	5.7	-	-	-	-	-	-	-	-	-		
Hexanoic acid 1-methylethyl ester	-	-	259301	9.0	-	-	-	-	-	-	-	75541	8.8	-	-	-	-	-	-	-	-		
3-Hydroxybutanal	-	-	-	-	110932	11.0	-	-	-	-	-	-	-	-	-	-	-	-	-	-	-		
Hexanoic acid	225356	9.1	869046	6.9	326937	12.7	629298	10.1	263959	10.8	630122	7.8	-	-	-	-	-	-	-	-	-		
2,2,6-Trimethylcyclohexanone	237697	11.6	321977	9.3	292571	15.5	208627	8.4	161823	11.0	174454	9.7	-	-	-	-	-	-	-	-	-		
(E)-3-hexenoic acid	289986	11.0	891388	6.6	386548	12.7	795329	8.6	329803	12.6	702755	7.8	-	-	-	-	-	-	-	-	-		
(E)-2-hexenoic acid	2200808	7.8	6883908	13.8	2018504	6.8	6218748	11.2	2121006	8.0	3199198	4.5	-	-	-	-	-	-	-	-	-		
Unidentified 4	-	-	-	-	-	-	-	-	-	-	-	-	-	-	-	-	43608	13.6	193210	13.4			
3,7-Dimethyl-1,6-octadien-3-ol	1146909	9.5	6150670	6.8	1905467	9.6	8028817	5.7	1560545	5.1	8345835	7.8	-	-	-	-	-	-	-	-	-		
Acetophenone	597398	6.7	532770	4.3	371239	8.9	431733	9.1	283239	10.3	480243	7.2	-	-	-	-	-	-	-	-	-		
Nonanal	588674	8.8	1258515	5.8	742400	12.0	861734	13.5	798200	11.7	1190221	8.6	-	-	-	-	-	-	-	-	-		
Undecane	310760	7.1	1317128	7.9	386640	11.8	369052	11.5	294210	9.3	1112521	13.3	-	-	-	-	-	-	-	-	-		
Hexanoic acid 2-methylpropyl ester	-	-	421035	11.5	391327	12.4	272051	11.1	351609	9.0	142626	12.6	-	-	-	-	-	-	-	-	-		
Butanoic acid (Z)-3-hexen-1-yl ester	-	-	279709	9.5	232273	8.9	227936	8.4	281197	9.3	301900	13.2	-	-	-	-	-	-	-	-	-		
5-Ethylidihydro-2 (3H)-furanone	-	-	-	-	-	-	114257	7.0	-	-	-	-	-	-	-	-	-	-	-	-	-		
1,7,7-trimethyl-bicyclo [2.1.1]-heptan-2-one	2480627	14.2	1260762	12.3	3274923	7.6	3065696	8.7	3224477	8.6	3854460	7.2	322760	10.1	131619	10.1	-	-	-	-	-	-	
Unidentified 5	-	-	-	-	395433	8.9	895256	9.9	369424	10.6	1034065	9.2	-	-	-	-	-	-	-	-	-	-	
3-Cyclohexene-1-methanol	-	-	1114660	11.0	-	-	1367938	10.6	-	-	1850328	13.0	-	-	-	-	-	-	-	-	-	-	
Decanal	280553	8.8	611634	12.7	312411	65.0	390081	7.4	-	-	1291819	8.8	-	-	-	-	-	-	-	-	-	-	
Octanoic acid	-	-	233713	9.6	-	-	226751	10.6	-	-	-	-	-	-	-	-	-	-	-	-	-	-	
Unidentified 6	265004	10.3	-	-	-	-	-	-	-	-	-	-	-	-	-	-	-	-	-	-	-	-	
2,6,6-Trimethyl-1-cyclohexen-1-carboxaldehyde	-	-	435940	6.1	339083	17.7	552066	8.9	308982	14.8	614935	13.7	-	-	-	-	-	-	-	-	-	-	
Unidentified 7	-	-	-	-	-	-	-	-	-	-	-	-	1506662	8.9	-	-	-	-	-	-	-	-	-
4-Heptanone	545535	7.1	1394436	9.7	687303	13.4	1774030	10.4	618478	10.3	2189027	8.2	140597	8.6	87399	8.6	-	-	-	-	-	-	-
Unidentified 8	-	-	254164	11.8	-	-	222611	9.6	310671	15.4	-	-	-	-</td									

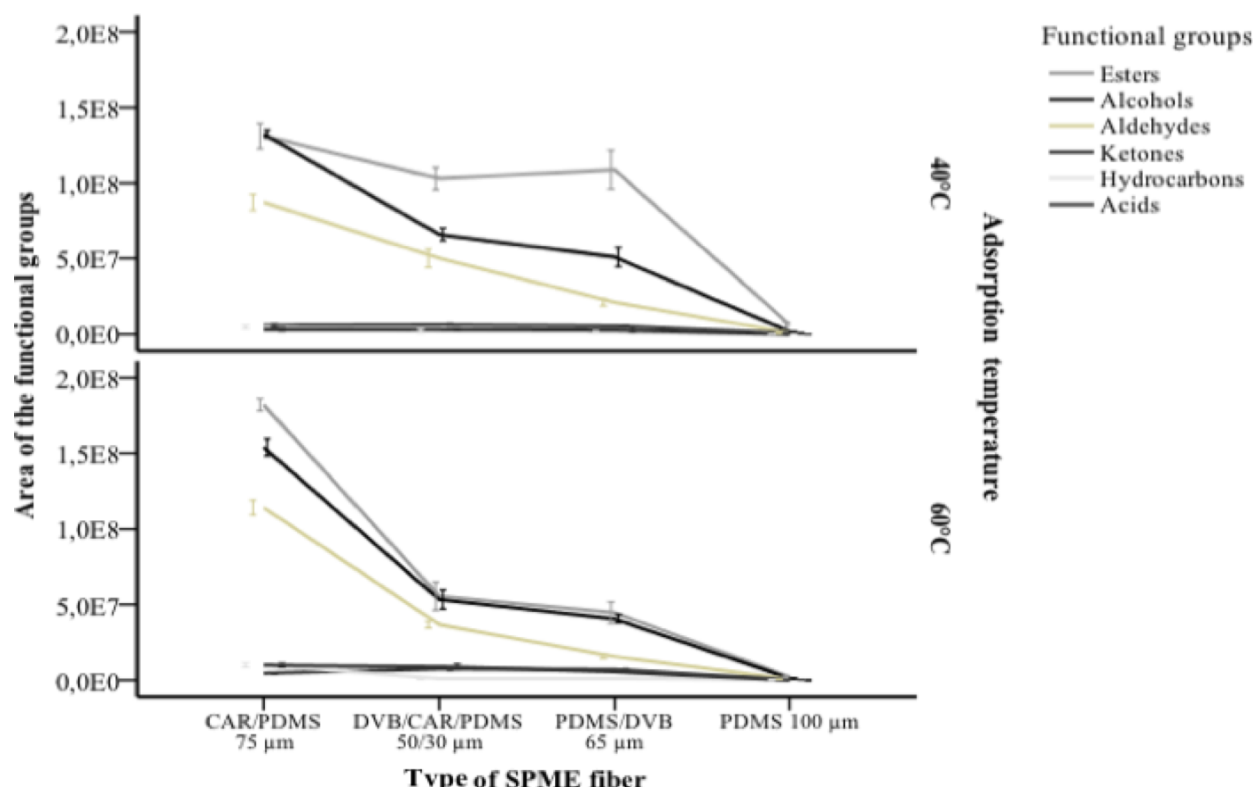


Figure 2. Areas of the functional groups from lulo pulp by GC/MS using different HS-SPME fibers and adsorption temperatures.

Table 3. T test of mean comparison for independent samples applied to the areas of functional groups obtained by HS-SPME/GC-MS and SDE/GC-MS.

		Levene test quality of variances		T test for equality of means						
				F	Sig.	t	gl	Sig. (bilateral)	Difference of means	Difference of standard error
										95% confidence interval of the difference
Esters	Equal variances are assumed	6.085	0.036	-24.46	9	0.000	-94264792	3852873	-1.030E8	-85548986
	Equal variances are not assumed			-26.32	6.76	0.000	-94264792	3581263	-1.028E8	-85737039
Alcohols	Equal variances are assumed	0.802	0.394	-37.75	9	0.000	-1.248E8	3306690	-1.323E8	-1.173E8
	Equal variances are not assumed			-38.81	8.94	0.000	-1.248E8	3216035	-1.321E8	-1.175E8
Aldehydes	Equal variances are assumed	4.946	0.053	10.93	9	0.000	74997733	6858963	59481680	90513785
	Equal variances are not assumed			11.93	5.80	0.000	74997733	6283756	59493714	90501751
Hydrocarbons	Equal variances are assumed	15.568	0.003	-21.75	9	0.000	-9863187	453486	-10889044	-8837330
	Equal variances are not assumed			-19.63	4.00	0.000	-9863187	502382	-11258024	-8468350
Ketones	Equal variances are assumed	14.901	0.004	4.65	9	0.001	13428672	2884563	6903336	19954008
	Equal variances are not assumed			5.14	5.02	0.004	13428672	2610189	6728241	20129103
Acids	Equal variances are assumed	11.228	0.009	33.74	9	0.000	710703624	21061589	663058998	758348250
	Equal variances are not assumed			37.30	5.00	0.000	710703624	19052916	661745002	759662247

Comparison between volatile compounds obtained by HS-SPME with other extraction methods

Considering that HS-SPME is a modern method, Table 4 shows the volatile compounds extracted by HS-SPME in the current study, which have previously been reported using other extraction methods from the lulo species *S. quitoense* (27, 28, 31, 32) and *S. vestissimum* (33). Fourteen out of the 28 volatile compounds previously reported belong to the esters and alcohols, for instance: acetic acid ethyl ester, 3-hexen-1-ol acetate, butanoic acid methyl ester, (E)-2-butenoic acid methyl ester, acetic acid, hexanal, (E)-2-hexenal, and (Z)-3-hexen-1-ol. On the contrary, some volatile compounds obtained by HS-SPME were not previously identified when analyzing the species of the fruit through the traditional methods such as: (Z)-2-penten-1-ol acetate, pentanal, acetic acid pentyl ester, butanoic acid (Z)-3-hexen-1-yl ester, 1-penten-3-one, 4-heptanone, and 6,7-dodecanodione. These compounds had lower areas than most of the other volatiles obtained from the same analysis, thus its difficulty of recovering using traditional methods, where there are higher losses compared to HS-SPME, could be related to the low sensitivity of these methods. As a matter of fact, the thermal degradation of these compounds during the conventional extraction should not be discarded.

Sensorial relevance of some of the compounds obtained

In regard to the HS-SPME method, there are referents on the extraction and analysis of odor active volatiles from dried lulo solids using the CAR/PDMS/DVB fiber. Among the compounds identified in the current study, hexanal, (E)-2-hexenal, and (Z)-3-hexen-1-ol were described as green odor volatiles. In addition, the compounds methyl butanoate, methyl hexanoate, and methyl benzoate had a fruity odor; whereas acetic acid, and benzoic acid were associated with descriptors of vinegar and rancid, respectively (31). The compounds (Z)-3-hexen-1-ol, hexyl acetate, and (Z)-3-hexenyl acetate have also been considered as relevant volatiles for curuba (*Passiflora mollissima* (Kunth) L. H. Bailey) (34), whereas hexanal showed a grassy flavor in pink Colombian guavas (*Psidium guajava* L.) (35).

Table 4. Volatile compounds obtained by HS-SPME/GC-MS that have previously been reported in lulo pulp using other different extraction methods.

Volatile compounds	<i>S. quitoense^a</i>		<i>S. quitoense^b</i>	<i>S. quitoense^c</i>	<i>S. quitoense^d</i>	<i>S. vestissimum^e</i>
	Colombia	Costa Rica				
Acetic acid methyl ester				+		
Acetic acid ethyl ester	+	+	+	+		+
Acetic acid hexyl ester	+	+	+			+
3-Hexen-1-ol acetate	+	+		+		+
Acetophenone	+	+				
Acetic acid	+	+	+		+	+
Hexanoic acid				+		
(E)-3-hexenoic acid	+	+				
(E)-2-hexenoic acid	+	+				
Octanoic acid			+			
Butanoic acid methyl ester				+	+	+
(E)-2-Butenoic acid methyl ester	+	+	+	+		+
Decane			+			+
3,7-dimethyl-1,6-octadien-3-ol						+
(E)-2-Hexenal			+	+	+	+
(E)-3-Hexen-1-ol	+	+				
(E,E)-2,4-hexadienal				+		
Hexanal	+	+		+	+	
1-Hexanol	+	+	+			
o-xylene						+
3-Pentanol	+	+				+
1-Penten-3-ol		+				
Methyl propionate						+
Toluene				+		+
Undecane			+			+
(Z)-3-Hexen-1-ol			+	+	+	+
(Z)-2-heptenal			+			
(Z)-2-penten-1-ol		+		+		

^a= Extraction with solvent, pentane/ether [2:1] (12). ^b= Extraction with supercritical CO₂ (13). ^c= Extraction with solvent, dichloromethane/ethyl ether [7:3] (31). ^d= SDE, with ethyl ether/pentane [1:1] (32). ^e= SDE, with pentane/diethyl ether [1:1] (33).

Conclusions

This study allowed to select the most efficient HS-SPME fiber for the extraction of volatile compounds for the first time in lulo pulp, as well as to compare the extracted volatiles with those recovered by a traditional method such as SDE. Among the tested solvents, ethyl acetate was the most appropriate solvent for the extraction using SDE/GC-MS; statistically higher areas for esters, alcohols, aldehydes, ketones, and acids were obtained. Also SPME fibers coated with CAR/PDMS promoted a higher efficiency in the extraction; with esters as were the main group of compounds. The differences between the mean areas of acids, aldehydes, and ketones by using SDE/GC-MS and the higher abundances of esters, alcohols, and hydrocarbons through HS-SPME/GC-MS indicated complementarity between these extraction methods. Finally, by using HS-SPME/GC-MS, the compounds (Z)-2-penten-1-ol acetate, pentanal, acetic acid pentyl ester, butanoic acid (Z)-3-hexen-1-yl ester, 1-penten-3-one, 4-heptanone, and 6,7-dodecanodione were obtained, which were not identified in previous studies by traditional extraction methods.

Acknowledgements

The researchers express their gratitude to the Administrative Department of Science, Technology and Innovation (Colciencias, Colombia) for their contribution in financing their study process (call for grant number 528-2011).

References

1. Pino, J.; Febles, Y. Odour-active compounds in banana fruit cv. Giant Cavendish. *Food Chem.* **2013**, *141*, 795–801. DOI: <http://dx.doi.org/10.1016/j.foodchem.2013.03.064>.
2. Chen, M.; Chen, X.; Wang, X.; Ci, Z.; Liu, X.; He, T. *et al.* Comparison of headspace solid-phase microextraction with simultaneous steam distillation extraction for the analysis of the volatile constituents in Chinese apricot. *Agric. Sci. China.* **2006**, *5*, 879–884. DOI: [http://dx.doi.org/10.1016/s1671-2927\(06\)60139-9](http://dx.doi.org/10.1016/s1671-2927(06)60139-9).
3. Arizala, M.; Monsalvo, A.; Betancourt, C.; Salazar, C.; Lagos, T. Evaluación de solanaceas silvestres como patrones de lulo (*Solanum quitoense* Lam.) y su reacción a *Fusarium* sp. *Rev. Cienc. Agric.* **2011**, *28*, 147–160.
4. Brunerie, P.; Maugeais, P. Comparison of volatile components in two naranjilla fruit (*Solanum quitoense* Lam.) pulp from different origin. *Dev. Food Sci.* **1992**, *29*, 163–174. DOI: <https://doi.org/10.1016/b978-0-444-88834-1.50019-3>.
5. Parada, F.; Guerrero, E.; Suárez, M.; Duque, C. Obtención de esencias de lulo (*Solanum quitoense* L.) utilizando CO₂ supercrítico. *Rev. Colomb. Quim.* **1993**, *22*, 53–62.
6. Suárez, M.; Duque, C.; Wintoch, H.; Schreier, P. Glycosidically bound aroma compounds from the pulp and the rind of lulo fruit (*Solanum vestissimum* D.). *J. Agr. Food Chem.* **1991**, *39*, 1643–1645. DOI: <https://doi.org/10.1021/jf00009a022>.
7. Mejía, C.; Gaviria, D.; Duque, A.; Rengifo, L.; Aguilar, E.; Alegría, A. Physicochemical characterization of the lulo (*Solanum quitoense* Lam.) castilla variety in six ripening stages. *Vitae* **2012**, *19*, 157–165.
8. Grant, S.; Golding, J.; McGlasson, W.; Williams, M. The relationship between ethylene and aroma volatiles production in ripening climacteric fruit. *Dev. Food Sci.* **1998**, *40*, 375–384. DOI: [https://doi.org/10.1016/s0167-4501\(98\)80061-7](https://doi.org/10.1016/s0167-4501(98)80061-7).
9. Márquez, C. Caracterización fisiológica, físico-química, reológica, nutracéutica, estructural y sensorial de la guanábana (*Annona muricata* L. cv. ELITA). Tesis de Doctorado, Universidad Nacional de Colombia, Medellín, Colombia, 2009.
10. Ceva-Antunes, P.; Ribeiro, H.; Carvalho, C.; Antunes, O. Analysis of volatile composition of siriguela (*Spondias purpurea* L.) by solid phase microextraction (SPME). *Food Sci. Technol.* **2006**, *39*, 437–443. DOI: <https://doi.org/10.1016/j.lwt.2005.02.007>.
11. Matich, A.; Young, H.; Allen, J.; Wang, M.; Fielder, S.; McNeilage, M. *et al.* *Actinidia arguta*: volatile compounds in fruit and flowers. *Phytochemistry.* **2003**, *63*, 285–301. DOI: [https://doi.org/10.1016/s0031-9422\(03\)00142-0](https://doi.org/10.1016/s0031-9422(03)00142-0).
12. Almora, K.; Pino, J.; Hernández, M.; Duarte, C.; González, J.; Roncal, E. Evaluation of volatiles from ripening papaya (*Carica papaya* L., var. Maradol roja). *Food Chem.* **2004**, *86*, 127–130. DOI: <https://doi.org/10.1016/j.foodchem.2003.09.039>.
13. Pino, J.; Cuevas-Glory, L.; Marbot, R.; Fuentes, V. Volatile compounds of grosella (*Phyllanthus acidus* [L.] Skeels) fruit. *Rev. CENIC, Cienc. Quim.* **2008**, *39*, 3–5.
14. Aurore, G.; Ginies, C.; Ganou-parfait, B.; Renard, C.; Fahrasmane, L. Comparative study of free and glycoconjugated volatile compounds of three banana cultivars from French West Indies: Cavendish, Frayssinette and Plantain. *Food Chem.* **2011**, *129*, 28–34. DOI: <https://doi.org/10.1016/j.foodchem.2011.01.104>.
15. Restrepo, P.; Duque, C. Componentes volátiles de la gulupa *Passiflora maliformis*. *Rev. Colomb. Quim.* **1988**, *17*, 57–63.
16. Min, S.; Zhang, Q. Effects of commercial-scale pulsed electric field processing on flavor and color of tomato juice. *J. Food Sci.* **2003**, *68*, 1600–1606. DOI: <http://dx.doi.org/10.1111/j.1365-2621.2003.tb12298.x>.
17. Qin, G.; Tao, S.; Cao, Y.; Wu, J.; Zhang, H.; Huang, W. *et al.* Evaluation of the volatile profile of 33 *Pyrus ussuriensis* cultivars by HS-SPME with GC-MS. *Food Chem.* **2012**, *134*, 2367–2382. DOI: <http://dx.doi.org/10.1016/j.foodchem.2012.04.053>.
18. Yang, D.; Balandrán-Quintana, R.; Ruiz, C.; Toledo, R.; Kays, S. Effect of hyperbaric, controlled atmosphere, and UV treatments on peach volatiles. *Postharvest Biol. Technol.* **2007**, *51*, 334–341. DOI: <http://dx.doi.org/10.1016/j.postharvbio.2008.09.005>.
19. Cai, J.; Liu, B.; & Su, Q. Comparison of simultaneous distillation extraction and solid-phase microextraction for the determination of volatile flavor components. *J. Chromatogr. A.* **2001**, *930*, 1–7. DOI: [http://dx.doi.org/10.1016/s0021-9673\(01\)01187-6](http://dx.doi.org/10.1016/s0021-9673(01)01187-6).
20. Pino, J. Odour-active compounds in papaya fruit cv. Red Maradol. *Food Chem.* **2014**, *146*, 120–126. DOI: <http://dx.doi.org/10.1016/j.foodchem.2013.09.031>.
21. Soler, S.; De Oliveira, W.; Ré-Poppi, N.; Simionatto, E.; Carasek, E. Volatile compounds of leaves and fruits of *Mangifera indica* var. *coquinho* (Anacardiaceae) obtained using solid phase microextraction and hydrodistillation. *Food Chem.* **2011**, *127*, 689–693. DOI: <http://dx.doi.org/10.1016/j.foodchem.2010.12.123>.
22. Nunes, C.; Coimbra, M.; Saraiva, J.; Rocha, S. Study of the volatile components of a candied plum and estimation of their contribution to the aroma. *Food Chem.* **2008**, *111*, 897–905. DOI: <http://dx.doi.org/10.1016/j.foodchem.2008.05.003>.
23. Cheong, M.; Liu, S.; Zhou, W.; Curran, P.; Yu, B. Chemical composition and sensory profile of pomelo (*Citrus grandis* (L.) Osbeck) juice. *Food Chem.* **2012**, *135*, 2505–2513. DOI: <http://dx.doi.org/10.1016/j.foodchem.2012.07.012>.
24. Santos, T.; Nogueira, P. Volatile components of mangaba fruit (*Hancornia speciosa* Gomes) at three stages of maturity. *Food Chem.* **2006**, *95*, 606–610. DOI: <https://doi.org/10.1016/j.foodchem.2005.01.038>.
25. Pontes, M.; Marques, J.; Câmara, J. Headspace solid-phase microextraction-gas chromatography-quadrupole mass spectrometric methodology for the establishment of the volatile composition of *Passiflora* fruit species. *Microchem. J.* **2009**, *93*, 1–11. DOI: <https://doi.org/10.1016/j.microc.2009.03.010>.
26. Diniz, F.; Pereira, T.; Maio, M.; Monteiro, A. Volatile and non-volatile chemical composition of the white guava fruit (*Psidium guajava*) at different stages of maturity. *Food Chem.* **2007**, *100*, 15–21. DOI: <https://doi.org/10.1016/j.foodchem.2005.07.061>.
27. Pandit, S.; Chidley, H.; Kulkarni, R.; Pujari, K.; Giri, A.; Gupta, V. Cultivar relationships in mango based on fruit volatile profiles. *Food Chem.* **2009**, *114*, 363–372. DOI: <https://doi.org/10.1016/j.foodchem.2008.09.107>.
28. El Arem, A.; Flaminii, G.; Saafi, E.; Issaoui, M.; Zayene, N.; Ferchichi, A. *et al.* Chemical and aroma volatile compositions of date palm (*Phoenix dactylifera* L.) fruits at three maturation stages. *Food Chem.* **2011**, *127*, 1744–1754. DOI: <https://doi.org/10.1016/j.foodchem.2011.02.051>.

29. Dharmawan, J.; Barlow, P.; Curran, P. Characterisation of volatile compounds in selected citrus fruits from Asia. *Dev. Food Sci.* **2006**, *43*, 319-322. DOI: [https://doi.org/10.1016/s0167-4501\(06\)80076-2](https://doi.org/10.1016/s0167-4501(06)80076-2).
30. Meret, M.; Brat, P.; Mertz, C.; Lebrun, M.; Gü nata, Z. Contribution to aroma potential of Andean blackberry (*Rubus glaucus* Benth.). *Food Res. Int.* **2011**, *44*, 54–60. DOI: <https://doi.org/10.1016/j.foodres.2010.11.016>.
31. Forero, D.; Orrego, C.; Grant, D.; Osorio, C. Chemical and sensory comparison of fresh and dried lulo (*Solanum quitoense* Lam.) fruit aroma. *Food Chem.* **2015**, *169*, 85-91. DOI: <https://doi.org/10.1016/j.foodchem.2014.07.111>.
32. Suárez, M.; Duque, C. Volatile constituents of lulo (*Solanum vestissimum* D.) fruit. *J. Agr. Food Chem.* **1991**, *39*, 1498-1500. DOI: <https://doi.org/10.1021/jf00008a026>.
33. Mora, R.; Pinzón, M. Principales constituyentes volátiles del aroma de lulo “La Selva” durante la maduración. V Seminario Nacional e Internacional de Frutales. Manizales, **2004**, 261-267.
34. Conde-Martínez, N.; Sinuco, D.; Osorio, C. Chemical studies on curuba (*Passiflora mollissima* (Kunth) L. H. Bailey) fruit flavour. *Food Chem.* **2014**, *157*, 356-363. DOI: <https://doi.org/10.1016/j.foodchem.2014.02.056>.
35. Steinhäus, M.; Sinuco, D.; Polster, J.; Osorio, C.; Schieberle, P. Characterization of the key aroma compounds in pink guava (*Psidium guajava* L.) by means of aroma re-engineering experiments and omission tests. *J. Agric. Food Chem.* **2009**, *57*, 2882-2888. DOI: <https://doi.org/10.1021/jf803728n>.

Article citation:

Corpas, E. J.; Taborda, G.; Tapasco, O. A.; Ortiz, A. Comparison between extraction methods to obtain volatiles from lulo (*Solanum quitoense*) pulp. *Rev. Colomb. Quim.* **2016**, *45* (3), 12-21. DOI: <http://dx.doi.org/10.15446/rev.colomb.quim.v45n3.61359>.

Oman Zuas^{1*}, Muhammad R. Mulyana¹, Harry Budiman¹



¹Gas Analysis Laboratory, Metrology in Chemistry Research Group, Research Centre for Metrology, Indonesian Institute of Sciences (Pusat Penelitian Metrologi-LIPI), Building 456, Kawasan PUSPIPTEK Serpong 15314, Tangerang, Banten, Indonesia.

*Corresponding author: oman.zuas@lipi.go.id

Recibido: 14 de Julio de 2016. Aceptado: 23 de Agosto de 2016.

Analytical method validation of GC-FID for the simultaneous measurement of hydrocarbons (C₂-C₄) in their gas mixture

Abstract

An accurate gas chromatography coupled to a flame ionization detector (GC-FID) method was validated for the simultaneous analysis of light hydrocarbons (C₂-C₄) in their gas mixture. The validation parameters were evaluated based on the ISO/IEC 17025 definition including method selectivity, repeatability, accuracy, linearity, limit of detection (LOD), limit of quantitation (LOQ), and ruggedness. Under the optimum analytical conditions, the analysis of a gas mixture revealed that each target component was well-separated with high selectivity property. The method was also found to be precise and accurate. The method linearity was found to be high with good correlation coefficient values ($R^2 \geq 0.999$) for all target components. It can be concluded that the GC-FID developed method is reliable and suitable for determination of light C₂-C₄ hydrocarbons in their gas mixture. The validated method was successfully applied to the estimation of light C₂-C₄ hydrocarbons in natural gas samples, showing high performance repeatability with relative standard deviation (RSD) less than 1.0% and good selectivity with no interference from other possible components.

Keywords: method validation, hydrocarbons, GC-FID, ISO/IEC 17025.

Validación de un método analítico GC-FID para la medida simultánea de hidrocarburos (C₂-C₄) en una mezcla gaseosa

Resumen

Se validó una cromatografía de gases precisa, acoplada con un detector de ionización de llama (GC-FID) para el análisis simultáneo de hidrocarburos ligeros (C₂-C₄) en su mezcla gaseosa. Los parámetros de validación se evaluaron con base en la definición de la ISO/IEC 17025, que incluye selectividad del método, precisión y repetibilidad, exactitud, linealidad, límite de detección (LOD), límite de cuantificación (LOQ) y robustez. Bajo las condiciones analíticas óptimas, el análisis de la mezcla gaseosa mostró que cada analito de interés fue separado adecuadamente con alta selectividad. Se encontró también que el método fue preciso y exacto; la linealidad fue alta y con buen coeficiente de correlación lineal ($R^2 \geq 0.999$) para todos los analitos. Se puede concluir que el método GC-FID es confiable y apropiado para la determinación de hidrocarburos ligeros C₂-C₄ en una mezcla gaseosa. El método validado ha sido exitosamente aplicado a la valoración de hidrocarburos ligeros C₂-C₄ en muestras de gas natural, mostrando alta repetibilidad con desviación estándar relativa (RDS) menor al 1% y buena selectividad sin interferencias de otros posibles componentes.

Palabras clave: validación de método analítico, hidrocarburos, GC-FID, ISO/IEC 17025.

Validação de uma metodologia analítica GC-FID para a medida simultânea de hidrocarbonetos (C₂-C₄) em uma mistura gasosa

Resumo

Foi avaliada uma cromatografia gasosa precisa, equipada com um detector de ionização de chama (CG-FID) para a análise simultânea de hidrocarbonetos ligeiros (C₂-C₄) em uma mistura gasosa. Os parâmetros de validação foram avaliados baseados na definição da ISO/IEC 17025, que incluiu seletividade do método, precisão e repetibilidade, exatidão, linearidade, limite de detecção (LOD), limite de quantificação (LOQ) e robustez. Baixo as condições analíticas ótimas, a análise da mistura gasosa mostrou que cada analito foi separado adequadamente com alta seletividade. Também foi encontrado que o método foi preciso e exato; a linearidade foi alta e com bom coeficiente de correlação linear ($R^2 \geq 0.999$) para todos os analitos. Pode-se concluir que o método GC-FID é confiável e apropriado para a determinação de hidrocarbonetos ligeiros C₂-C₄ em uma mistura gasosa. O método avaliado tem sido exitosamente aplicado à valoração de hidrocarbonetos ligeiros C₂-C₄ em amostras de gás natural mostrando alta repetibilidade com desvio-padrão relativo menor funcional. ao 1% e boa seletividade sem interferências de outros possíveis componentes.

Palavras-Chave: validação do método analítico, hidrocarbonetos, CG-FID, ISO/IEC 17025.

Introduction

Non-methane hydrocarbons (NMHCs in short) are typically low molecular weight (C_1 - C_{10}) species in the hydrocarbon chain. The NMHCs have become important in industry and environment. In chemical industries, some natural sources of NMHCs (such as methane, propane, and butane) have more popular feedstock and their trading supply are highly demanded (1). Furthermore, NMHCs, generated by anthropogenic activities, (fuel and biomass burning, vehicles, solvent usage, and oil refineries) have been detected in the atmosphere and they have grown environmental and public health concern (2, 3). Regardless of their importance, it is necessary to reassess measurement practice in order to provide accurate and reliable data of the NMHCs concentration. This necessity is related to the fact that accurate and reliable data are used as the basis for decision making related to both for market price in industrial purpose and regulatory enforcement for the environmental monitoring program.

According to ISO/IEC 17025, a reliable and accurate result can only be obtained by using a validated method. In any testing laboratory, method validation is a part of quality assurances to declare that a high quality of analytical result is provided (4). In general, method validation refers to a documented procedure used by a laboratory to assure that the method performance for the determination of a particular analyte meets the required criteria (5-7). This paper presents results on the validation of a GC-FID method for the measurement of five components of light hydrocarbons (C_2 - C_4) including ethylene, propane, propylene, isobutane, and n-butane in their gas mixture. The evaluation was based on the ISO/IEC 17025 definition (8, 9) and it was emphasized on the following validation parameters: method selectivity, repeatability, accuracy, linearity, limit of detection (LOD), limit of quantification (LOQ), and ruggedness. The validated method was successfully employed in the assay of light C_2 - C_4 hydrocarbons in natural gas samples.

Materials and methods

Materials

Certified gas standards for C_2 - C_4 hydrocarbon mixture (GS-1 in short) were purchased from Mesa Specialty Gases and Equipment (CA, USA). A series of GS-1 (denoted as GS-1a to GS-1d), having concentration as listed in Table 1, was used as test standard in all experimental runs. Another GS (denoted as GS-2) was only used for method accuracy assessment. Both certified GS-1 and GS-2 with relative uncertainty $\pm 2\%$ are traceable to National Institute of Standards and Technology (NIST), USA.

Instrumentation

Separation of C_2 - C_4 hydrocarbons from their mixture was performed on a packed-column (Coated GC Packing 23% SP-1700, 80/100 Chromosorb PAW, 30 ft x 1/8 inch SS from Supelco) installed on a GC system Model 6890 (Hewlett Packard Agilent, CA, USA), equipped with a flame ionization detector (FID). The optimized analytical conditions for the GC-FID method are tabulated (Table 2).

Table 1. Typical concentration (%mol/mol) of C_2 - C_4 hydrocarbon in N_2 matrix.

Gas components	Certified Gas Standard (GS)				
	GS-1				GS-2
	GS-1a	GS-1b	GS-1c	GS-1d	
Ethylene	0.38	0.48	0.59	1.00	0.49
Propane	3.05	3.8	4.65	8.05	3.88
Propylene	13.11	16.6	20.64	37.04	16.97
Isobutane	5.42	6.78	8.36	14.97	6.93
n-butane	1.56	1.95	2.39	3.97	1.99
Nitrogen	matrix	matrix	matrix	matrix	matrix

Table 2. Optimized analytical conditions of the GC-FID.

Apparatus	Agilent 6890 GC System
Sample loop	2 mL, stainless steel
Valve box temperature	100 °C
Oven/Column temperature	55 °C
Running time	60 min
Gas carrier	Helium ultra-high purity grade (99.999%)
Carrier gas flow rate	207 kPa (7.0 mL/min)
Detector temperature:	165 °C
H ₂ flow	40 mL/min
Air flow	400 mL/min

Gas chromatography analysis

A certain volume of gas standard was injected into a GC system under optimized analytical conditions (Table 2). The output signal was monitored using GC ChemStation version Rev. A.10.02 (1757), which was installed on a LG personal computer (Processor AMD Richland A4-7300-HD 8470D, LG International Corp.). The data was estimated by automated integration of the area under the resolved chromatographic profile.

Procedure for method validation

All data obtained from the GC-FID measurement were used for the method validation. The assessment parameters (selectivity, repeatability, linearity, LOD, LOQ, and ruggedness) were calculated by adopting some procedures, as they can be found everywhere in published literature (4, 5, 10-16). In a typical experiment, the calculation procedure is described as follows: selectivity of the method was determined by injecting the gas standard (GS-1) and it was evaluated in term of retention time (t_R) and selectivity factor (α); repeatability was established by measuring the response of the GS-1 standard and expressed as percentage relative standard deviation (% RSD) of seven replications injection under the same operating condition over a short time interval (in the same day); accuracy was evaluated by comparing the concentration of GS-1 standard against another independent gas standard (GS-2).

Furthermore, to investigate the linearity, a series of GS-1 standard (GS-1a to GS-1d as listed in Table 1) was used. The injection of each gas standard was conducted in seven replications and then the linearity was estimated from the calibration curve. The calibration curve was constructed by plotting peak area of each component in the GS-1 standard (GS-1a to GS-1d) as a function of their concentration. The LOD and LOQ were established at a signal-to-noise ratio (S/N) of 3 and 10, respectively, of the chromatogram at the lowest concentration point of each component. Ruggedness was evaluated by small changing in flow rate of carrier gas during analysis (from 6.5 to 7.5 mL/min with 0.5 mL/min flow rate different as listed in Table 7).

Selectivity, repeatability, accuracy, linearity, LOD and LOQ, and ruggedness were defined as follows:

Selectivity

The selectivity refers to the capability of GC method to discriminate and quantify the response of target component in the presence of other components as interference (5, 10). The selectivity is the relative retention of two adjacent peaks; hence, it is highly dependent on the change of the t_R values of the two corresponding target gas components.

Repeatability

The repeatability precision of method refers to the closeness between measured values resulting from an independent measurement using the same equipment, under the same analytical condition, by the same operator and within short intervals of time (5, 10). Theoretically, the determination of the repeatability was conducted by the prediction of relative standard deviation (%RSD) of precision using Horwitz function [1] (14):

$$CV - \text{Horwitz} (\%) = 2^{(1-0.5\log c)} \quad [1]$$

where C is the concentration of gas component stated in decimal fraction. The requirement of %RSD for repeatability is between 0.5 and 0.75 of a theoretical value determined by Horwitz function. In a word, the repeatability of the method is categorized acceptable when the %RSD is less than 0.67 of the %CV- Horwitz (0.67CV-Horwitz) (7).

Accuracy

Method accuracy refers to the closeness of agreement between measured and accepted (true) concentration of target component. The accuracy value is dependent on two factors i.e., the bias and precision. The bias of a method is the difference between the measured value and the value from certificate of reference standard, which was calculated using an expression below [2] (4, 6, 7):

$$C\Delta = \bar{X} - Y \quad [2]$$

where \bar{X} is the average of measured reference standard value, and Y is value from certificate of reference standard. For assessing the method accuracy, precision of an analytical method (σ) from repeatability and reproducibility is included. In addition, the uncertainty value from certificate of reference standard is also included for estimating the σ value. Thus, the value of σ is obtained by combining those three components by using the following expression [3] (6, 7):

$$\sigma = \sqrt{S_b^2 + \frac{S_w^2}{n} + \mu_{RM}^2} \quad [3]$$

where S_b is the standard deviation from reproducibility (inter day precision); S_w is the standard deviation from repeatability (intra day precision), and μ_{RM} is the uncertainty of standard GS-2 as stated in the certificate. The acceptance criteria is set according to the ISO Guide 33:2000 (15). In such ISO Guide, no bias is found if the observed bias ($C\Delta$) value falls within $\pm 2\sigma$ at confidence level 95% [4]:

$$-2\sigma < C\Delta < 2\sigma \quad [4]$$

Linearity

Method linearity is defined as the ability of the method to demonstrate that the test results are proportional to the concentration of sample (5, 7, 10). Investigation of method linearity for C₂-C₄ measurement was conducted by generating a calibration curve using different concentration levels of C₂-C₄ gas standards. Each concentration level was analyzed using GC-FID in six replications (n = 6).

LOD and LOQ

LOD of an analytical method refers to the lowest amount of analyte that can be detected which is not necessarily quantified as an exact value. Meanwhile, LOQ is the lowest concentration of an analyte that can be quantitatively determined with appropriate precision (5, 10). In a GC measurement, both LOD and LOQ are important. The LOD and LOQ were calculated based on signal to noise ratio, which are 3:1 and 10:1, respectively.

Ruggedness

The ruggedness of an analytical method is the method capacity to generate some results which remains unaffected by minor changes of the experimental conditions during analysis (5, 10). In this study, the ruggedness of the method was assessed by investigating the effect of small change on the flow rate of the carrier gas used as the mobile phase for gas component separation in the column of GC-FID system.

Assay of hydrocarbon in natural gas samples

Two natural gas samples were obtained commercially from Indonesian State Oil and Natural Gas Mining Company (PERTAMINA) located in North of Jakarta. The natural gas samples were analyzed by the validated method without any special treatment.

Results and discussion

Practically, in every method validation process for a GC technique, performing development of the method is the initial step, which can be carried out by optimizing the conditions of the GC for the measurement of the target component. Figure 1 depicts a typical chromatogram of C_2 - C_4 gas component obtained under optimum analytical conditions of the GC-FID instrument (Table 2). As can be seen from Figure 1, all gas components were well separated with their retention times (t_R) as listed in Table 3. No other interference peaks could be found, indicating that the development of the GC method was achieved successfully (12). Thus, the method validation process could be conducted.

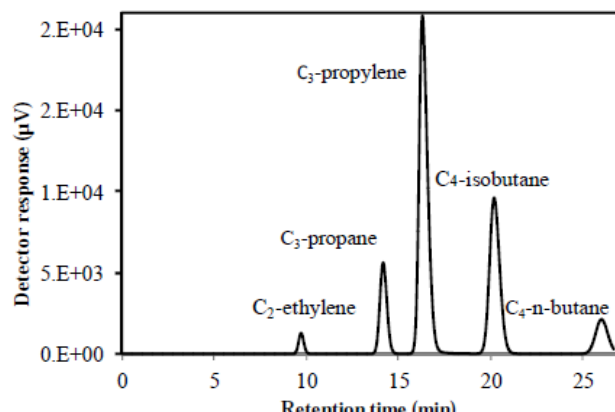


Figure 1. A typical chromatogram of C_2 - C_4 under optimized analytical conditions, showing a good separation property.

Selectivity

As discussed above, no interfering peak of one gas component relative to others could be observed (Figure 1), resulting in excellent selectivity factor (α) (Table 3) with α values larger than 1.0 (13).

Repeatability

From the calculation result, the % of CV- Horwitz for each individual gas component as found to be less than 0.67 CV-Horwitz as listed in Table 4, indicating that the method is repeatable.

Table 3. Retention time and selectivity factor.

Hydrocarbon components (C_2 - C_4)	Parameter	
	Retention time (t_R , min)	Selectivity factor (α)
C_2 -Ethylene	9.71	
		2.55
C_3 -Propane	14.14	
		1.29
C_3 -Propylene	16.22	
		1.42
C_4 -Isobutane	20.14	
		1.44
C_4 -n-Butane	25.96	

Table 4. %RSD and CV-Horwitz.

Gas Component	Concentration (% mol/mol)	Repeatability %RSD (n=6)	CV-Horwitz	0.67 x CV-Horwitz
C_2 -Ethylene	0.49	0.13	4.45	2.98
C_3 -Propane	3.88	0.13	3.26	2.19
C_3 -Propylene	16.97	0.14	2.61	1.75
C_4 -Isobutane	6.93	0.13	2.99	2.00
C_4 -n-butane	1.99	0.14	3.61	2.42

Accuracy

From the Table 5, it can be observed that the measured values of all C_2 - C_4 hydrocarbons fall within $\pm 2\sigma$; thus, it can be concluded that no evidence of bias can be found in the analytical method used under this study.

Table 5. Accuracy data of the GC-FID for the measurement of C_2 - C_4 in their mixture.

Parameters	Ethylene	Propane	Propylene	Isobutane	n-butane
Bias (% mol/mol)	-0.002	-0.020	-0.098	-0.039	-0.014
Precision of method, σ (% mol/mol)	0.010	0.015	0.058	0.024	0.013
$\pm 2\sigma$ (% mol/mol)	0.019	0.030	0.117	0.048	0.026

Linearity

The linearity data of the method are listed in Table 6. As it can be seen from Table 6, excellent linearity was obtained for all gas components with correlation coefficient values (R^2) equal or greater than 0.999. Thus, the method may fit for purpose for the determination of C₂-C₄ gas in their mixture.

Table 6. Data indicating linearity of the method for all gas component and their LOD and LOQ values (n = 6).

Gas component	Slope	Intercept	Linear range (% mol/mol)	R^2	LOD ($\mu\text{mol/mol}$)	LOQ ($\mu\text{mol/mol}$)
Ethylene	5.77E+04	4231.30	0.38-1.00	0.999	270	910
Propane	4.43E+04	21468.00	3.05-8.05	1.000	500	1660
Propylene	4.55E+04	103553.00	13.11-37.04	0.999	770	2560
Isobutane	6.17E+04	48379.00	5.42-14.97	1.000	520	1720
N-Butane	5.89E+04	11574.00	1.56-3.97	1.000	450	1490

LOD and LOQ

For any quantification process producing a value below the LOD and LOQ level may lead to yield in a high measurement uncertainty; thus an unreliable measurement would occur. In addition, practically, the LOD and LOQ assessment are equally important in comparison to other method validation parameters. At a LOD level, only qualitative analysis is possible to be evaluated, while at a LOQ level, both quantitative and qualitative analysis are possible. However, at the LOQ level, the quantitative analysis performed may produce inaccuracy and imprecise result, leading to a high uncertainty contribution on the final analytical results (4). Table 6 tabulates the LOD and LOQ values for all gas components. As it can be seen in Table 6, the lowest LOD value was found to be 270 $\mu\text{mol/mol}$ for ethylene, and the highest LOD values was found to be 770 $\mu\text{mol/mol}$ for propylene. Correspondingly, the LOQ of ethylene (910 $\mu\text{mol/mol}$) and propylene (2560 $\mu\text{mol/mol}$) were found to have the same trend as the lowest and the highest LOQ value, respectively.

This is a reasonably accepted finding because the concentration of ethylene (0.38 % mol/mol) and propylene (13.11 % mol/mol), as the lowest and the highest concentration among all other components (Table 6), respectively, were used as the basis for calculating the LOD/LOQ. Since the value of LOD/LOQ obtained from an analytical measurement is generally concentration dependent; therefore, the value of LOD/LOQ could be decreased by decreasing the concentration of the component used for LOD/LOQ calculation.

Ruggedness

As can be seen in Table 7, in all flow rate levels, both retention time and percentage peak area were found to be within acceptable limit with very low standard deviation (SD). Thus, small changes on the GC-FID experimental conditions in term of flow rate variation did not have any effect on the results of analytical measurement. Although, a massive change on the flow rate level of carrier gas has been reported to significantly affect the results of a GC measurement (16).

Assay of natural gas samples

The validated method was applied for the analysis of light hydrocarbons (C₂-C₄) in two natural gas samples. The primary analysis results indicated that the concentration of the target components (C₂-C₄) in the natural gas sample was higher than the linear concentration range of the standard gas mixture (Table 6). This implies that a dilution step is required. Therefore, the natural gas samples were then properly diluted by using ultra high pure helium (99.999% purity) with a dilution factor of 6, and the final concentration is shown in Table 8. It can be seen from Table 8 that all the target components (C₂-C₄) in the natural gas samples were detected and found at high concentration, except for propylene. Propylene may also exist in the natural gas sample but it cannot be detected by the GC-FID system under the experimental condition of this study. In addition, Figure 2 displays a typical chromatogram of a natural gas sample after the analysis using the validated method. Chromatogram in Figure 2 indicates that the method was selective for the analysis of C₂-C₄, and no interference from other components could be observed.

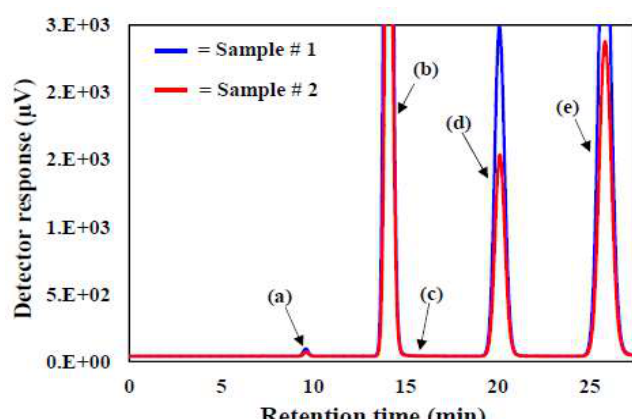
Table 7. Results of the ruggedness study.

Carrier gas flow rate (mL/min)	Level	Ethylene		Propane		Propylene		Isobutane		n-butane	
		t _R (min)	Peak area (%)								
6.5	-0.5	9.888	1.882	14.452	11.456	16.694	50.843	20.586	28.24	26.459	7.603
7	0	9.736	1.882	14.232	11.452	16.438	50.821	20.27	28.239	26.054	7.601
7.5	0.5	9.472	1.883	13.887	11.46	16.054	50.815	19.816	28.227	25.494	7.596
Mean		6.699	1.822 ±	14.190	11.546	16.395	50.826	20.224 ±	28.235	26.002	7.600
± SD		± 0.21	0.001	± 0.29	± 0.01	± 0.32	± 0.02	0.39	± 0.01	± 0.49	± 0.01

Note: The GS-2 was used for producing the data with concentration as listed in Table 1.

Table 8. The final concentration (% mol/mol) of C_2 - C_4 in natural gas samples

Sample #	Ethylene	Propane	Propylene	Isobutane	n-butane
1	0.033 ^a (0.03) ^b	23.236 ^a (0.42) ^b	ND	4.947 ^a (0.12) ^b	17.997 ^a (0.09) ^b
2	0.049 ^a (0.01) ^b	14.210 ^a (0.11) ^b	ND	0.591 ^a (0.72) ^b	9.516 ^a (0.09) ^b

^an = 3 (triplicate) and ^b%RSD.**Figure 2.** Chromatogram of natural gas samples analyzed using the developed and validated method, showing the presence of C_2 - C_4 gas components: (a) ethylene, (b) propane, (c) propylene, (d) isobutane, and (e) n-butane

Conclusions

In this study, the developed GC-FID method for the analysis of the C_2 - C_4 hydrocarbons (including ethylene, propane, propylene, isobutane, and n-butane) provides good selectivity toward separation of individual gas components from their mixture. Moreover, the results of each validation parameter, based on the ISO/IEC 17025, indicated that the validated method provides a sufficient evidence for proving a reliable GC-FID method for the measurement of C_2 - C_4 hydrocarbon in their gas mixture. The developed and validated method could also be extended to the analysis of real natural gas samples. Hence, the use of such validated method may keep the degree of user confidence regarding their analytical data.

Acknowledgement

The authors gratefully acknowledged the Indonesian Government for financially supporting this study within the scope of LIPI's project "Strengthening Chemical Metrology Competency and Infrastructure" under Project No. SP.DIPA-079.01.2.664833/2016. The authors are also very much thankful to anonymous reviewers for their valuable comments, which helped the authors to improve the manuscript.

References

- Zyryanova, M.M.; Badmaev, S.D.; Belyaev, V.D.; Amosov, Y.I.; Snitnikov, P.V.; Kirillov, V.A. et al. Catalytic reforming of hydrocarbon feedstocks into fuel for power generation units. *Catal. Ind.* **2013**, *5*, 312-317. DOI: <http://dx.doi.org/10.1134/S2070050413040107>.
- Williams, J. Organic trace gases: an overview. *Environ. Chem.* **2014**, *1*, 125-136. DOI: <http://dx.doi.org/10.1071/EN04057>.
- Thompson, C.R.; Hueber, J.; Helming, D. Influence of oil and gas emissions on ambient atmospheric non-methane hydrocarbons in residential areas of Northeastern Colorado. *Elem. Sci. Anth.* **2014**, *2*, 000035. DOI: <http://dx.doi.org/10.12952/journal.elementa.000035>.
- Budiman, H.; Zuas, O. Validation of analytical method for determination of high level carbon dioxide (CO_2) in nitrogen gas (N_2) matrix using gas chromatography thermal conductivity detector. *Periódico Tchê Química.* **2015**, *12*, 7-16.
- European Guide: The Fitness for Purpose of Analytical Methods A Laboratory Guide to Method Validation and Related Topics. 1998. Available at <https://www.eurachem.org/>.
- Taverniers, I.; Loose, M.D.; Van Bockstaele, E. Trends in quality in the analytical laboratory, II: Analytical method validation and quality assurance. *Trac-Trend Anal. Chem.* **2004**, *23*, 535-552. DOI: <http://dx.doi.org/10.1016/j.trac.2004.04.001>.
- Taverniers, I.; Van Bockstaele, E.; Loose, M.D. Trends in quality in the analytical laboratory. I. Traceability and measurement uncertainty of analytical results. *Trends in Anal. Chem.* **2004**, *23*, 480-490. DOI: [http://dx.doi.org/10.1016/S0165-9936\(04\)00733-2](http://dx.doi.org/10.1016/S0165-9936(04)00733-2).
- ISO/IEC 17025: General requirements for the competence of testing and calibration laboratories. 2nd Edition, Switzerland. 2005.
- ALACC Guide 3: How to Meet ISO 17025 Requirements for Method Verification. The Analytical Laboratory Accreditation Criteria Committee. 2007.
- NATA: Guidelines for the validation and verification of quantitative and qualitative test methods. The National Association of Testing Authorities (NATA). 2013. Available at <http://www.nata.com.au/>.
- Styarini, D.; Zuas, O.; Hamim, N. Validation and uncertainty estimation of analytical method for determination of benzene in beverages. *Eurasian. J. Anal. Chem.* **2011**, *6*, 159-172.
- Di Marco, G.; de Andrade, M.; Felipe, C.; Alfieri, F.; Gooding, A.; Silva, H. T. J.; et al. Determination of sirolimus blood concentration using high-performance liquid chromatography with ultraviolet detection. *Ther. Drug Monit.* **2003**, *25*, 558-264. PMID: 14508378.
- Guaratini, T.; Cardozo, K. H. M.; Pinto, E.; Colepicolo, P. Comparison of diode array and electrochemical detection in the C30 reverse phase HPLC analysis of algae carotenoids. *J. Braz. Chem. Soc.* **2003**, *20*, 1609-1616. DOI: <http://dx.doi.org/10.1590/S0103-50532009000900007>.
- Linsinger, T. P. J.; Josephs, R. D. Limitations of the application of the Horwitz equation. *Trac. Trends in Anal. Chem.* **2006**, *25*, 1125-1130. DOI: <http://dx.doi.org/10.1016/j.trac.2006.11.002>.
- ISO Guide 33: Guide 33: Uses of certified reference materials. The International Organization for Standardization. 2000.
- Zuas, O.; Budiman, H. Estimating precision and accuracy of GC-TCD method for carbon dioxide, propane and carbon monoxide determination at different flow rate of carrier gas. *Hem. Ind.* **2016**, *4*, 451-459. DOI: <http://dx.doi.org/10.2298/HEMIND150315051Z>.

Article citation:

Zuas, O.; Mulyana, M. R.; Budiman, H. Analytical method validation of GC-FID for the simultaneous measurement of hydrocarbons (C_2 - C_4) in their gas mixture. *Rev. Colomb. Quím.* **2016**, *45* (3), 22-27. DOI: <http://dx.doi.org/10.15446/rev.colomb.quim.v45n3.58085>.

Gustavo Gutiérrez¹, Mónica A. Gordillo², Manuel N. Chaur^{2,*}



UNIVERSIDAD
NACIONAL
DE COLOMBIA

¹Departamento de Ciencias Farmacéuticas, Universidad Icesi, Cali-Colombia

²Departamento de Química, Universidad del Valle, A.A., 25360 Cali-Colombia.

*Autor para correspondencia: manuel.chaur@correounivalle.edu.co

Recibido: 10 de Mayo de 2016. Aceptado: 8 de Septiembre de 2016.

A DFT study on Dichloro {(E)-4-dimethylamino-N'-[(pyridin-2-yl)methylidene-κN]benzohydrazide-κO}M²⁺ (M = Zn, Cu, Ni, Fe, Mn, Ca and Co) complexes: Effect of the metal over association energy and complex geometry

Abstract

The molecular geometry of (E)-4-dimethylamino-N'-[(pyridin-2-yl)methylidene-κN]benzohydrazide ($C_{15}H_{16}N_4O$) complexed with M^{2+} ($M=Zn, Cu, Ni, Fe, Mn, Ca$ and Co) ions was calculated, using density functional theory (B3LYP) with 6-31G(d, p) basis set. Vibrational frequencies were computed in order to verify the absence of imaginary vibrational frequencies, fact that confirms the global minimum in geometry optimization. Molecular geometry parameters (bond lengths and angles) for Cu^{2+} and Zn^{2+} complexes were compared with crystallographic data previously reported, showing good correlation. Binding energies for all complexes were computed at the B3LYP/6-31G++(d, p) level of theory. These calculations indicate that Cu-L is the lowest favorable complex, Cu^{2+} corresponds to the smallest cation on the present study. On the other hand, Ca-L, one of the less favorable complex, corresponds to the largest cation analyzed in the present study. Molecular orbital analysis was carried out showing variations in $\Delta E_{\text{HOMO-LUMO}}$ values as a function of the metallic ion employed.

Keywords: Hydrazones, Binding energies, Single-Point, DFT, complexes.

Un estudio DFT en complejos Dicloro {(E)-4-dimetilamino-N'-[(piridin-2-il) metilideno-κN] benzohidrazida-κO} M²⁺ (M = Zn, Cu, Ni, Fe, Mn, Ca y Co): efecto del metal sobre la energía de asociación y la geometría del complejo

Resumen

La geometría molecular de la (E)-4-dimethylamino-N'-[(piridin-2-il) metilideno-κN] benzohidrazida ($C_{15}H_{16}N_4O$) acomplejada con iones M^{2+} ($M=Zn, Cu, Ni, Fe, Mn, Ca$ y Co) se calculó usando la teoría funcional de densidad (B3LYP) empleando un conjunto de bases 6-31G(d, p). Las frecuencias vibracionales fueron calculadas con el propósito de comprobar la ausencia de frecuencias vibracionales imaginarias, hecho que confirma el mínimo global en la optimización de la geometría. Los parámetros de la geometría molecular (longitudes de enlace y ángulos) para los complejos de Cu^{2+} y Zn^{2+} fueron comparados con datos cristalográficos previamente reportados, mostrando una buena correlación. Las energías de asociación para todos los complejos fueron determinadas a un nivel de teoría B3LYP/6-31G++(d, p) mostrando que el complejo menos favorable es Cu-L, correspondiente al catión más pequeño del estudio. Por otro lado Ca-L, uno de los menos estables, corresponde al catión más grande analizado. Se llevó a cabo un análisis de orbitales moleculares en el cual los complejos exhibieron diferentes valores de $\Delta E_{\text{HOMO-LUMO}}$ en función del metal empleado.

Palabras clave: hidrazona, energía de asociación, SPE, DFT, complejos.

Um estudo DFT nos complexos Dicloro {(E)-4-dimetilamino-N'-[(piridin-2-il) metilideno-κN] benzohidrazida-κO} M²⁺ (M = Zn, Cu, Ni, Fe, Mn, Ca y Co): efeito do metal sobre a energia de associação e a geometria do complexo

Resumo

A geometria molecular da (E)-4-dimethylamino-N'-[(piridin-2-il) metilideno-κN] benzohidrazida ($C_{15}H_{16}N_4O$) acomplexada com íons M^{2+} ($M=Zn, Cu, Ni, Fe, Mn, Ca$ y Co) foi calculada usando a teoria funcional da densidade (B3LYP) utilizando um conjunto de bases 6-31G(d, p). As frequências vibracionais foram calculadas com o objetivo de comprovar a ausência de freqüências vibracionais imaginárias, fato que confirma o mínimo global na otimização da geometria. Os parâmetros da geometria molecular (longitudes de enlace e ângulos) para os complexos de Cu^{2+} y Zn^{2+} foram comparados com dados cristalográficos previamente reportados e mostraram boa correlação. As energias de associação para todos os complexos foram determinadas ao nível de teoria B3LYP/6-31G++(d, p) mostrando que o complexo menos favorável é Cu-L, correspondente ao cátion mais pequeno do estudo. Por outro lado Ca-L, um dos menos estáveis, corresponde ao cátion mais grande analisado. Foi feita uma análise de orbitais moleculares no qual os complexos exibiram diferentes valores de $\Delta E_{\text{HOMO-LUMO}}$ em função do metal utilizado.

Palavras-Chave: hidrazona, associação de energia, SPE, DTF, complexos.

Introduction

Hydrazones are compounds with interesting properties in various research fields such as pharmacology (1-3) antibiotics (4), analytical purposes (5) among others (6-7). In this particular case, the interest is specially focused on the multiple hydrazones dynamics that are important features to the configurational dynamics (imine bond) and the ability to coordinate (terpyridine-like). These characteristics confer applicability in the development of molecular machines and systems for information storage (8-9). Pyridine-2-carboxaldehyde, aryl or acyl hydrazone derivatives exhibit thermal or photo-induced reversible E/Z isomerization where the Z-isomer is in a thermodynamic metastable state stabilized by an intramolecular hydrogen bond (10-12). Additionally, the terpyridine-like framework of most hydrazones allows them to coordinate metal centers (9, 13). Induced isomerization and metal coordination constitute configurational changes in the short term. Reversible chemical identity modifications are available as well and represent constitutional dynamics, which are especially useful for long-term information storage applications (14).

Density Functional Theory (DFT) methods have been widely used for calculating molecular optimized geometries and spectral properties, for instance NMR (15), UV (16), IR (17) and Raman (18), with good correlations with those obtained experimentally. In this sense, one of the most widely used method in computational chemistry is the Becke's three-parameter hybrid (19) and Lee, Yang and Parr correlation functional (B3LYP) (20). This method has proven to be an especially useful approach in the computational study of inorganic (21) and organometallic complexes (22), as well as organic compounds. For instance, in a previous work it was found good correlation between the experimental data of a 2-pyridinecarboxaldehyde derivative and its computed results at two levels of theory (12).

Typically, DFT studies may or may not use diffuse s and p functions for non-hydrogen (6-31G+) atoms and also hydrogen atoms (6-31G++), but the use of d-polarization functions at least for non-hydrogen atoms (6-31G (d)) (23) in organic systems seems mandatory in order to obtain reasonable accuracy; the use of basis that employ polarization functions for all atoms (6-31G (d, p)) is common (24, 25).

Furthermore, Sangeetha *et al.* (26) reported the crystal structure and other spectral properties of (E)-4-dimethylamino-N'-(pyridin-2-yl)methylidene]benzohydrazide copper (II) complex. Previously, the crystal structure of the same ligand participating in a Zn (II) complex was reported by this research group (27). Nevertheless, as far as it is known, there are no theoretical studies for the titled complexes reported in literature. In that way, in order to understand the effect of metallic ion over complex properties, the full-optimized geometric parameters of the titled ligand ($C_{15}H_{16}N_4O$) uncomplexed and associated with four transition metallic ions in the ground state, association energies, and Highest Occupied- and Lowest Unoccupied Molecular Orbitals (HOMO-LUMO) energy gaps were calculated. In this order of ideas, improving the comprehension about complex formation may lead to the development of coordination brakes capable of performing a controlled movement or result in the rational use of certain metal ions in dynamic combinatorial chemistry. Therefore, these results may show the possible use of this kind of complexes in supramolecular structures with specific applications among them in metalo-supramolecular chemistry, coordination polymers based on hydrazones and molecular machines.

Calculations

Molecular geometries of the free ligand and its M²⁺ (M = Zn, Cu, Ni, Fe, Mn, Ca and Co) complexes in the ground state were optimized by DFT:B3LYP method with 6-31G (d, p) basis set. Theoretical IR spectra were computed at the same level of theory to confirm the absence of imaginary frequencies, and single-point energy calculations were performed using B3LYP/6-31G++ (d, p) employing Gauss View 5 as a graphic interface (28) and Gaussian 09W64 (29) for running the calculations. Binding energies were calculated as described by Lee (30) using equation [1].

$$\Delta E = E_{\text{complex}} - (E_{M^{2+}} + E_{C_{15}H_{16}N_4O}) \quad [1]$$

where E_{complex} is the single-point energy (SPE) of the complex, $E_{M^{2+}}$ is the computed SPE for the chloride salt of each metal and $E_{C_{15}H_{16}N_4O}$ is the ligand SPE.

Results and discussion

The crystal morphology of 2-pyridine-carboxaldehyde-4-dimethylaminobenzoylhydrazone is monoclinic with space group P21/c and it is presented as an ethanolic solvate with cell dimensions $a = 6.670$ (4) Å, $b = 29.778$ (3) Å, $c = 8.010$ (2) Å and $V = 1575.96$ Å³ (31). The optimized geometry was calculated at the DFT: B3LYP / 6-31G (d, p) level of theory with a good theoretical-experimental correlation, the relative error was lower than 2.7% for both, bond lengths and angles.

On the one hand, the crystal structure of the copper complex is monoclinic with an space group C2/c and cell dimensions $a = 19.849$ (3) Å, $b = 17.675$ (2) Å, $c = 11.876$ (2) Å and $V = 3386.91$ Å³ (26). Likewise, the zinc complex exhibits a monoclinic geometric structure with an space group P21/c and cell dimensions $a = 19.849$ (3) Å, $b = 13.586$ (5) Å, $c = 7.598$ (9) Å and $V = 1670.36$ Å³ (27). Since there are no crystallographic reports for the aforementioned ligand complexed with more metals than copper and zinc, theoretical-experimental correlation is only possible for the mentioned metals; correlation graphs of selected geometrical parameters are shown in Figure 1.

Accordingly, linear regression is an useful tool in comparative studies of two set of data where the slope is a proportion between response variation and input variables, thus, a perfect correlation would have a slope equal to one. Higher or lower values represent over or underestimation of the calculated values regarding the experimental data, respectively. The intercept is, by definition, the value of the response variable when the input is equal to zero, hence, negative or positive intercept values represent quantitatively the over- or underestimation of calculations.

Finally, R^2 values provide the percentage of response variability that is explained by the variation of the independent variable, thus, the difference between R^2 value and one represents an indirect measure of random error (32). In that way, the calculations in this research are slightly overestimated for bond angles and bond lengths in the zinc complex and underestimated in the copper complex. The latter showed the higher random error.

The biggest discrepancies for both complexes are related with the angle and length of the chlorine-metal bond. This error is explained by the high influence of intermolecular interactions in solid phase, neglected in these computational calculations, which assume an isolated molecule in the gas phase; N—H \cdots Cl along [001] direction stacking.

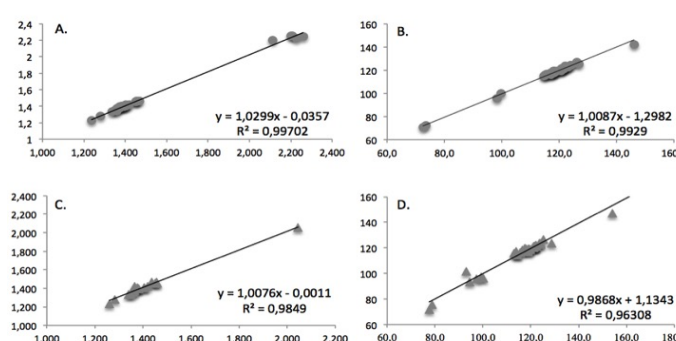


Figure 1. Theoretical (y-axis) – Experimental (x-axis) correlation graphs of selected molecular geometric parameters: A. Zinc complex bond lengths. B. Zinc complex bond angles. C. Copper complex bond lengths. D. Copper complex bond angles.

Therefore, we excluded the aforementioned bonds in error rate calculations. On the one hand, copper complex showed acceptable average errors of 1.12 and 1.46% for bond lengths and angles respectively. On the other hand, zinc complex report 0.83 and 0.66% for bond lengths and angles, respectively.

Results from SPE calculations were performed at DFT: B3LYP/6-31G+(d, p) level of theory for the full-optimized geometries of the titled ligand, the ligand complexed with zinc, copper, nickel, manganese, iron, calcium and cobalt, and the chloride of each metal without restrictions, as well as metallic center geometry parameters are presented below in Table 1. The optimized structure of each complex along with the ORTEP representation of the zinc complex's structure is shown in Figure 2.

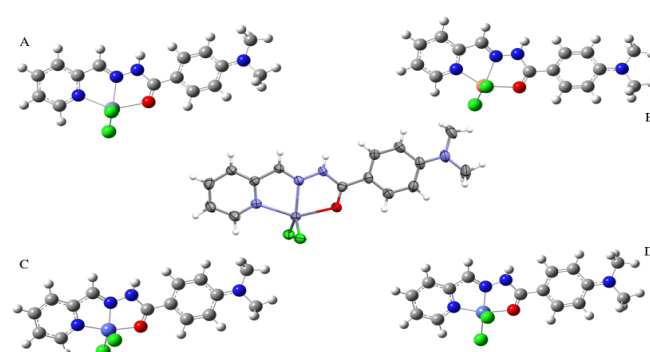


Figure 2. Fully optimized structures of A. Zinc, B. Copper, C. Calcium, D. Manganese complexes and at the center, the ORTEP representation of the zinc complex's structure.

Table 1. Metallic center geometry parameters and association energy values Cu²⁺ and Zn²⁺ bond angle and length data/error percentage respect to crystallographic results.

Distance (Å)							
Bond	Ni ²⁺	Cu ²⁺	Zn ²⁺	Co ²⁺	Fe ²⁺	Mn ²⁺	Ca ²⁺
N ₁ -M	1.886	2.053/0.39	2.254/2.208	1.908	1.935	1.985	2.627
N ₂ -M	1.841	2.187/10.33	2.2/4.00	1.862	1.789	1.820	2.603
O ₁ -M	1.920	2.192/5.89	2.252/2.22	1.971	2.021	2.045	2.457
Cl ₁ -M	2.469	2.256/11.39	2.244/0.67	2.327	2.243	2.223	2.628
Cl ₂ -M	2.201	2.222/0.765	2.225/0.135	2.237	2.233	2.227	2.623
Angle (°)							
Atom set	Ni ²⁺	Cu ²⁺	Zn ²⁺	Co ²⁺	Fe ²⁺	Mn ²⁺	Ca ²⁺
N ₁ -N ₂ -O ₁ *	99.39	103.92	110.06	101.09	104.23	105.43	114.23
N ₁ -M-O ₁	162.13	146.85/4.94	141.84/2.93	162.84	164.62	162.68	122.30
N ₁ -M-N ₂	82.77	75.58/4.26	72/2.22	82.06	82.68	81.56	61.81
N ₂ -M-O ₁	81.87	71.77/8.12	70.86/2.31	81.07	81.95	81.12	62.22
Cl-M-Cl	112.08	141.66/26.94	131.49/10.72	124.01	143.38	143.67	133.81
Ionic radio (Å)	0.77	0.570	0.610	0.81	0.78	0.83	1.16
Association energy (kcal/mol)	-44.9	-25.8	-26.2	-61.8	-55.0	-74.8	-31.06

*Ligand showed 124.68°

Association energy results showed that the most favorable complex formation is the one formed between the ligand and manganese (II) (-74.8 kcal/mol) while the less favorable complexes are those formed with Copper and Zinc 2+ ions (-25.8 and -26.2 kcal/mol, respectively). Noteworthily, figures 2A and 2B show that although Cu²⁺ and Zn²⁺ ions are capable of fitting in the N-N-O pocket of the ligand, the small size of these ions results in longer distances between the metal cations and atoms, from the ligand, participating in the coordination framework.

Ca²⁺ is the largest ion under the present study and, as observed in figure 2C, is too voluminous fit in the N-N-O pocket inducing again longer distances, decreasing the effectiveness of interaction and therefore the complex stability in both cases. Nickel (II) complex showed a particular behavior since exhibits the less N₁-N₂-O₁ angle while N₁-MO₁ angle and the N₁-M, O₁-M and N₂-M distances are comparable to other complexes (Co, Fe or Mn, i. e.) indicating an especial structural modification of the ligand closing the N₁-O distance, probably to promoting the interaction ligand-metal.

Since HOMO-LUMO is mainly a mathematical model that represents electronic density around atoms and not directly experimentally observable parameters, usually they are physically explained as the ionization potential and electron affinity, respectively. However, HOMO-LUMO energy gap and other interactions between both molecular orbitals studied in Frontier Molecular Orbitals Theory (FMOT) are important for chemical reactivity of molecular systems. As observed in figure 3 the ligand and the zinc complex HOMO-LUMO transitions are characterized by a subtle electronic displacement from the phenyl-hydrazone moiety to the pyridine ring. In contrast, other complexes have the HOMO localized at the metallic center and their HOMO-LUMO transitions are characterized by an electronic displacement towards the phenyl-hydrazone and pyridine ring moieties, this is specially observed for the copper complex.

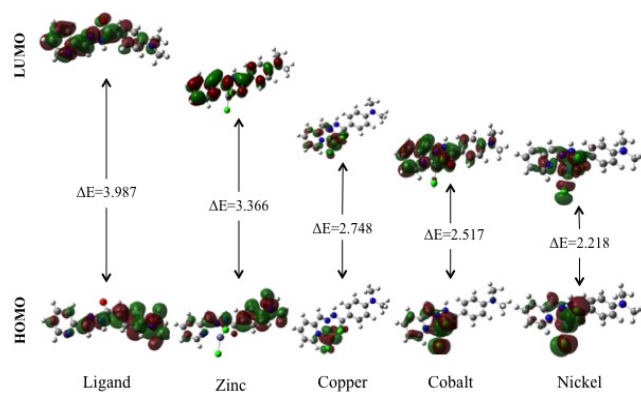


Figure 3. Selected complexes HOMO-LUMO energy gap. ΔE values are presented in eV.

Conclusions

Optimized geometries of the titled ligand and their respective complexes of seven metallic 2+ ions (Zn, Cu, Ni, Mn, Fe, Ca and Co) were calculated and compared with crystallographic reports for the ligand, zinc and copper complexes with good theoretical-experimental correlation.

The main discrepancy between crystal and calculated structures was found in the chloride-metal-chloride geometry due to computed geometries that were carry out in gas phase for an isolated molecule, approach that neglects intermolecular interactions observed in the solid state structure (N—H···Cl along [001] direction stacking, i. e.). Association energy calculations showed that the most favorable complex formation occurs in presence of Mn²⁺ while Zn²⁺, Ca²⁺ and Cu²⁺ are the less favorable complexes.

Acknowledgments

We greatly thank to Vicerrectoría de Investigaciones and Centro de Excelencia en Nuevos Materiales (CENM) from Universidad del Valle for their generous financial support.

References

- Giziroglu, E.; Aygün, M.; Sarikurkcu, C.; Kazar, D.; Orhan, N.; Firinki, H. *et al.* Synthesis, characterization and antioxidant activity of new dibasic tridentate ligands: X-ray crystal structures of DMSO adducts of 1,3-dimethyl-5-acetylbarbituric acid o-hydroxybenzoyl hydrazone copper(II) complex *Inorg. Chem. Commun.* **2013**, *36*, 199-205. DOI: <https://doi.org/10.1016/j.inoche.2013.09.013>.
- Kovács, D.; Wölfling, J.; Szabó, N.; Szécsi, M.; Minörös, R.; Zupkó, I. *et al.* Efficient access to novel androsteno-17-(1',3',4')-oxadiazoles and 17β-(1',3',4')-thiadiazoles via N-substituted hydrazone and N,N'-disubstituted hydrazine intermediates, and their pharmacological evaluation in vitro *Eur. J. Med. Chem.* **2015**, *98*, 13-29. DOI: <http://dx.doi.org/10.1016/j.ejmech.2015.05.010>.
- Rollas, S. Küçükgüzel, *Molecules*, **12**, 1910 (2007).
- Sridhar, S.K.; Saravanan, M.; Ramesh, A. Synthesis and antibacterial screening of hydrazones, Schiff and Mannich bases of isatin derivatives. *Eur. J. Med. Chem.*, **2001**, *36* (7), 615-625. DOI: [http://dx.doi.org/10.1016/s0223-5234\(01\)01255-7](http://dx.doi.org/10.1016/s0223-5234(01)01255-7).
- Suvarapu, L.N.; Seo, Y.K.; Baek, S. O.; Ammireddy, V.R. Review on analytical and biological applications of hydrazones and their metal complexes. *E-J. Chem. (Online)*, **2012**, *9* (3), 1288-130. DOI: <https://doi.org/10.1155/2012/534617>.
- Su, X.; Aprahamian, I.; Hydrazone-based switches, metallo-assemblies and sensors. *Chem. Soc. Rev.* **2014**, *43* (6), 1963-1981. DOI: <https://doi.org/10.1039/c3cs60385g>.
- van Dijken, D. J.; Kovaricek, P. S.; Ihrig, P.; Hecht, S. Acylhydrazones as Widely Tunable Photoswitches. *J. Am. Chem. Soc.* **2015**, *137* (47), 14982-14991. DOI: <https://doi.org/10.1021/jacs.5b09519>.
- Chaur, M.N.; Collado, D.; Lehn, J. M. Configurational and constitutional information storage: multiple dynamics in systems based on pyridyl and acyl hydrazones. *Chem. Eur. J.* **2011**, *17* (1), 248-258. DOI: <http://dx.doi.org/10.1002/chem.201002308>.
- Romero, E.; D'Vries, R.; Zuluaga, F.; Chaur, M. Multiple dynamics of hydrazone based compounds. *J. Braz. Chem. Soc.* **2015**, *26* (3) 1255-1273. DOI: <https://doi.org/10.5935/0103-5053.20150092>.
- Landge, S.M.; Tkatchouk, E.; Benítez, D.; Lanfranchi, D. A.; Elhabiri, M.; Goddard, W. *et al.* Isomerization mechanism in hydrazone-based rotary switches: lateral shift, rotation, or tautomerization? *J. Am. Chem. Soc.* **2011**, *133* (25), 9812-9823. DOI: <https://doi.org/10.1021/ja200699v>.
- Chaur, M. N. Aroylhydrazones as potential systems for information storage: photoisomerization and metal complexation. *Rev. Colomb. Quím.* **2012**, *41* (3), 349-358.

12. Gordillo, M.A.; Soto-Monsalve, M.; Gutiérrez, G.; D'vries, R.; Chaur, M. N. Theoretical and experimental comparative study of a derivative from 2-pyridinecarboxaldehyde which exhibits configurational dynamics *J. Mol. Struc.* **2016**, *1119*, 286-295. DOI: <https://doi.org/10.1016/j.molstruc.2016.04.055>.
13. Fernández, M. A.; Barona, J. C.; Polo, D.; Chaur, M. N. Photochemical and electrochemical studies on lanthanide complexes of 6-(hydroxymethyl) pyridine-2-carboxaldehyde [2-methyl-pyrimidine-4, 6-diyl] bis-hydrazone. *Rev. Colomb. Quim.* **2014**, *43* (1), 5-11.
14. Lehn, J. M. Conjecture: Imines as unidirectional photodriven molecular motors—motional and constitutional dynamic devices. *Chem. Eur. J.* **2006**, *12* (23), 5910-5915. DOI: <https://doi.org/10.1002/chem.200600489>.
15. Bagno, A.; Saielli, G. Addressing the stereochemistry of complex organic molecules by density functional theory - NMR. *WIREs Comput. Mol. Sci.* **2015**, *5* (2), 228-240. DOI: <https://doi.org/10.1002/wcms.1214>.
16. Preat, J.; Jacquemin, D.; Wathélet, V.; Fontaine, M.; Perpète, E.A. Thioindigo dyes: highly accurate visible spectra with TD-DFT. *J. Phys. Chem. A*, **2006**, *128* (6), 2072-2083. DOI: <https://doi.org/10.1021/ja056676h>.
17. Wang, Y.; Liu, Q.; Qiu, L.; Wang, T.; Yuan, H. Lin, J. *et al.* Molecular structure, IR spectra, and chemical reactivity of cisplatin and transplatin: DFT studies, basis set effect and solvent effect. *Spectrochim. Acta, Part A* **2015**, *150*, 902-908.
18. Sudha, S.; Sundaraganesan, N.; Kurt, M.; Cinar, M.; Karabacak, M. FT-IR and FTRaman spectra, vibrational assignments, NBO analysis and DFT calculations of 2-amino-4-chlorobenzonitrile. *J. Mol. Struc.* **2011**, *985*, 148. DOI: <http://dx.doi.org/10.1016/j.molstruc.2010.10.035>.
19. Becke, A. D. Density - functional thermochemistry. III. The role of exact exchange. *J. Chem. Phys.* **1993**, *98*, 5648-5652. DOI: <http://dx.doi.org/10.1063/1.464913>.
20. Lee, C.; Yang, W.; Parr, R.G. Development of the colle-salvetti correlation energy formula into a functional of the electron density. *Phys. Rev. B* **1988**, *37*, 785-789. DOI: <http://dx.doi.org/10.1103/physrevb.37.785>.
21. Dudev, T.; Lim, C. Tetrahedral vs octahedral zinc complexes with ligands of biological interest: a DFT/CDM study. *J. Am. Chem. Soc.* **2000**, *122* (45), 11146-11153. DOI: <http://dx.doi.org/10.1021/ja0010296>.
22. Bagno, A.; Rastrelli, F.; Saielli, G. Toward the complete prediction of the ¹H and ¹³C NMR spectra of complex organic molecules by DFT methods: application to natural substances. *Chem. Eur. J.* **2006**, *12* (21), 5514-5525. DOI:<https://doi.org/10.1002/chem.200501583>
23. Rablen, P. R.; Lockman, J. W.; Jorgensen, W. L. Ab initio calculations on hydrogen-bonded complexes of small organic molecules with water. *J. Chem. Phys. A* **1998**, *102* (21), 3782-3797. DOI: <https://doi.org/10.1021/jp980708o>.
24. Szemik-Hojniak, A.; Oberda, K.; Deperasińska, I.; Nizhnik, Y. P.; Jerzykiewicz, L. A negligible CT character of the lowest excited state of a novel complex of zinc tetraphenylporphyrin with axially bonded 2-(4-methoxy-trans-styryl)quinoline-1-oxide ligand: Experimental studies and TD DFT/CAM B3LYP [6-31G(d,p)] calculations. *Polyhedron* **2015**, *88*, 190-198. DOI: <http://dx.doi.org/10.1016/j.poly.2014.12.025>.
25. Maxwell, C. I.; Mosey, N. J.; Stan Brown, R. DFT Computational study of the methanolytic cleavage of DNA and RNA phosphodiester models promoted by the dinuclear Zn(II) complex of 1,3-Bis(1,5,9-triazacyclododec-1-yl)propane. *J. Am. Chem. Soc.* **2013**, *135* (45), 17209-17222. DOI: <https://doi.org/10.1021/ja4088264>.
26. Sangeetha, N. R.; Pal, S.; Anson, C. E. Powell, A. K.; Pal, S. A one-dimensional assembly of copper(II) polyhedra via dual use of hydrogen-bonding and π - π interaction *Inorg. Chem. Commun.* **2000**, *3* (8), 415-419. DOI: [http://dx.doi.org/10.1016/s1387-7003\(00\)00103-9](http://dx.doi.org/10.1016/s1387-7003(00)00103-9).
27. Chaur, M. Dichlorido{(E)-4-dimethylamino-N'-(pyridin-2-yl)methylidenejN] benzohydrazide-jO}zinc *Acta Crystallogr. Sect. E: Struct. Rep. Online* **2013**, *69*, m27. DOI: <https://doi.org/10.1107/s1600536812049355>.
28. GaussView, Version 5, Dennington, R.; Keith, T.; Millam, J. *Semicem Inc.*, Shawnee Mission, KS, 2009
29. Gaussian 09, Revision D.01, Frisch, M. J.; Trucks, G. W.; Schlegel, H. B. *et al.*, Gaussian, Inc., Wallingford CT, 2009.
30. Lee, G. Y. DFT studies of the zinc complexes of DNA bases *Bull. Korean Chem. Soc.* **2006**, *27* (3), 419-422. DOI: <https://doi.org/10.5012/bkcs.2006.27.3.419>.
31. Sangeetha, N. R.; Pal, S.; Pal S. Copper(II)-activated transformation of azomethine to imidate: synthetic and structural studies. *Polyhedron* **2000**, *19* (28), 2713-2717. DOI: [https://doi.org/10.1016/s0277-5387\(00\)00595-7](https://doi.org/10.1016/s0277-5387(00)00595-7).
32. Stockl, D.; Dewitte, K.; Thienpont L.M. Validity of linear regression in method comparison studies: is it limited by the statistical model or the quality of the analytical input data? *Clin. Chem.* **1998**, *44* (11), 2340-2346.

Article citation:

Gutiérrez, G.; Gordillo, M. A.; Chaur, M. N. A DFT study on Dichloro {(E)-4-dimethylamino-N'-(pyridin-2-yl) methylidene- κ N] benzohydrazide- κ O}M²⁺ (M = Zn, Cu, Ni, Fe, Mn, Ca and Co) complexes: Effect of the metal over association energy and complex geometry *Rev. Colomb. Quim.* **2016**, *45* (3), 28-32. DOI: <http://dx.doi.org/10.15446/rev.colomb.quim.v45n3.57351>.



Johana Rodríguez Ruiz¹, Adolfo Pájaro Payares^{1,2}, Edgardo Meza Fuentes^{2,*}

¹Grupo de Investigación en Procesos de la Industria Petroquímica. SENA-centro para la Industria Petroquímica, Cartagena, Bolívar, Colombia

²Grupo de Estudios en Materiales y Combustibles, Programa de Química, Universidad de Cartagena, Cartagena, Colombia.

*Autor para correspondencia: emezaf@unicartagena.edu.co

Recibido: 15 de Junio de 2016. Aceptado: 9 de Septiembre de 2016.

Síntesis y caracterización estructural de hidrotalcitas de Cu-Zn-Al

Resumen

Las hidrotalcitas pueden ser usadas en áreas como catálisis, medicina, química ambiental, entre otras. Dependiendo de los metales presentes, los sólidos derivados de la calcinación de hidrotalcitas también son usados debido a su carácter básico, efecto de memoria y alta área superficial específica. En este estudio se describen algunas características de hidrotalcitas a base de Cu-Zn-Al. Los análisis se realizaron usando AAS, DRX, FTIR, TGA y DSC. En el espectro FTIR se observó que, en los sólidos con mayor cantidad de cobre, la banda del estiramiento O•H ($M\bullet OH$, $H\bullet OH$) se desplazó a valores más bajos de número de onda, debido a que la densidad electrónica de los grupos OH se orienta hacia el centro metálico de cobre. En todos los sólidos se observó la formación de la fase hidrotalcita, y de la fase $Cu(OH)_2$ en los sólidos con mayor contenido de cobre, lo que puede ser atribuido al efecto Jahn-Teller. Los resultados mostraron que los sólidos con mayor contenido de cobre colapsan en temperaturas menores. En todas las muestras se observaron eventos como: descomposición de la estructura HTLc, formación de óxidos metálicos y descomposición decarbonatos que quedaron ocluidos en los poros de los sólidos debido al colapso de la estructura laminar.

Palabras clave: hidrotalcitas, cobre, colapso de estructura.

Synthesis and structural characterization of Zn-Al-Cu hydrotalcites

Abstract

Hydrotalcite-like compounds have been used in catalysis, medicine, environmental chemistry, and other applications. Depending on the metals present, the solids obtained by calcination can be used due to their basicity, memory effect, and high specific surface area. This study describes some characteristics of hydrotalcites based on Cu-Zn-Al. The solids were characterized by AAS, XRD, FTIR, DSC and TGA. In the FTIR spectra it was observed that in the solids with higher copper contents the band signed to O•H stretching ($M\bullet OH$, $H\bullet OH$) was moved to lower wave number values, because electron density of hydroxide groups orients toward the metallic copper center. In all materials hydrotalcite phase formation was observed and the $Cu(OH)_2$ phase in solids with higher copper content was detected, fact attributed to the Jahn-Teller effect. Results indicate that the collapse of the structure occurs at lower temperatures in the case of solids with higher copper content. In all the tested materials the decomposition of the HTLc structure and the formation of metal oxides was observed, as well as decomposition of carbonate ions occluded in the solid due to the collapse of the lamellar structure.

Palavras clave: Hydrotalcite, copper, collapse of structure.

Síntese e caracterização estrutural de hidrotalcitas de Cu-Zn-Al

Resumo

Os compostos do tipo hidrotalcita podem ser usados nas áreas de catalise, medicina, química ambiental, entre outras. Dependendo dos metais presentes, os sólidos obtidos pela calcinação de hidrotalcitas também podem ser usados devido a propriedades tais como: caráter básico, efeito de memória e elevada área superficial específica. Neste estudo descrevem-se algumas características das hidrotalcitas baseadas em Cu-Zn-Al. Na caracterização dos sólidos usaram-se as técnicas AAS, DRX, FTIR, TGA e DSC. Observou-se nos sólidos com maior conteúdo de cobre que o estiramento O•H ($M\bullet OH$, $H\bullet OH$) se desloca a valores menores de numero de onda, devido a que a densidade eletrônica dos grupos hidróxido se orienta em direção ao centro metálico de cobre. Em todos os materiais observou-se a fase hidrotalcita e nos sólidos com maior conteúdo de cobre foi detectada a fase $Cu(OH)_2$, fato atribuído ao efeito Jahn-Teller. Os resultados indicam que o colapso da estrutura acontece em temperaturas menores no caso dos sólidos com maior conteúdo de cobre. Em todos os materiais observaram-se decomposição da estrutura HTLc, formação de óxidos metálicos, e a decomposição dos íons carbonato que ficaram ocluídos nos sólidos devido ao colapso da estrutura lamelar.

Palavras-Chave: hidrotalcitas, cobre, colapso da estrutura.

Introducción

Los hidróxidos dobles laminares (HDLs) o compuestos del tipo hidrotalcita (HTLc) pertenecen al tipo de arcillas aniónicas que poseen una estructura representada por la siguiente fórmula:



Donde M(II) y M(III) corresponden a metales con cargas 2+ y 3+, respectivamente; el término Anx/n corresponde a la presencia de un anión que estabiliza la carga positiva, generada por la incorporación del metal en estado de oxidación 3+ en la red de un hidróxido de un metal divalente (1, 2).

El término hidrotalcita (HTLc) corresponde al compuesto con la fórmula general $Mg_6Al_2(OH)_{16}CO_3\bullet H_2O$, donde la fracción atómica del Al³⁺ corresponde a 0,25 y la del Mg²⁺ a 0,75 de los metales presentes (1). La estructura de las hidrotalcitas se fundamenta en la brúctita [Mg(OH)₂] que posee una geometría laminar de alta simetría, donde el catión Mg²⁺ está situado en el centro de un octaedro y coordinado a seis grupos OH. En este compuesto los octaedros comparten los lados formando láminas planas e infinitas que se apilan unas sobre otras y que se mantienen unidas a través de interacciones de tipo puente de hidrógeno (2, 3).

Cuando en la estructura de la brúctita los iones Mg²⁺ son sustituidos por iones trivalentes con radios atómicos similares al del magnesio, se generan cargas positivas a lo largo de las láminas, las cuales deben ser compensadas con la presencia de aniones que se incorporan en los espacios existentes entre una lámina y otra. Sin embargo, debido a que los aniones no ocupan todo el espacio entre las láminas, quedan espacios libres en los que se depositan moléculas de agua (4, 5).

Los cationes M²⁺ más estudiados en la literatura son Mg²⁺, Fe²⁺, Ni²⁺, Co²⁺, Zn²⁺ y Cu²⁺, mientras que los cationes M³⁺ más comunes son Al³⁺, Cr³⁺ y Fe³⁺, pudiendo ser usados todos los cationes con radios iónicos entre 0,5 e 0,8 Å (1, 5). Las hidrotalcitas no se limitan a poseer en su estructura solo un catión divalente y otro trivalente, ya que estas cantidades pueden variar siempre y cuando la suma de los iones divalentes y trivalentes esté en el límite de los valores de x necesarios para que ocurra la formación de la estructura. En este contexto se han sintetizado hidrotalcitas que contienen cobre y zinc (6, 7), cobre y cobalto (8), níquel y zinc (7) y otras combinaciones (1).

Las hidrotalcitas están constituidas por celdas unitarias ortorrómicas con una simetría R-3m y un valor del parámetro *c*, que es tres veces la distancia entre dos láminas sucesivas. El parámetro de celda *c* es determinado por el tamaño y por la cantidad de aniones presentes entre las láminas, mientras que el parámetro de celda *a*, depende del tipo y de la cantidad de los cationes presentes (2). En cuanto a los aniones, el más estudiado es el carbonato, debido a su estabilidad y a que se descompone en dióxido de carbono por efecto de la temperatura. Otros aniones empleados en la síntesis de hidrotalcita son: F⁻, Cl⁻, Br⁻, I⁻, (ClO₄)⁻, (NO₃)⁻, (ClO₃)⁻, (IO₃)⁻, OH⁻, (CrO₄)²⁻ (1, 2), así como polioxometalatos y aniones orgánicos (9).

Debido a las propiedades químicas de las hidrotalcitas, estas pueden dar origen a una gran variedad de productos a través de tratamientos térmicos que permiten obtener óxidos mixtos o mezclas de óxidos con propiedades que permiten diferentes propósitos: elevada área superficial específica, buena estabilidad térmica, alta dispersión y carácter básico. Estas propiedades han conducido a que dichos materiales hayan recibido mucha atención y aplicación en diversas áreas. En medicina, por ejemplo, las hidrotalcitas pueden ser utilizadas como agentes en el tratamiento de úlceras pépticas a través de la adsorción de la pepsina cargada negativamente dentro de las superficies cargadas positivamente. A nivel industrial se usan como componentes en los materiales de PVC, lo que permite que se conserve la fuerza y blancura del PVC durante más tiempo (10).

Las hidrotalcitas también son potencialmente útiles como catalizadores o precursores de catalizadores, ya que se pueden usar para formar óxidos metálicos mixtos con altas áreas superficiales y con un carácter básico que las hace útiles en varias reacciones. Algunos ejemplos del uso de hidrotalcitas del tipo Mg-Al para la generación de catalizadores activos y selectivos son la hidrogenación de metil-benzoato a benzaldehído, la reducción de aldehídos a alcoholes y la fotodegradación de compuestos fenólicos por medio de alquilaciones de fenol con 1-propanol y 2-propano. Del mismo modo, se han utilizado catalizadores a base de níquel y cobre, obtenidos apartir de precursores del tipo hidrotalcita en reacciones de reforma de metano y de alcoholes (6, 11-13) y reacción de desplazamiento de vapor de agua (7, 14), entre otras.

Este estudio se centra en las características de hidrotalcitas a base de cobre, zinc y aluminio en la obtención de catalizadores para reacciones de purificación y aumento de la producción de hidrógeno, a través de la reacción WGS (7) y reforma de metanol (15). Los resultados revelaron la formación de la estructura del tipo hidrotalcita en todos los materiales. También se observó que la composición de los materiales puede contribuir con la estabilidad térmica y con la formación de una o dos fases en los sólidos, notándose que en los materiales con mayor contenido de cobre el efecto Jahn-Teller conduce a la formación de partículas de hidróxido de cobre (II).

Materiales y métodos

Preparación de los materiales

Se prepararon los precursores de los catalizadores con estructura del tipo hidrotalcita (HTLc) por el método sal-base a pH constante (1). Para la síntesis de los precursores se mezcló una solución salina que contenía nitrato de cobre ($Cu(NO_3)_2\bullet 6H_2O$) de grado analítico (marca Merck), nitrato de zinc ($Zn(NO_3)_2\bullet 6H_2O$) de grado analítico (marca Merck) y nitrato de aluminio ($Al(NO_3)_3\bullet 9H_2O$) de grado analítico (marca Merck) con una segunda solución que contenía hidróxido de potasio (KOH) de grado analítico (marca Vetec) y carbonato de potasio (K_2CO_3) de grado analítico (marca Vetec), manteniendo el pH a 8,3 y bajo agitación durante 2 h a 65 °C. El sólido formado se separó por filtración al vacío y se lavó con agua desionizada hasta la eliminación total de la especie nitrato; el material resultante se secó a 60 °C durante 24 h. Las muestras obtenidas fueron codificadas de acuerdo al número de moles de los metales presentes en cada sólido presentados en la Tabla 1.

Tabla 1. Relación molar Cu/Zn y Cu/Al y parámetros de celda calculados por difracción de rayos X. Dp: Diámetro de Partícula; TC: Temperatura de colapso de la estructura HTLc.

Muestra	Relación Cu/Zn	Relación Cu/Al	Parámetro <i>c</i> (Å)	Parámetro <i>a</i> (Å)	Dp* (nm)	TC (°C)
Cu _{0.50} Zn _{0.25} Al _{0.25}	2,10	2,10	21,76	3,06	8,5	139
Cu _{0.37} Zn _{0.37} Al _{0.25}	1,00	1,54	22,48	3,07	9,6	158
Cu _{0.44} Zn _{0.22} Al _{0.33}	2,10	1,40	21,81	3,03	8,5	163
Cu _{0.33} Zn _{0.33} Al _{0.33}	1,00	1,00	22,63	3,07	21,6	166

*Calculado por la Ecuación de Scherrer usando el plano (0 0 3) (11).

Caracterización de los materiales

Los sólidos sintetizados fueron caracterizados usando espectroscopía de absorción atómica (AAS), espectroscopía en la región del infrarrojo medio con transformada de Fourier (FTIR), análisis termogravimétrico (TGA), calorimetría diferencial de barrido (DSC) y difracción de rayos X (DRX). La determinación del contenido de los metales por (AAS) en los sólidos sintetizados se realizó en un equipo Unicam Modelo Solaar 969, previa disolución de los sólidos en medio ácido.

Los DRX de los sólidos del tipo hidrotalcita fueron obtenidos en un equipo BRUKER modelo D8 ADVANCE, usando radiación CuK α 1, generada a 40 kV y 30 mA, en el intervalo de medición de 10-80° 2 θ usando un paso de 0,02 °/s.

Los análisis FTIR fueron realizados en un equipo Shimadzu, modelo IRAffinity, en la región entre 4000 y 400 cm $^{-1}$. Para estos análisis, las muestras fueron dispersadas en bromuro de potasio en una relación 1:100 y después prensadas en pastillas que fueron analizadas en la región de número de onda antes mencionada.

Los análisis de TGA y DSC fueron realizados en un equipo TA Instruments Modelo SDT Q600, en el intervalo de temperaturas de 30 a 1000 °C en un flujo de aire de 50 mL/min y una velocidad de calentamiento de 10 °C/min.

Resultados y discusión

Las relaciones molares y los códigos usados para identificar los sólidos sintetizados son mostrados en la Tabla 1. Las relaciones molares obtenidas a través espectrometría de absorción atómica muestran un alto grado de correspondencia entre los valores teóricos (Cu/Zn = 2,0 o 1,0; Cu/Al = 1,5 o 1,33) y los obtenidos experimentalmente, lo cual comprueba la efectividad del método de síntesis.

Los gráficos de difracción de rayos X (Figura 1) confirman la presencia de la estructura hidrotalcita en todos los sólidos. Sin embargo, en los materiales con menor contenido de aluminio se observaron señales que indican la formación de algunas partículas de hidróxido de cobre [Cu(OH)₂]. Esto puede atribuirse al efecto Jahn-Teller que presentan los compuestos de Cu(II), donde ocurre una distorsión de la simetría octaédrica que conduce a la estabilización de los compuestos, afectando la formación de la fase hidrotalcita en estos materiales (15).

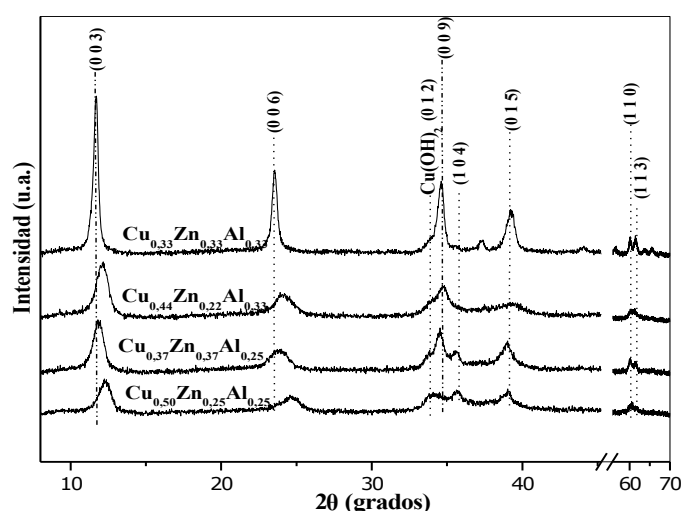


Figura 1. Difractogramas de rayos X de los sólidos sintetizados.

En este sentido, se observa que el aumento del metal trivalente ayuda a estabilizar la estructura del tipo hidrotalcita, debido al distanciamiento de las unidades de Cu(OH)₂, disminuyendo así el efecto Jahn-Teller.

El sólido Cu_{0.33}Zn_{0.33}Al_{0.33} presentó el difractograma con los picos correspondientes a la estructura HTLc más estrechos y simétricos, lo que indica que en este material la presencia de mayor cantidad de zinc y de aluminio permite tener un material en el cual los átomos de cobre están menos próximos entre sí, disminuyendo la posibilidad de ocurrencia del efecto Jahn-Teller, lo cual favoreció la formación de la fase hidrotalcita. Lo anterior se verifica a través del mayor tamaño de partícula (Dp) de la fase de la estructura HTLc de este material (Tabla 1). En los otros materiales el menor tamaño de las partículas es atribuido a la presencia de la fase Cu(OH)₂ que puede actuar como una barrera entre las partículas de la estructura HTLc, disminuyendo su tamaño.

En relación al parámetro de celda *c* (Tabla 1), los valores no mostraron una tendencia asociada al aumento del anión carbonato en la estructura, lo que puede ser asociado a la presencia de partículas de hidróxido de cobre, las cuales pueden estar presentes tanto en la superficie de los sólidos, como en las regiones interlaminares. En el caso del parámetro de celda *a*, los materiales con más contenido de zinc presentaron mayores valores, debido a que este elemento posee mayor radio atómico (0,74 Å) que el cobre (0,72 Å).

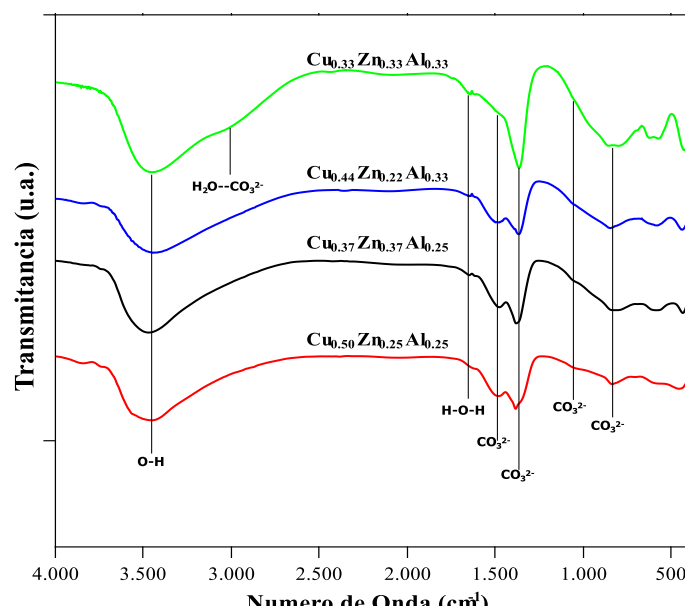


Figura 2. Espectros FTIR de los sólidos sintetizados.

Los espectros FTIR de los sólidos muestran varias bandas que son características de las estructuras HTLc que contienen el anión carbonato (Figura 2). Se observa que, en los sólidos con las cantidades más altas de cobre la banda originada por el estiramiento O-H (M-OH, H-OH) se desplaza ligeramente hacia valores más bajos de número de onda. Esto se debe a que la densidad electrónica del grupo OH se orienta hacia el centro metálico de cobre por su baja densidad electrónica en el orbital 4s ($3d^{10} 4s^1$), lo que conduce a la disminución de la frecuencia de vibración O-H en relación a otros elementos de la primera serie de transición (16).

En todos los sólidos se observó una banda a 1525 cm^{-1} , característica de los iones carbonato, que está relacionada con el modo vibracional resultante de la disminución de la simetría D_{3h} de los iones carbonato hacia la simetría C_{2v} , debido a la interacción de este anión con los grupos OH presentes en las láminas positivas (4). La banda a 1370 cm^{-1} (v_3), característica también del ion carbonato fue observada en todos los espectros y las bandas que aparecen por debajo de 1000 cm^{-1} son atribuidos a los enlaces metal-oxígeno (M-O-H) presentes en las láminas (4).

La banda asociada a la interacción entre las moléculas de agua y los iones carbonato ($3000\text{-}3100\text{ cm}^{-1}$) fue observada únicamente en el espectro de la muestra $\text{Cu}_{0.33}\text{Zn}_{0.33}\text{Al}_{0.33}$, lo cual puede deberse al mayor contenido de carbonato y al mayor espacio entre las láminas registrado en este sólido, como se observó a través de los valores del parámetro c . Lo anterior contribuye con el aumento del volumen en el que pueden estar ubicadas las moléculas de agua, facilitando su difusión e interacción con los carbonatos presentes.

A través de los análisis de termogravimetría y calorimetría diferencial de barrido (Figura 3) se evidenció que la estructura HTLc del sólido $\text{Cu}_{0.50}\text{Zn}_{0.25}\text{Al}_{0.25}$ es la menos estable, colapsando a 139°C (Tabla 1), mientras que en el caso de los otros materiales el colapso ocurrió en temperaturas más altas y próximas entre sí. Este hecho concuerda con la presencia de la fase $\text{Cu}(\text{OH})_2$ observada por DRX, lo cual comprueba la incidencia del efecto Jahn-Teller en la estabilidad de la estructura HTLc.

En todos los sólidos se evidenciaron varios procesos durante el calentamiento que están relacionados con la salida de agua fisisorbida en la superficie de los sólidos y la que está presente entre las láminas de la estructura. Seguido a este proceso, los aniones carbonato y grupos hidróxido se descompusieron y se formaron óxidos de cobre y zinc, a temperaturas inferiores a 350°C , y óxidos de aluminio entre 400 y 500°C .

En relación con el calor necesario para que ocurran los procesos característicos de la descomposición de hidrotalcitas (curva de DSC), se observa que el mayor requerimiento energético para la salida del agua antes del colapso se registra en los sólidos con mayor contenido de aluminio, lo que puede atribuirse a que este elemento forma hidróxidos con multitud de cavidades que retienen mayor cantidad de agua; esto se evidencia a través de los gráficos de TGA de los materiales. Despues de la salida de moléculas de agua, ocurren reacciones de descomposición de los grupos hidróxidos y de los aniones carbonato, con el subsecuente colapso de la estructura HTLc y la formación de los óxidos metálicos. En todos los materiales se originó un segundo pico en temperaturas inferiores a 350°C que está asociado a los procesos de descomposición ya mencionados. Posteriormente, a temperaturas mayores se observaron picos atribuidos a la formación de los óxidos de aluminio o de aluminatos.

En temperaturas superiores a 600°C se observaron pérdidas de masa que pueden deberse a la salida de CO_2 , producto de la descomposición de los aniones carbonato que quedaron ocluidos en los poros de los sólidos debido al colapso de la estructura, o que pudieron haber reaccionado con los iones metálicos presentes para formar especies del tipo $(\text{Cu},\text{Zn})\text{Al}_x\text{O}_y(\text{CO}_3)_z$ que también se descomponen a altas temperaturas liberando CO_2 (17).

Conclusiones

El método de síntesis permitió obtener la estructura HTLc en todos los materiales, sin embargo, el aumento del contenido de cobre condujo a la formación de pequeñas cantidades de la fase $\text{Cu}(\text{OH})_2$ que limitan el crecimiento de las partículas de la estructura HTLc y disminuyen la estabilidad térmica de los sólidos formados. Todos los materiales presentaron señales asociadas a la presencia de las especies características de hidrotalcitas que contenían el ion carbonato. Se observó que el aumento del contenido de aluminio condujo a una mayor retención de moléculas de agua en la zona interlaminares y a una mayor interacción entre estas y los iones carbonato, así como al aumento de la estabilidad térmica de los sólidos. El efecto Jahn-Teller se evidenció a través de la formación del $\text{Cu}(\text{OH})_2$ en los sólidos con mayor cantidad de cobre y en el aumento de la frecuencia de vibración Cu-O-H en estos materiales. Se observó que la descomposición de la fase HTLc a bajas temperaturas conduce al encapsulamiento de aniones carbonato al interior de los sólidos, bien sea en la forma del CO_2 , producto de reacciones de descomposición o como especies del tipo $(\text{Cu},\text{Zn})\text{Al}_x\text{O}_y(\text{CO}_3)_z$, que pueden formarse por la reacción con los iones metálicos presentes, las cuales se descomponen en temperaturas mayores de 600°C .

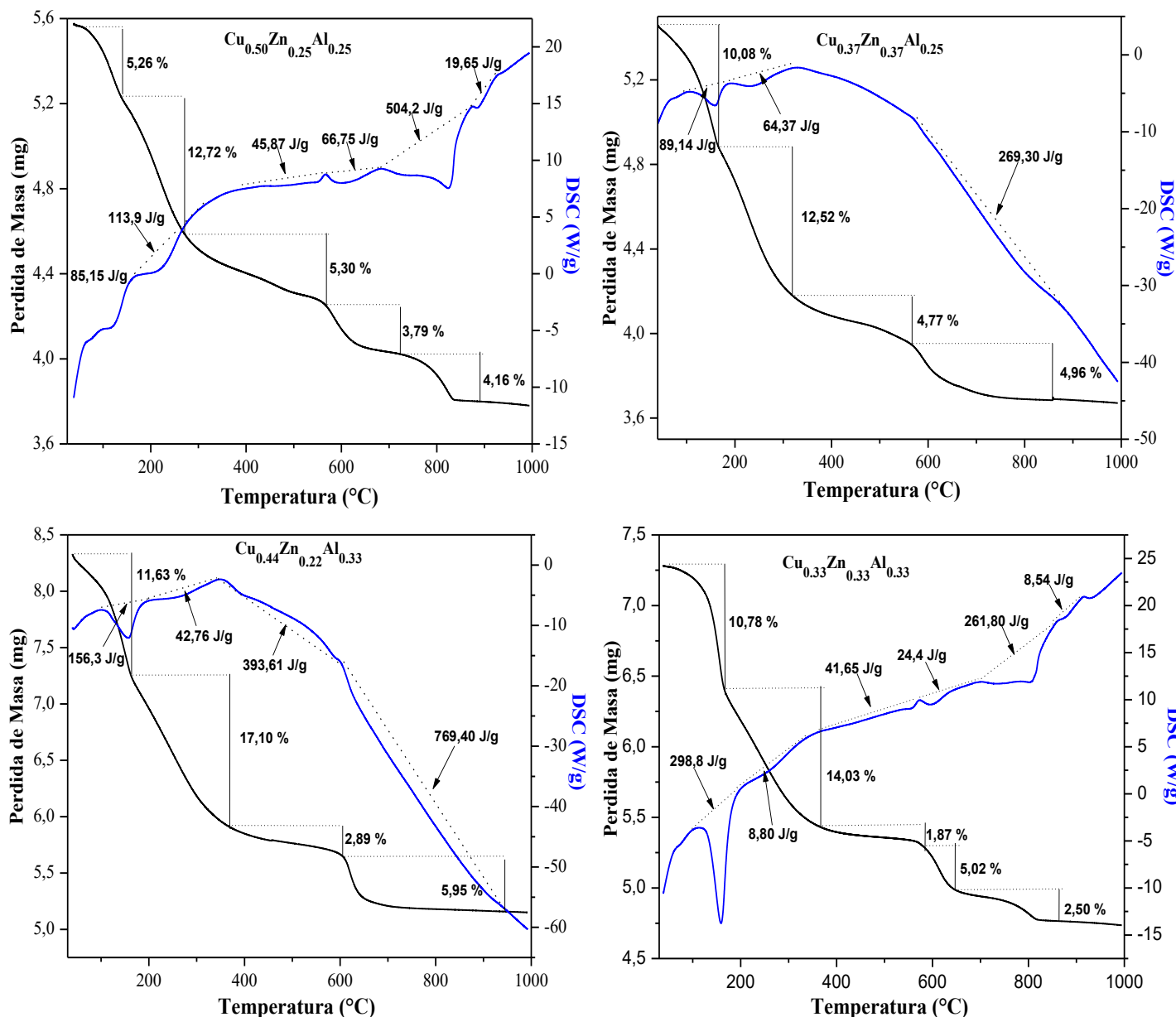


Figura 3. Curvas de TGA y DSC de los sólidos sintetizados.

Referencias

- Cavani, F.; Trifiro, F.; Vaccari, A. Hydrotalcite-type anionic clays: preparation, properties and application. *Catal. Today* **1991**, *11*, 173-301. DOI: [https://doi.org/10.1016/0920-5861\(91\)80068-k](https://doi.org/10.1016/0920-5861(91)80068-k).
- Crepaldi, E.L.; Barros Valim.; J. Hidróxidos duplos lamelares: síntese, estrutura, propriedades e aplicações. *Quím. Nova* **1998**, *21*, 300-311. DOI: <https://doi.org/10.1590/s0100-40421998000300011>.
- Pascale, F.; Tosoni, S.; Zicovich-Wilson, C.; Ugliengo, P.; Orlando, R.; Dovesi, R. Vibrational spectrum of brucite, Mg(OH)₂: a periodic ab initio quantum mechanical calculation including OH anharmonicity. *Chem. Phys. Letters* **2004**, *396*, 308-315. DOI: <http://dx.doi.org/10.1016/j.cplett.2004.08.047>.
- Melián-Cabrera, I.; López Granados, M.; Fierro, J. L. G. Thermal decomposition of a hydrotalcite-containing Cu-Zn-Al precursor: thermal methods combined with an in situ DRIFT study. *Phys. Chem. Chem. Phys.* **2002**, *4*, 3122-3127. DOI: <https://doi.org/10.1039/b201996e>.

5. Goh, K.; Lim, T.; Dong, Z. Application of layered double hydroxides for removal of oxyánions: A review. *Water Res.* **2008**, *42*, 1343-1368. DOI: <https://doi.org/10.1016/j.watres.2007.10.043>.
6. Jiang, L.; Ye, Binghuo; Wei, Kemei. Effects of CeO₂ on structure and properties of Ni-Mn-K/bauxite catalysts for water-gas shift reaction. *J. Rare Earth.* **2008**, *26*, 352-356. DOI: [https://doi.org/10.1016/s1002-0721\(08\)60094-0](https://doi.org/10.1016/s1002-0721(08)60094-0).
7. Meza-Fuentes, E.; Costa Faro, A.; Freitas Silva, T.; Mansur Assaf J.; Rangel M. A comparison between copper and nickel-based catalysts obtained from hydrotalcite-like precursors for WGSR. *Catal. Today*, **2011**, *171*, 290-296. DOI: <https://doi.org/10.1016/j.cattod.2011.03.082>.
8. Iglesias, A. H.; Ferreira, O. P.; Gouveiaab, D. X.; Souza Filho, A. G.; de Paiva, J.A.C.; Mendes Filho, J.; Alves, O. L. Structural and thermal properties of Co-Cu-Fe hydrotalcite-like compounds. *J. Solid. State. Chem.*, **2005**, *178*, 142-152. DOI: <http://dx.doi.org/10.1016/j.jssc.2004.10.039>.
9. Newman, S. P.; Jones, W. Synthesis, characterization and applications of layered double hydroxides containing organic guests. *New J. Chem.*, **1998**, *22*, 105-115. DOI: <https://doi.org/10.1039/a708319j>.
10. Gupta S.; Agarwal, D.; Banerjee, S. Thermal stabilization of poly (vinyl chloride) by hydrotalcites, zeolites, and conventional stabilizers. *J. Vinyl. Addit. Techn.* **2009**, *15*, 164-170. DOI: <https://doi.org/10.1002/vnl.20196>.
11. Touahra, F.; Sehailia, M.; Ketir, W.; Bachari, K.; Chebout, R.; Trari, M.; Cherifi, O.; Halliche, D. Effect of the Ni/Al ratio of hydrotalcite-type catalysts on their performance in the methane dry reforming process. *Applied Petrochem Res.* **2016**, *6*, 1-13. DOI: <http://dx.doi.org/10.1007/s13203-015-0109-y>.
12. Dębek, R.; Motak, M.; Duraczynska, D.; Launay, F.; Galvez, M.; Grzybek, T.; Da Costa, P. Methane dry reforming over hydrotalcite-derived Ni-Mg-Al mixed oxides: The Influence of Ni content on catalytic activity, selectivity and stability. *Catal. Sci. Technol.* **2016**, *6* (17), 6705-6715. DOI: <http://dx.doi.org/10.1039/c6cy00906a>.
13. Espinal, R.; Taboada, E.; Molins, E.; Chimentao R.; Medina, F.; Llorca, J. Ethanol Steam Reforming Over Hydrotalcite-Derived Co Catalysts Doped with Pt and Rh. *Topics in Catal.* **2013**, *56* (18), 1660-1671. DOI: <https://doi.org/10.1007/s11244-013-0100-8>.
14. Meza Fuentes, E.; Cadete Santos Aires, F. J.; Prakash, S.; da Costa Faro, A.; de Freitas Silva, T.; Mansur Assaf J.; Rangel M. The effect of metal content on nickel-based catalysts obtained from hydrotalcites for WGSR in one step. *Inter. J. Hydrogen Energy* **2014**, *39*, 1-14. DOI: <https://doi.org/10.1016/j.ijhydene.2013.10.114>
15. Costantino, U.; Marmottini, F.; Sisani, M.; Montanari, T.; Ramis, G.; Busca, G.; Turco, M.; Bagnasco, G. Cu-Zn-Al hydrotalcites as precursors of catalysts for the production of hydrogen from methanol. *Solid State Ionics* **2005**, *176*, 2917-2922. DOI: <http://dx.doi.org/10.1016/j.ssi.2005.09.051>.
16. Wang, X.; Andrews, L. Infrared spectra of M(OH)_{1,2,3} (M = Mn, Fe, Co, Ni) molecules in solid argon and the character of first row transition metal hydroxide bonding. *J. Phys. Chem. A*, **2006**, *110*, 10035-10045. DOI: <http://dx.doi.org/10.1021/jp0624698>
17. Kannan, S.; Rives, V.; Knözinger, H. High-temperature transformations of Cu-rich hydrotalcites. *J. Solid. State. Chem.* **2004**, *177*, 319-331. DOI: <https://doi.org/10.1016/j.jssc.2003.08.023>

Article citation:

Rodríguez-Ruiz, J.; Pájaro-Payares, A.; Meza-Fuentes, E. Síntesis y caracterización estructural de hidrotalcitas de Cu-Zn-Al. *Rev. Colomb. Quim.* **2016**, *45* (3), 33-38. DOI: <http://dx.doi.org/10.15446/rev.colomb.quim.v45n3.61381>.



Mónica A. Gordillo¹, Fabio Zuluaga¹, Manuel N. Chaur^{1,*}

¹Grupo de Investigación Síntesis y Mecanismos de Reacción en Química Orgánica (SIMERQO)
Departamento de Química, Universidad del Valle, A.A., 25360 Cali, Colombia.

*Autor para correspondencia: manuel.chaur@correo.univalle.edu.co

Recibido: 6 de Junio de 2016. Aceptado: 27 de Septiembre de 2016.

Acylhydrazone-based dynamic combinatorial libraries: study of the thermodynamic/kinetic evolution, configurational and coordination dynamics

Abstract

The kinetic and thermodynamic selectivity of acylhydrazone formation in dynamic combinatorial libraries (DCL) is described. Competition reactions were generated from hydrazides: isoniazid, 4-nitro-benzohydrazide, 4-dimethylamino-benzohydrazide, and nicotinic hydrazide as well as the aldehyde derivatives: benzaldehyde and 2-pyridine-carboxaldehyde. The obtained species and the distribution of the DCLs were monitored by ¹H-NMR spectroscopy finding that those acylhydrazones containing the 4-dimethylamino-benzohydrazide moiety are both the kinetic and thermodynamic product of their respective libraries. Configurational and coordination dynamics for some of these libraries were also investigated. The obtained results allowed the study of the redistribution of components and the amplification of one or more products using light and metal ions as physical and chemical templates, respectively.

Keywords: dynamic combinatorial chemistry, acylhydrazones, coordination and configurational dynamics.

Librerías combinatorias dinámicas basadas en acil-hidrazone: estudio del desarrollo termodinámico/cinético, dinámicas de configuración y de coordinación

Resumen

Se describe la selectividad cinética y termodinámica de la formación de acil-hidrazone en bibliotecas combinatorias dinámicas (DCL). Se generaron reacciones competitivas a partir de hidrazidas: isoniazida, 4-nitro-benzohidrazida, 4-dimetilamino-benzohidrazida y hidrazida nicotínica; así como a partir de los derivados de aldehído: benzaldehído y 2-piridin-carboxaldehído. Las especies obtenidas y la distribución de los DCLs fueron monitoreados mediante espectroscopía ¹H-NMR, encontrándose que las acil-hidrazonas que contenían la 4-dimetilamino-benzohidrazida son tanto el producto cinético, como el termodinámico de sus respectivas bibliotecas. También se investigaron las dinámicas de configuración y de coordinación para algunas de estas bibliotecas. Los resultados obtenidos permitieron estudiar la redistribución de los componentes y la amplificación de uno o más productos usando luz e iones metálicos como plantillas físicas y químicas, respectivamente.

Palabras clave: bibliotecas combinatorias dinámicas, acil-hidrazonas, dinámicas de coordinación y configuración.

Livrarias combinatórias dinâmicas baseadas na acil-hidrazone: estudo da evolução cinética/termodinâmica, dinâmicas de configuração e da coordenação

Resumo

É descrita a seletividade cinética e termodinâmica da formação de acil-hidrazonas em livrarias combinatórias dinâmicas (DLC). Foram geradas reações competitivas a partir das hidrazidas: isoniazida, 4-nitro-benzohidrazida, 4-dimetilamino-benzohidrazida e hidrazida nicotínica; além dos derivados de aldeído: benzaldeído e 2-piridin-carboxaldeído. As espécies obtidas e a distribuição dos DLCs foram monitorados mediante espectroscopia ¹H-NMR, foi encontrado que as acil-hidrazonas que continham à 4-dimetilamino-benzohidrazida são tanto o produto cinético como o termodinâmico de suas respectivas livrarias. Também investigaram-se as dinâmicas de configuração e coordenação para algumas destas livrarias. Os resultados obtidos permitem estudar a redistribuição dos componentes e a amplificação de um ou mais produtos usando luz e íons metálicos como modelos físicos e químicos, respectivamente.

Palavras-Chave: livrarias combinatórias dinâmicas, acil-hidrazonas, dinâmicas de coordenação e configuração.

Introduction

Dynamic combinatorial chemistry (DCC) is a powerful tool to study and create complex chemical systems in a relative simple manner. DCC was defined by Sanders as molecular or supramolecular combinatorial chemistry under thermodynamic control (1). When a system is formed by molecular fragments that can react with each other, combining them, a mixture of many compounds that interconverts constantly, will be obtained, i.e. building blocks are connected together by reversible bonds which are continuously forming and breaking in the reaction medium (Figure 1). This product mixture is known as Dynamic Combinatorial Library (DCL). The system is reversible and it is in equilibrium, thus, any external effect could shift this equilibrium. A clean-cut example of these systems and relating Emil Fisher's concept is placing a template in the system, which fits precisely with one member of the library, and subsequently amplify or shift the equilibrium towards the formation of a product (2).

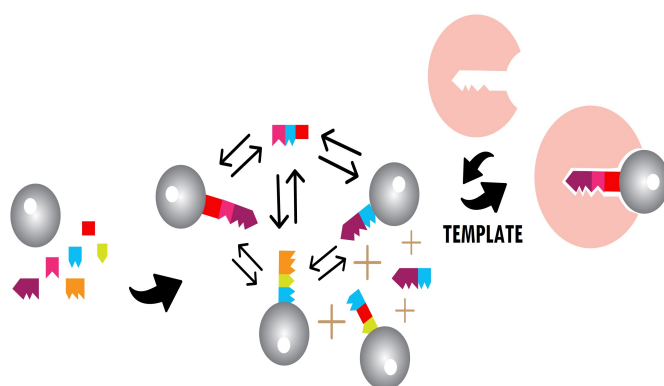


Figure 1. Formation of a DCL from "building blocks" and the addition of a template, which causes amplification of the member forming the more stable complex.

DCC and DCL's have been widely used for the synthesis and identification of small molecular receptors (3-7). These tools have also helped to generate effective ligands for biomacromolecules and biosensors (8-10), synthesis of catalysts (11-13), crosslinked materials (14-16), capsules and cages (17-19), self-replication (20), nanomachines (21), among others.

Based on previous work done by Lehn's group (22-24), we have chosen a set of four hydrazides and two aldehydes as building blocks in order to generate several dynamic combinatorial libraries. These building blocks were selected since the acylhydrazones, which can be formed, have a number of characteristics that make them attractive for DCL's formation: i) unlike the hydrazones, the acylhydrazones have a much weaker double bond making them favorable to perform exchange reactions; ii) these compounds have an imino double bond, which has been widely investigated in our research group and it is known that is sensitive to light (25-26); iii) some of these compounds have coordination sites in their chemical structure that serve as tridentate ligand to coordinate to cation metals. Having in mind these characteristics, we have analyzed how the distributions of the formed libraries vary by the presence of the metals and UV light as external stimuli. For this purpose, nuclear magnetic resonance technique was used as a tool for monitoring the evolution of the dynamic library.

Materials and methods

All starting materials, reagents and solvents, were purchased from Sigma-Aldrich and Alfa Aesar. The hydrazides were used without any further purification. The benzaldehyde was distilled under reduced pressure. ^1H and ^{13}C -NMR spectra were taken in a 400 MHz Bruker UltraShield spectrometer. UV-Vis spectra were recorded in a Shimadzu UV-1700 PharmaSpec spectrophotometer.

Standard procedure for the preparation of acylhydrazones

One eq of aldehyde **A-B** was added to an ethanol solution (5.0 mL) of the corresponding hydrazide **1-4** (1 eq) with 5.0 μL of glacial acetic acid. The mixture was heated under reflux of ethanol for 3 to 6 h. The resulting precipitate was collected by vacuum filtration and recrystallized from cold ethanol to afford the pure acylhydrazones in their *E*-configuration.

Standard procedure for the preparation of DCLs

The DCLs were prepared by mixing in a sealed NMR tube (under inert atmosphere of N_2 , done in a Aldrich AtmosBag) 1 eq of the corresponding aldehydes (225 μL) and acylhydrazines (225 μL) in $\text{DMSO}-d_6$ or CD_3OD at 25 °C. The starting time of reaction ($t = 0$) was considered as the time in which the solution of aldehydes was poured into the NMR tube and entered in contact with the hydrazines solution. ^1H -NMR spectroscopy was used as a tool to monitor the evolution of the library. For those experiments involving UV radiation, a 250 W mercury lamp was used as an UV source. The NMR tube was irradiated while pouring the reagents; in a second experiment the NMR tube with the compounds was allowed to equilibrate during 24 h. Afterwards, the tube was irradiated during 1 h. For the addition of metal ions, solutions of the corresponding M^{2+} ion were standarized by atomic absorption spectroscopy calculating the concentration in a calibration curve.

Results and discussion

When mixing aldehydes and hydrazines redacción: a large number of ^1H -NMR signals are obtained making difficult to identify the products. Therefore, each possible acylhydrazone, as part of the library, was synthesized from each corresponding hydrazide and aldehyde derivatives, according to a methodology reported previously (22) (Figure 2). The reactions were monitored by thin layer chromatography (TLC), and the spectroscopic data were consistent with the proposed structures (*E* configuration) of compounds **A-1** to **B-4** (Figure 3). Details of the synthesis were described in the Materials and methods section.

The synthesis was performed with the aim to identify characteristic signals in the ^1H -NMR spectra of each acylhydrazone. Signals found in the region between 11.5 and 12.5 ppm, which correspond to the N-H protons (as determined by 2D NMR techniques), were chosen to determine the distribution of the products on the libraries (see *Characterization data for acylhydrazones*) and further confirmed by DOSY experiments to corroborate the assignment of the N-H proton signals.

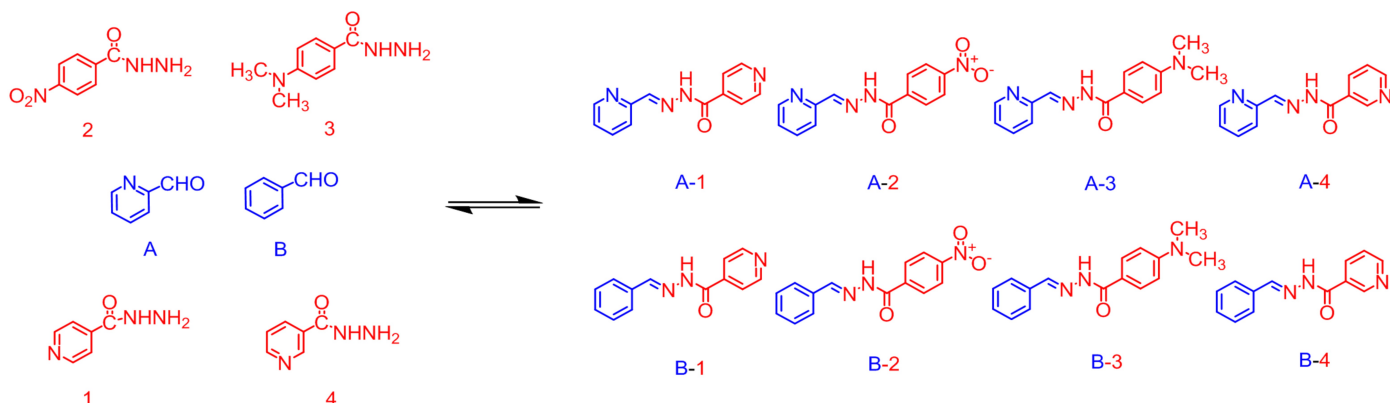


Figure 2. Building blocks (hydrazides and aldehydes) and constituent products of hydrazones-based libraries.

The fact that the signals of the N-H protons of each acylhydrazone appear at different chemical shifts, results from the type of substituent, which is present in every one of them, since they contain either electron-withdrawing groups, electron-releasing groups or an electronegative nitrogen at different positions on the ring.

Characterization data for acylhydrazones

2-pyridinecarboxaldehyde isonicotinoyl hydrazone (A-1): Using the method described above, the compound was synthesized and obtained in a 86% yield. M.p.: 166-167°C. Elemental analysis calcd. (%) for $C_{12}H_{10}N_4O$: C, 63.71; H, 4.46; N, 24.76; found: C, 62.37; H, 4.23; N, 23.82. FT-IR (ATR) ν/cm^{-1} 3292 (N-H), 1665 (C=O), 1539 (C=N). 1H -NMR (400 MHz, DMSO-*d*6) δ 12.28 (s, 1H), 8.84-8.78 (m, 2H), 8.64 (d, J 4.29 Hz, 1H), 8.48 (s, 1H), 8.03-7.97 (m, 1H), 7.91 (td, J 7.71, 1.56 Hz, 1H), 7.86-7.82 (m, 2H), 7.45 (ddd, J 7.27, 4.93, 1.07 Hz, 1H). ^{13}C -NMR (100.60 MHz, DMSO-*d*6) δ 161.93, 152.96, 150.44, 149.65, 149.23, 140.26, 137.04, 124.74, 121.61, 120.13.

2-pyridinecarboxaldehyde p-nitrobenzoyl hydrazone (A-2): Using the method described above, the compound was synthesized and obtained in a 96% yield. M.p.: 227-228°C. Elemental analysis calcd. (%) for $C_{13}H_{10}N_4O_3$: C, 57.78; H, 3.73; N, 20.73; found: C, 57.86; H, 3.72; N, 20.62. FT-IR (ATR) ν/cm^{-1} 3221 (N-H), 1659 (C=O), 1595(C=N). 1H -NMR (400 MHz, DMSO-*d*6) δ 12.31 (s, 1H), 8.64 (d, J 4.29 Hz, 1H), 8.49 (s, 1H), 8.39 (d, J 8.59 Hz, 2H), 8.17 (d, J 8.59 Hz, 2H), 8.01 (d, J 7.80 Hz, 1H) 7.94-7.87 (m, 1H) 7.47-7.42 (m, 1H). ^{13}C -NMR (100.60 MHz, DMSO-*d*6) δ 161.76, 152.96, 149.59, 149.38, 149.12, 138.80, 136.95, 129.26, 124.65, 123.69, 120.08.

2-pyridinecarboxaldehyde p-dimethylamino-benzoyl hydrazone (A-3): Using the method described above, the compound was synthesized and obtained in a 87% yield. M.p.: 224-225°C. Elemental analysis calcd. (%) for $C_{15}H_{16}N_4O$: C, 67.15; H, 6.05; N, 20.88; found: C, 67.19; H, 6.07; N, 20.78. FT-IR (ATR) ν/cm^{-1} 3244 (N-H), 1611(C=O), 1516(C=N). 1H -NMR (400 MHz, DMSO-*d*6) δ 11.77 (s, 1H), 8.60 (d, J 4.49 Hz, 1H), 8.45 (s, 1H), 7.95 (d, J 7.80 Hz, 1H), 7.88 (dd, J 7.61, 1.56 Hz, 1H), 7.83 (d, J 8.98 Hz, 2H), 7.39 (dd, J 7.41, 4.88 Hz, 1H), 6.76 (d, J 8.98 Hz, 2H), 3.00 (s, 6H). ^{13}C -NMR (100.60 MHz, DMSO-*d*6) δ 163.09, 153.66, 152.61, 149.48, 146.32, 136.83, 129.24, 124.12, 119.67, 119.08, 110.84, 39.51.

2-pyridinecarboxaldehyde nicotinoyl hydrazone (A-4): Using the method described above, the compound was synthesized and obtained in a 91% yield. M.p.: 148-150°C. Elemental analysis calcd. (%) for $C_{12}H_{10}N_4O$: C, 63.71; H, 4.46; N, 24.76; found: C, 58.63; H, 4.74; N, 22.81. FT-IR (ATR) ν/cm^{-1} 3474 (N-H), 1668(C=O), 1593 (C=N). 1H -NMR (400 MHz, DMSO-*d*6) δ 12.24 (s, 1H), 9.08 (d, J = 1.56 Hz, 1H), 8.82-8.75 (m, 1H), 8.63 (d, J = 4.68 Hz, 1H), 8.46 (s, 1H), 8.28 (d, J = 7.80 Hz, 1H), 8.00 (d, J = 7.80 Hz, 1H), 7.94-7.86 (m, 1H), 7.59 (dd, J = 7.80, 4.88 Hz, 1H), 7.48-7.40 (m, 1H). ^{13}C -NMR (100.60 MHz, DMSO-*d*6) δ 162.12, 153.10, 152.61, 149.70, 148.75, 148.73, 137.13, 135.73, 129.05, 124.76, 123.83, 120.20.

Benzaldehyde isonicotinoyl hydrazone (B-1): Using the method described above, the compound was synthesized and obtained in a 71% yield. M.p.: 198-199°C. Elemental analysis calcd. (%) for $C_{13}H_{11}N_3O$: C, 69.32; H, 4.92; N, 18.66; found: C, 68.73; H, 4.89; N, 18.38. FT-IR (KBr) ν/cm^{-1} 3455 (N-H), 1692 (C=O), 1566 (C=N). 1H -NMR (400 MHz, DMSO-*d*6) δ 12.11 (s, 1H), 8.79 (d, J 4.10 Hz, 2H), 8.46 (s, 1H), 7.83 (d, J 3.90 Hz, 2H), 7.78-7.74 (m, 2H), 7.47 (br. s., 3H). ^{13}C -NMR (100.60 MHz, DMSO-*d*6) δ 161.65, 150.33, 149.07, 140.47, 134.01, 130.41, 128.90, 127.27, 121.53.

Benzaldehyde p-nitrobenzoyl hydrazone (B-2): Using the method described above, the compound B-2 was obtained with a 79% yield. M.p.: 260-262°C. Elemental analysis calcd. (%) for $C_{14}H_{11}N_3O_3$: C, 62.45; H, 4.12; N, 15.61; found: C, 61.65; H, 4.15; N, 15.35. FT-IR (KBr) ν/cm^{-1} 3450 (N-H), 1656 (C=O), 1554 (C=N). 1H -NMR (400 MHz, DMSO-*d*6) δ 12.17 (s, 1H), 8.47 (s, 1H), 8.37 (d, J 8.59 Hz, 2H), 8.15 (d, J 8.78 Hz, 2H), 7.78-7.73 (m, 2H), 7.49-7.45 (m, 3H). ^{13}C -NMR (100.60 MHz, DMSO-*d*6) δ 161.61, 149.31, 149.03, 139.11, 134.06, 130.44, 129.21, 128.93, 127.31, 123.69.

Benzaldehyde p-dimethylamino-benzoyl hydrazone (B-3): Using the method described above, the compound was synthesized and obtained in a 82% yield. M.p.: 283-285°C. Elemental analysis calcd. (%) for $C_{16}H_{17}N_3O$: C, 71.89; H, 6.41; N, 15.72; found: C, 71.48; H, 6.50; N, 15.82. FT-IR (KBr) ν/cm^{-1} 3223 (N-H), 1614 (C=O), 1524 (C=N). 1H -NMR (400 MHz, DMSO-*d*6) δ 11.57 (br. s., 1H), 8.42 (br. s., 1H), 7.82 (d, J 8.78 Hz, 2H), 7.70 (d, J 6.63 Hz, 2H), 7.48-7.40 (m, 3H), 6.76 (d, J 8.98 Hz, 2H), 3.00 (s, 6H). ^{13}C -NMR (100.60 MHz, DMSO-*d*6) δ 163.07, 152.48, 145.96, 134.68, 129.69, 128.79, 126.84, 119.44, 110.81.

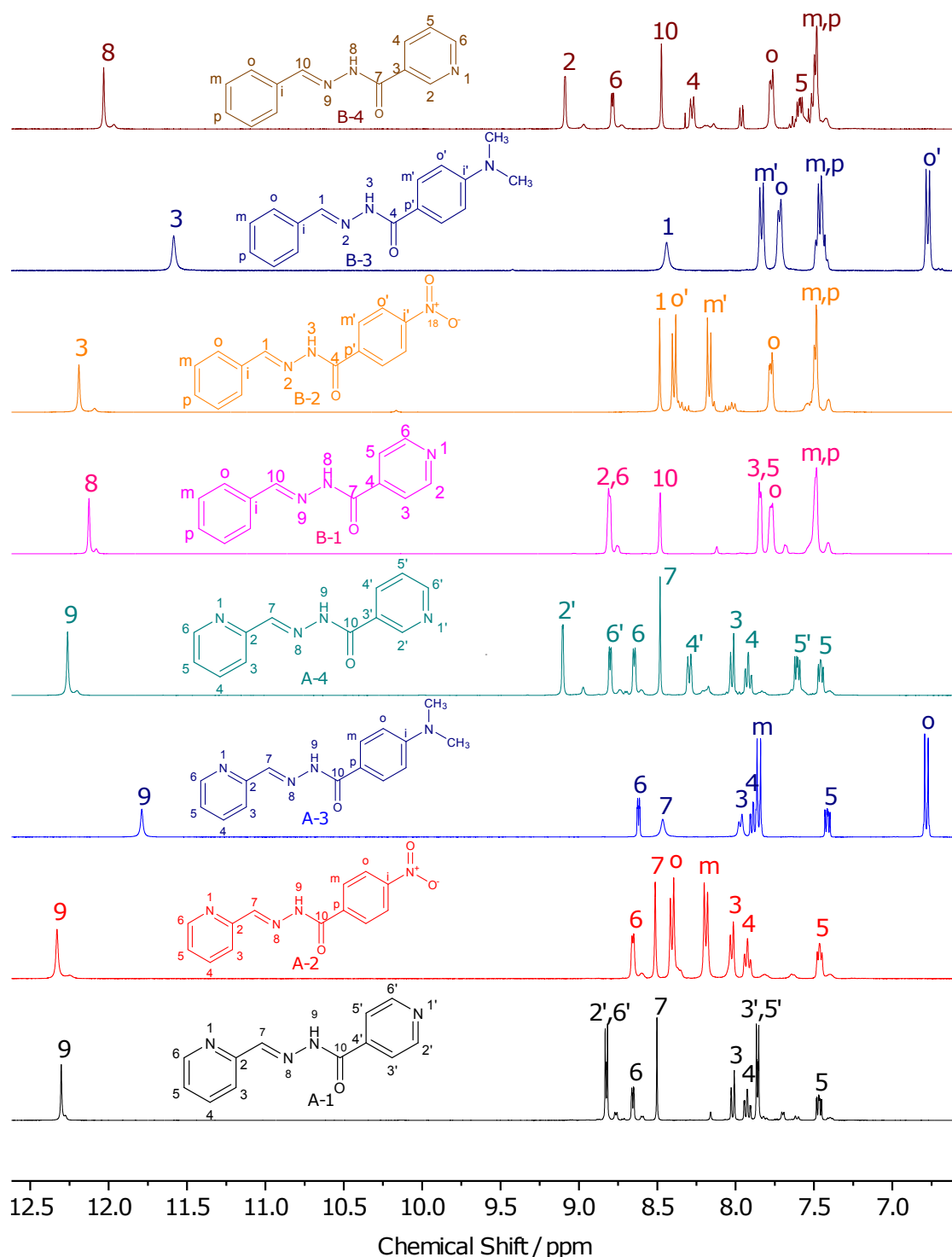


Figure 3. ¹H-NMR (400 MHz, DMSO-*d*6) spectra of the products of dynamical combinatorial libraries.

Benzaldehyde nicotinoyl hydrazone (B-4): Using the method described above, the compound was synthesized and obtained in a 70% yield. M.p.: 129–130°C. Elemental analysis calcd. (%) for C₁₃H₁₁N₃O: C, 69.32; H, 4.92; N, 18.66; found: C, 67.47; H, 4.94; N, 17.68. FT-IR (KBr) v/cm⁻¹ 3270 (N-H), 1653 (C=O), 1550 (C=N).

¹H-NMR (400 MHz, DMSO-*d*6) δ 12.01 (s, 1 H), 9.07 (d, J 1.17 Hz, 1 H), 8.77 (d, J 3.90 Hz, 1 H), 8.46 (s, 1 H), 8.26 (d, J 7.80 Hz, 1 H), 7.79–7.71 (m, 2 H), 7.57 (dd, J 7.80, 4.88 Hz, 1 H), 7.50–7.45 (m, 3 H). ¹³C-NMR (100.60 MHz, DMSO-*d*6) δ 161.67, 152.26, 148.54, 135.41, 134.10, 130.24, 129.22, 128.84, 128.52, 127.17, 123.58.

Competitive reactions of acylhydrazines 1-4 with aldehydes A and B

Two competitive reactions, named DCL-1 and DCL-2, were carried out from the hydrazides 1-4 and aldehyde **A** (DCL-1) or **B** (DCL-2) by mixing equimolar amounts of the respective building blocks in a NMR tube and using a deuterated solvent (Figure 2). The libraries with **A** and **B** were monitored for 320 min by ¹H-NMR spectroscopy, further time did not show any changes in the relative concentration of the DCL. The relative amount of acylhydrazone formed was calculated from the relative intensities of the corresponding signals and compared to an internal standard (1,4-dioxane). As shown in Figure 4 for DCL-1 and Figure 5 for DCL-2, the appearance of four new signals in the aforementioned region shows the formation of the four corresponding acylhydrazones (**A-1**, **A-2**, **A-3** and **A-4**).

From the NMR data, kinetic traces for acylhydrazone formation were plotted. Additionally, equilibrium distributions of the different acylhydrazones are shown in Figure 6. From these results, it is observed that **A-3** and **B-3** are the acylhydrazones kinetically and thermodynamically favored in their respective DCLs. The latter is understood based on the greater nucleophilicity of acylhydrazine 3.

Likewise, the highest rate of formation and stability of **A-3** and **B-3** may also be explained if we consider that the precursors of the other acylhydrazones have in their structure either one electron withdrawing group or an electronegative nitrogen in the aromatic ring, which by both inductive and resonance effects generate an electronic deficiency in the molecule, making it less reactive towards the nucleophilic attack of the nitrogen to the carbonyl group of the aldehyde (2).

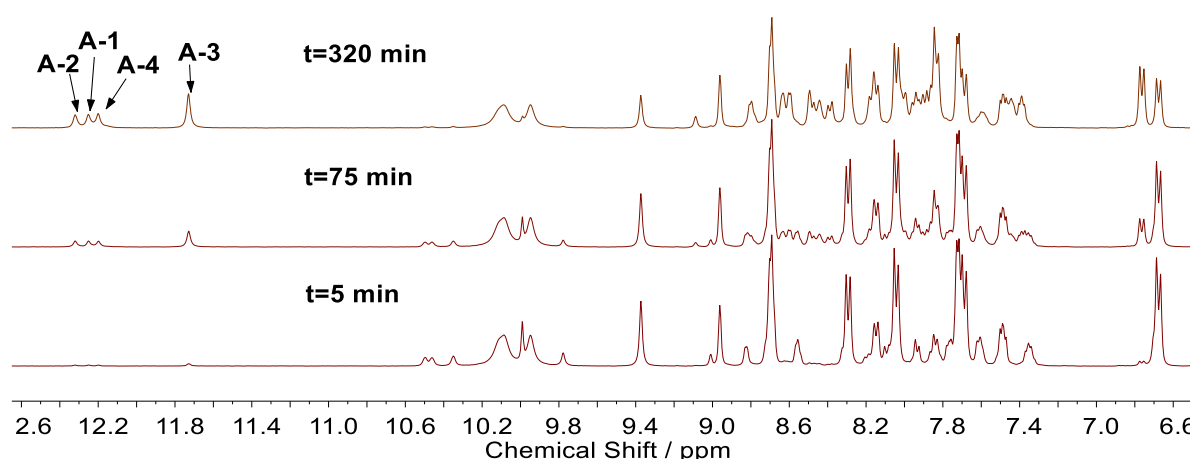


Figure 4. ¹H-NMR spectra at three selected (aleatorially) times of the DCL-1 formed by **1-4** and **A** in DMSO-*d*₆.

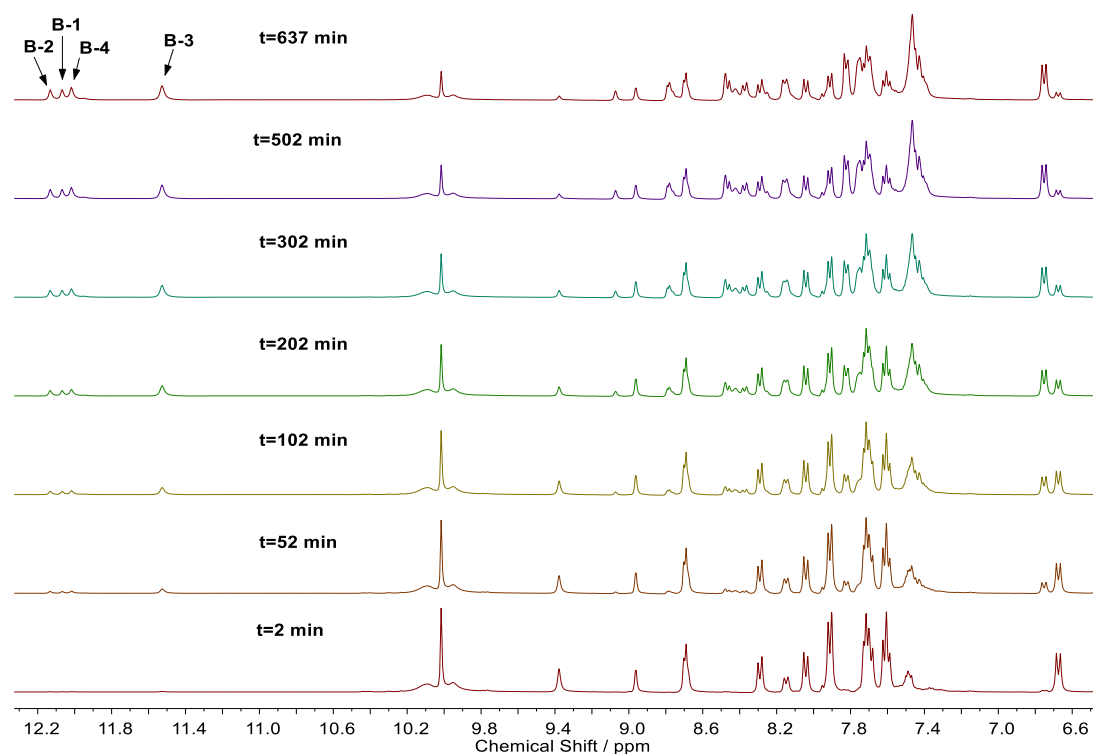


Figure 5. ¹H-NMR (400 MHz, DMSO-*d*6) spectra at different times of the library formed by **1-4** and **B** (DCL-2).

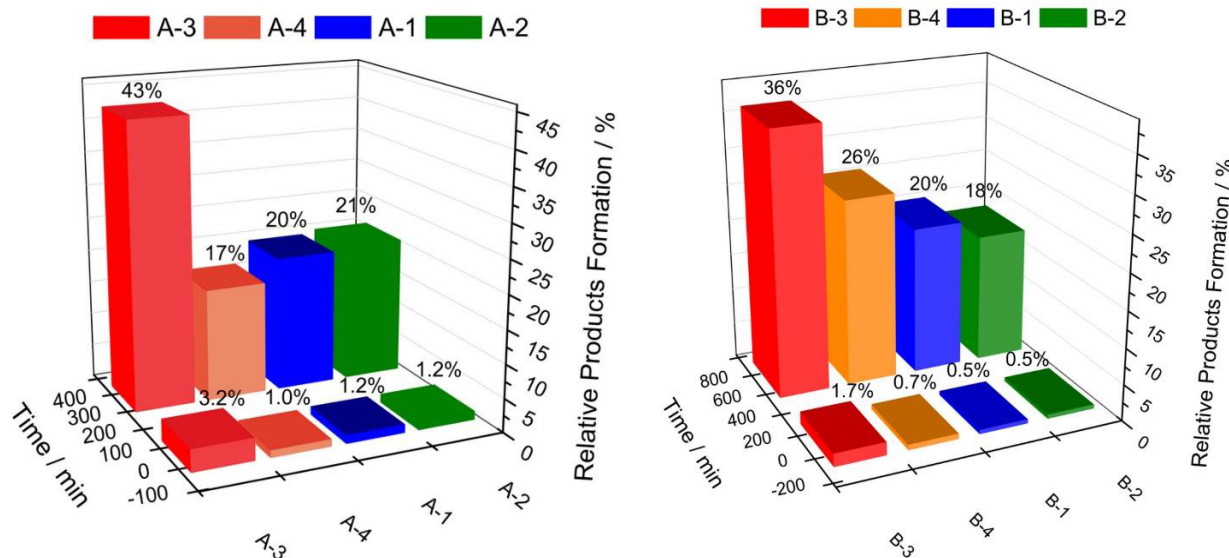


Figure 6. Equilibrium distributions of different acylhydrazones **A-1** to **A-4** (DCL-1, left) and **B-1** to **B-4** (DCL-2, right) in the DCL formed from aldehydes **A** and **B** and acylhydrazines **1-4**.

While in **A-3** and **B-3**, the dimethylamine group makes the molecule more electron-rich, thus conferring a higher reactivity for the nucleophilic attack, which is reflected in the greater proportion and the greater stability of this acylhydrazones. Although equilibrium was confirmed by a control experiment using different starting concentrations of previously prepared acylhydrazones reaching the same final distributions, it is important to remark that those distributions are reached in longer times which implies a slow amine interchange in the DCL. Despite that amine interchange can be increased by changing the nature of the solvent, this was not considered in this study to avoid issues with the solubility of the reagents.

DCL-3: hydrazides **1-4** plus aldehydes **A** and **B**

Aldehydes **A-B** were added to an equimolar mixture of hydrazides **1-4**. The reaction was monitored for 817 min, resulting in 168 ¹H-NMR spectra in total (some of them are shown in Figure 7).

Figure 8 shows the kinetic trace of the competition DCL reaction. According to the results, **A-3** is the kinetic product, not only for the larger nucleophilicity of acylhydrazine **3** but also for the larger electrophilicity of aldehyde **A**, which plays an important role in the reaction kinetics. Likewise, acylhydrazones formed from **A** were found in larger amounts than the ones formed from **B**.

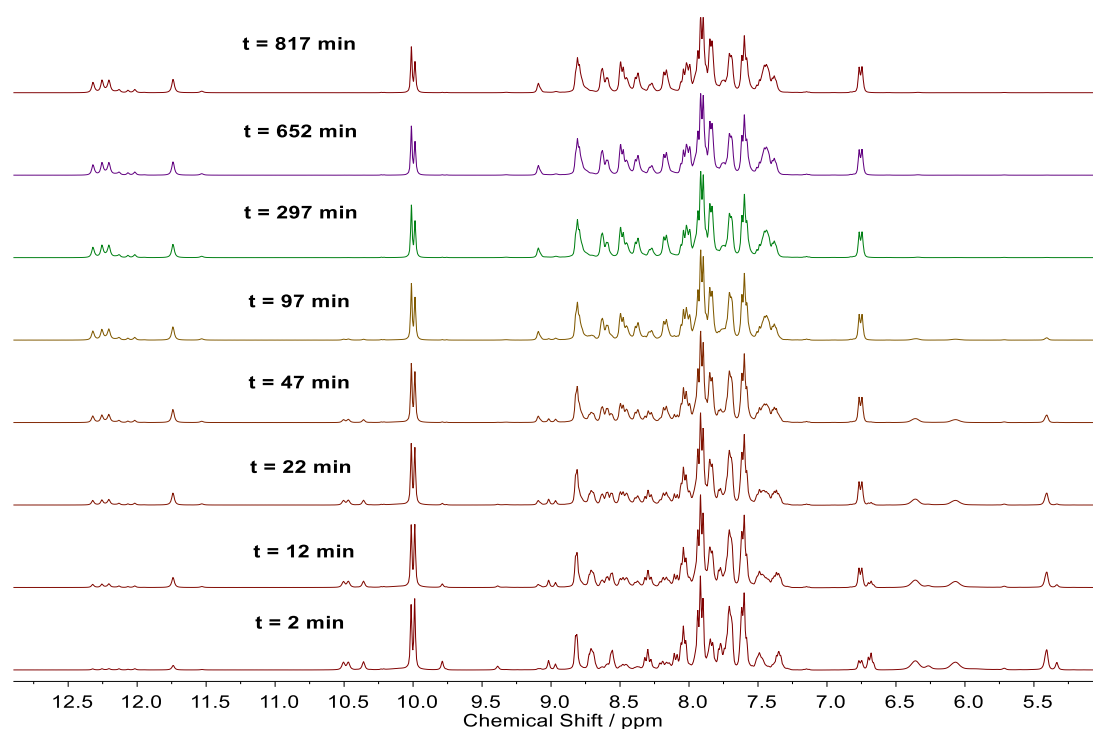


Figure 7. ¹H-NMR (400 MHz, DMSO-*d*₆) spectra at different times of the library formed by **1-4** and **A-B** (DCL-3).

This can be attributed to the electronegative nitrogen present in **A**, which by inductive effect causes the carbonyl group to be more electron deficient, making it more susceptible to nucleophilic attack. Noteworthy, data fit to a kinetic model is quite difficult for this system, however, within the first 8% of the reaction, the DCL follows a second order reaction with a 4-5% error, this allows to estimate that acylhydrazone **A-3** is generated in around 12-fold faster than its **B-3** counterpart. Interestingly, electrophilicity of the aldehyde is more important than acylhydrazine nucleophilicity in both, kinetic and thermodynamic control of the DCL. Upon equilibrium, **A**-containing acylhydrazones exhibit similar concentrations, which supports the dynamic character of the DCL.

The evident acylhydrazine interchange is probably due to the conjugation of the hydrazonic nitrogen (-NH-) with the carbonyl group which reduces the conjugation of this one with the imino group (C=N), making the latter a more reactive bond towards nucleophiles such as hydrazides or water (27). Therefore, the exchange reaction promotes another product to be formed at the expense of **A-3**, but still, at the end of the experiment ($t = 817$ min), this acylhydrazone continues to be the one with the highest percentage yield, therefore **A-3** is the thermodynamic product in the library. The difference between the greater proportion of acylhydrazones formed from **A**, as compared with the generated from **B**, confirms the higher reactivity of 2-pyridinecarboxaldehyde over benzaldehyde, due to the presence of an electronegative nitrogen atom in the ring.

Effect of UV light irradiation

Acylhydrazones formed from the aldehyde **A** exhibit, in the *Z* configuration, a thermodynamic stabilization by the formation of an intramolecular hydrogen bond between the amine hydrogen and the pyridine nitrogen upon photochemical isomerization. Meanwhile, the *Z* configuration of acylhydrazones from **B** do not exhibit this thermodynamic stabilization (25, 26). With this in mind, it was interesting to observe the effect of UV light irradiation on the acylhydrazone distribution of the DCLs. For this purpose, the library was formed only with hydrazides **1** and **4** as well as the aldehydes **A** and **B**, due to their solubility in MeOH-*d*₄.

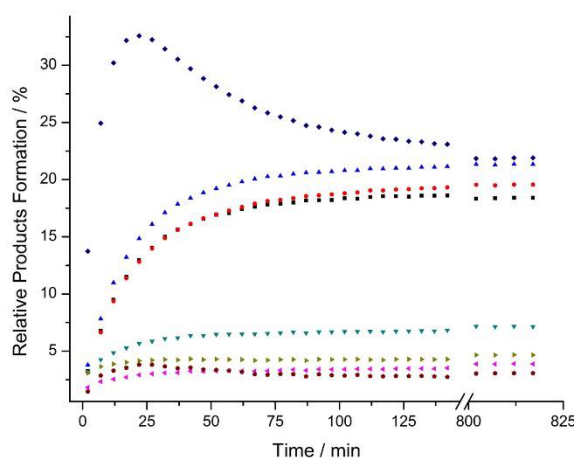


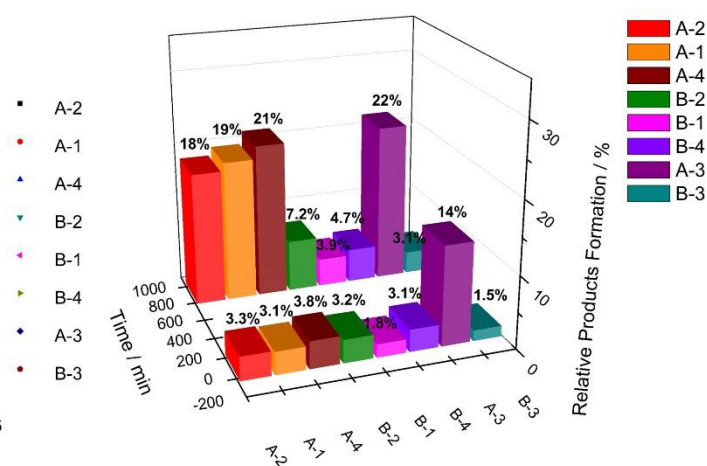
Figure 8. Kinetic trace of relative product formation over time of the library DCL-3.

The latter was used instead of DMSO-*d*₆ because photoisomerization experiments in DMSO-*d*₆ did not exhibit any appreciable changes, even after 150 min of UV irradiation, contrary to MeOH-*d*₄ (Figure 9). This contrasting result is due to the viscosity of DMSO which slows down the photoisomerization of hydrazone-based compounds (25-28).

In a typical procedure, a competition reaction was carried out until equilibrium was reached. Afterwards, the mixture was irradiated with UV light using a mercury lamp of 250 W. The competition reaction was monitored for 228 min. The relative concentrations of each acylhydrazone were calculated only at the end of the experiment and the results were 39/15/29/17% of **A-1/A-4/B-1/B-4**, respectively. The fact that those products containing the hydrazide **1** are in greater proportion, suggests that hydrazide **4** is less nucleophilic by the overall inductive effect that the N of the pyridine ring in position 3 has on the R group. Once the equilibrium was reached, the library was subjected to UV irradiation for 1 h and then was monitored by ¹H-NMR. It is remarkable the appearance of new signals in the spectra shown in Figures 10-12 which correspond to the *Z* isomers of compounds **A-1** and **A-4**.

The relative percentages shown in Table 1 were calculated by integrating those signals obtained in Figure 11 that are not overlapped and then by the subtraction between these and the overlapped ones, the integrals and therefore the percentages of the latters were obtained. From the distribution of acylhydrazones it can be observed that the product which is amplified after 60 min of UV light irradiation is the *Z* isomer of **A-1**, suggesting the adaptation of the library when a stimulus is applied. Vantomme *et al.* (27) also observed the same photoselection in a different DCL with similar yields of photoisomerization.

A second DCL was generated from the same building blocks (acylhydrazines **1** and **4** and aldehydes **A** and **B**) in the presence of UV light irradiation. For this purpose, the NMR tubes were irradiated with a mercury vapor lamp during 1 h before the reaction started. Afterwards, the ¹H-NMR spectra were taken to observe the distribution of the library (Figure 13). The amplified product for this DCL was the acylhydrazone **B-1** (Table 1). The presence of **A-1** and **A-4** *Z* isomers on the library proved that UV light is part of the system, however, this also indicates that whether UV light is added at the beginning or at the end of the reaction, the amplified product will be a different one.



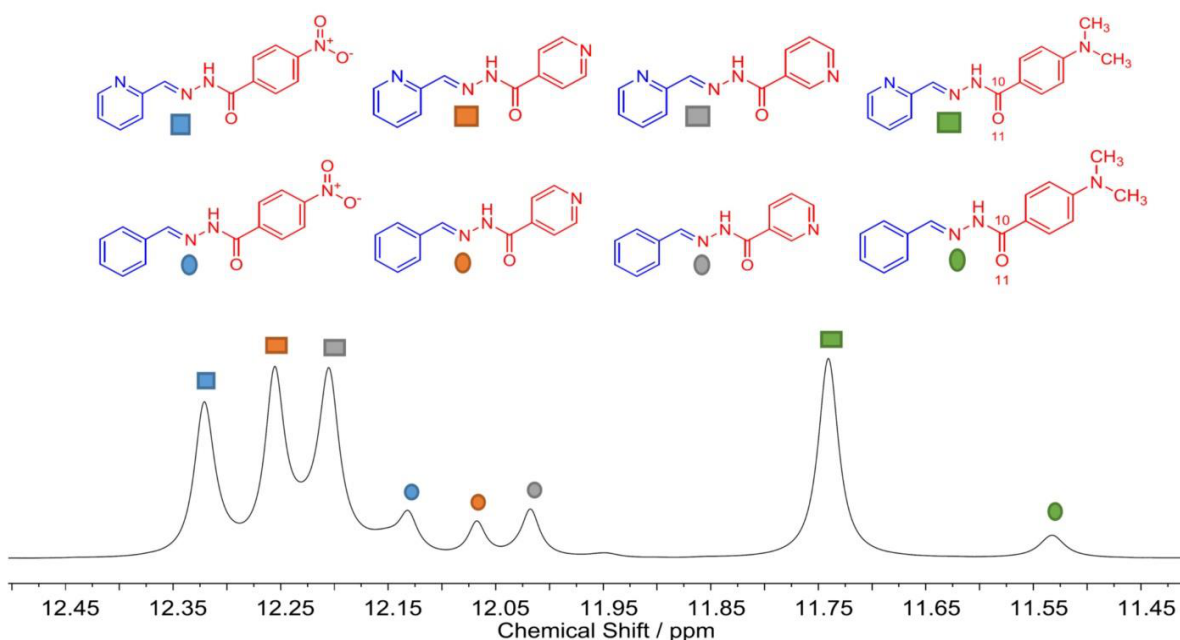


Figure 9. A portion of ^1H -NMR (400 MHz, $\text{DMSO}-d_6$) spectrum at $t = 817$ min and the assignment of signals.

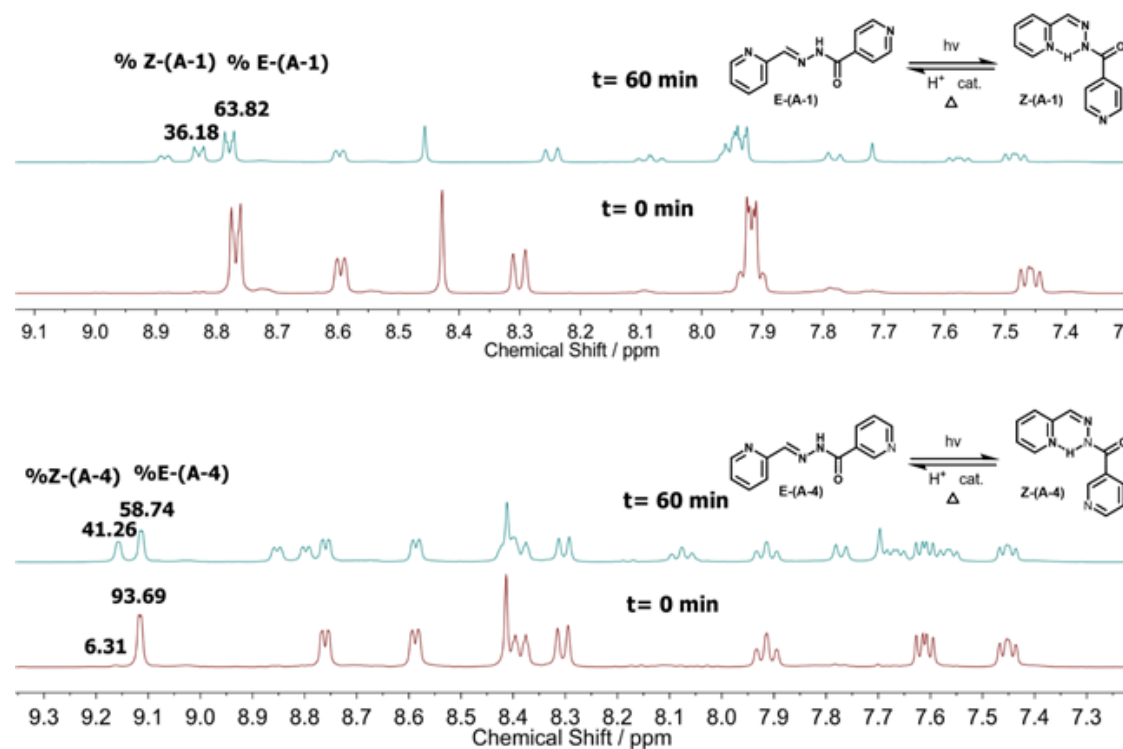


Figure 10. A portion of the ^1H -NMR (400 MHz, $\text{MeOH}-d_4$) spectra of acylhydrazones **A-1** (top) and **A-4** (bottom) taken at different times under UV irradiation.

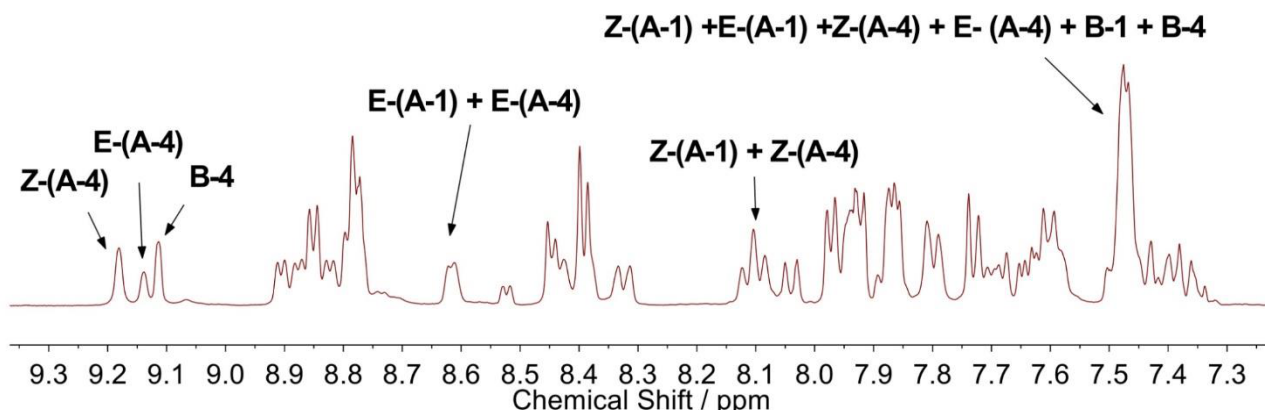


Figure 11. A portion of the ^1H -NMR spectra of the DCL-1 after 1h of irradiation in $\text{MeOH}-d_4$.

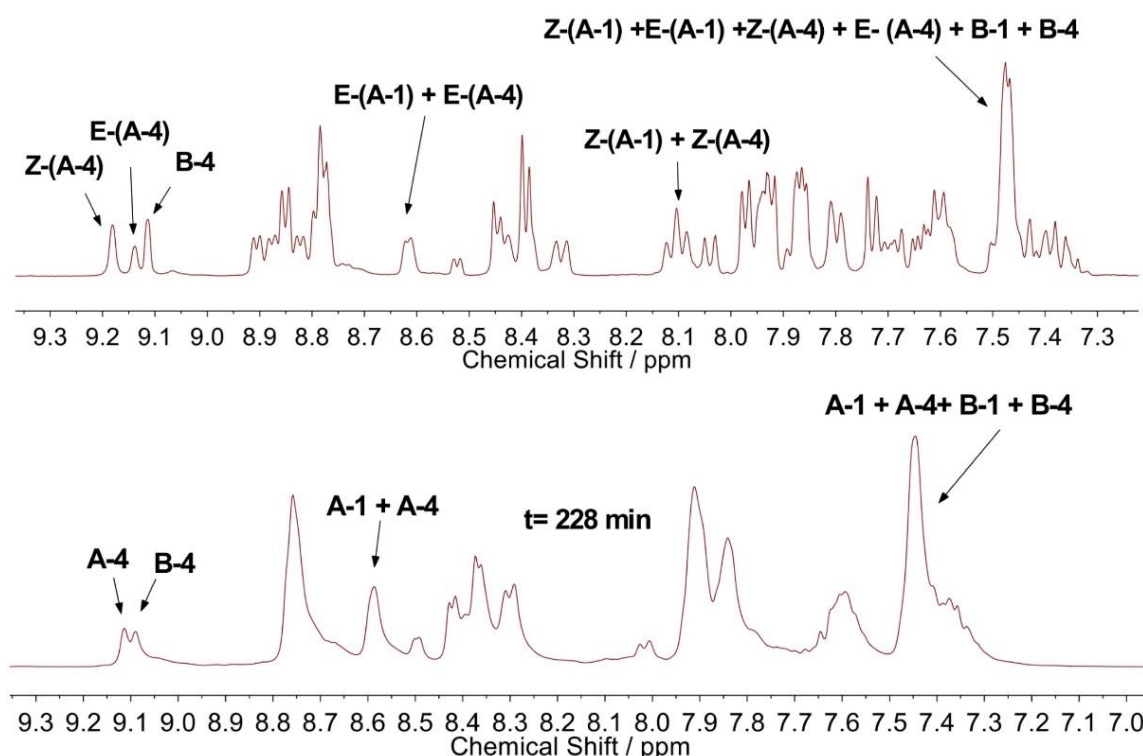


Figure 12. A portion of ^1H -NMR (400 MHz, $\text{MeOH}-d_4$) spectrum after irradiation with UV light.

Table 1. Relative percent of products observed in two DCL's

Acylhydrazone	Relative contribution (%)	
	DCL + UV light after equilibrium ^a	DCL + UV light from $t = 0^b$
(E)-A-1	13.5	12.8
(Z)-A-1	28.4	20.3
(E)-A-4	9.6	11.7
(Z)-A-4	18.6	12.0
B-1	11.5	24.7
B-4	18.4	18.5

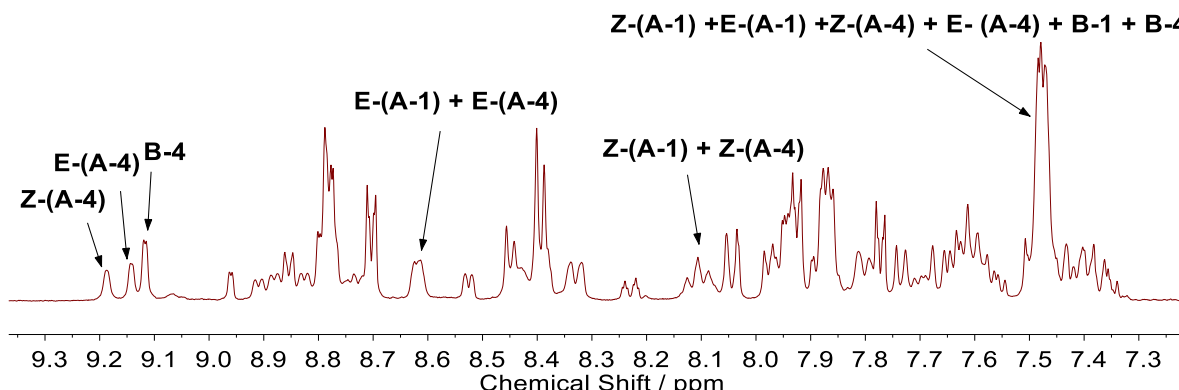


Figure 13. A portion of the ^1H -NMR spectra of the DCL in $\text{MeOH}-d_4$ irradiated with UV light at the beginning of reaction.

Noteworthy, in both cases the resulting product distribution is quite difficult to analyze even by the use of 2D NMR experiments, besides, once the UV light is removed the products concentrations do not go back to the previous distributions. These results imply that the system is in a metastable thermodynamic point due to the hydrogen bond formation (22, 25). In any case, these experiments proved the use of UV light as an irreversible template in DCL amplification and deserves further exploration.

Effect of the introduction of metal cations on DCL distributions

Finally, we wanted to explore the role of metal ions on DCL distributions, since it is well known that hydrazones and acylhydrazones derived from 2-pyridinecarboxaldehydes and 2-pyridinehydrazines or acylhydrazines are able to coordinate metal cations in a terpyrdine-like fashion (22, 25, 26). In this regard it can be thought that the introduction of metal ions can be used as a template to amplify acylhydrazones derived from aldehyde A. Accordingly, hydrazines **1** and **4** and aldehydes **A** y **B** were used to form the DCL; in addition, 0.5 eq of $\text{Zn}(\text{OTf})_2$ were added to the mixture, the reaction was monitored for 820 min. Comparing this library with other DCL in the present work (Figure 14) it was observed from the beginning of the reaction the appearance of only four N-H signals instead of eight corresponding to the formation of every possible acylhydrazone.

The ones that disappear, correspond to those acylhydrazones derived from aldehyde A, those which have a propitious structure to form a complex with Zn^{2+} by their tridentate NNO coordination site (28-32).

These signals disappearance are proof of the formation of ML_2 type complexes usually formed with this kind of ligands (22, 25-27). When they form a complex, these ligands are deprotonated, either because there is a relatively basic environment or because the enol form of the ligand predominates (32). Although it is known that the addition of this template (M^{2+} ions) results in the formation of such complexes, it is not possible to know which component is amplified, because the signals from each product are highly overlapped. Therefore, it is necessary to determine the binding and stability constants to have a clearer idea of what it is inside the solution.

Although DCLs have been studied with some detail over the last years, it is difficult to compare our results with the literature. Since, on one hand, most reports deal with the use of biological chemical templates and only one article introduces UV light to a DCL (based on aldehydes and hydrazines) obtaining similar results (27). On the other hand, metal ion selection has been studied for a more simple system (23) and similar to the present work a metalloselection was observed.

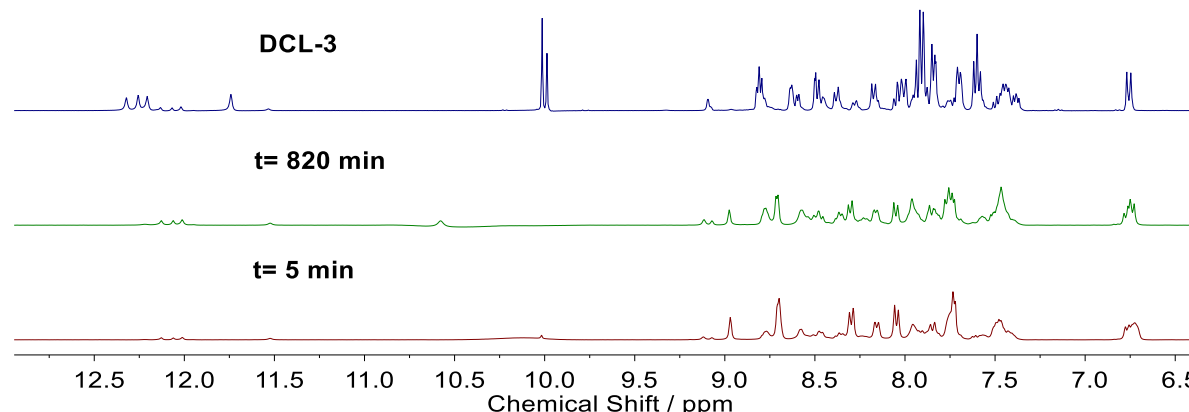


Figure 14. A portion of the ^1H -NMR spectra of the library formed from four hydrazides, both aldehydes and Zn^{2+} , in $\text{DMSO}-d_6$ and the spectrum of DCL-3.

Conclusions

Generation of dynamic combinatorial libraries derived from acylhydrazines **1-4** and aldehydes **A** and **B** were monitored by ¹H-NMR spectroscopy, achieving the calculation of the products distribution in time in most cases. The acylhydrazone **A-3** was both the kinetic and thermodynamic product of two of the formed libraries, confirming the greater nucleophilicity of the corresponding hydrazide due to the electron releasing character of the dimethylamino group and the higher electrophilicity of 2-pyridin-carboxaldehyde as compared with benzaldehyde, because of the presence of an electronegative nitrogen atom in its structure.

In competitive DCL reactions acylhydrazone products derived from hydrazide **1** (versus hydrazide **4**) were found in higher yields, suggesting that the reduced nucleophilicity of hydrazide **4** is due to the overall inductive effect that the pyridine ring N in position 3 has on the R group ($R=-(CO)-NH-NH_2$). Exposure to a physical stimulus such as irradiation with UV light, demonstrated that DCLs respond or adapt themselves to that stimulus, reorganizing and leading to the formation of a new library. In this particular case, it was also observed that depending on the time when the stimulus is added, the amplified product change, because the formation of the *E* isomer occurs first that the *Z* one, still in the presence of UV light.

Finally, the disappearance of the signals corresponding to the acylhydrazones NH_2 fragment derived from 2-pyridinecarboxaldehyde, by adding Zn^{2+} , demonstrates the formation of ML_2 type complexes and its amplification.

Acknowledgements

Authors are grateful to Vicerrectoría de Investigaciones and Centro de Excelencia en Nuevos Materiales (CENM) from Universidad del Valle (Colombia) for the financial support of this project. We also thank professor Julien Wist for his collaboration regarding NMR spectroscopy experiments.

References

- Corbett, P. T.; Leclaire, J.; Vial, L.; West, K. R.; Wieter, J. L.; Sanders, J. K. M. et al. Dynamic Combinatorial Chemistry. *Chem. Rev.* (Washington, DC, U. S.) **2006**, *106*, 3652. DOI: <http://dx.doi.org/10.1002/chin.200648268>.
- Cougnon, F. B. L.; Sanders, J. K. M. Evolution of Dynamic Combinatorial Chemistry. *Acc. Chem. Res.* **2012**, *45*, 2211. DOI: <https://doi.org/10.1021/ar200240m>.
- Custelcean, R. Dynamic chemistry of anion recognition. *Top. Curr. Chem.* **2012**, *322*, 193. DOI: https://doi.org/10.1007/128_2011_197.
- Bru, M.; Alfonso, I.; Burguete, M. I.; Luis, S. V. Anion-Templated Syntheses of Pseudopeptidic Macrocycles. *Angew. Chemie Int. Ed.* **2006**, *45*, 6155. DOI: <https://dx.doi.org/10.1002/anie.200602206>.
- Bru, M.; Alfonso, I.; Bolte, M.; Burguete, M. I.; Luis, S. V. Structurally disfavoured pseudopeptidic macrocycles through anion templation. *Chem. Commun.* **2011**, *47*, 283. DOI: <https://doi.org/10.1039/c0cc01784a>.
- Besenius, P.; Cormack, P. A. G.; Ludlow, R. F.; Otto, S.; Sherrington, D. C. Polymersupported cationic templates for molecular recognition of anionic hosts in water. *Chem. Commun.* **2008**, 2809. DOI: <https://doi.org/10.1039/b802982b>.
- Saggiomo, V.; Lüning, U. Transport of calcium ions through a bulk membrane by use of a dynamic combinatorial library. *Chem. Commun.* **2009**, 3711. DOI: <https://doi.org/10.1039/b902847a>.
- Verma, A.; Rotello, V. M. Surface recognition of biomacromolecules using nanoparticle receptors. *Chem. Commun.* **2005**, 303. DOI: <https://doi.org/10.1039/b410889b>.
- Ingerman, L. A.; Cuellar, M. E.; Waters, M. L. A small molecule receptor that selectively recognizes trimethyl lysine in a histone peptide with native protein-like affinity. *Chem. Commun.* **2010**, *46*, 1839. DOI: <https://doi.org/10.1039/c000255k>.
- Shi, B.; Stevenson, R.; Campopiano, D. J.; Greaney, M. F. Discovery of Glutathione S-Transferase Inhibitors Using Dynamic Combinatorial Chemistry. *J. Am. Chem. Soc.* **2006**, *128*, 8459. DOI: <https://doi.org/10.1021/ja058049y>.
- Vial, L.; Sanders, J. K. M.; Otto, S. A catalyst for an acetal hydrolysis reaction from a dynamic combinatorial library. *New J. Chem.* **2005**, *29*, 1001. DOI: <https://doi.org/10.1039/b505316a>.
- Gasparini, G.; Prins, L. J.; Scrimin, P. Exploiting Neighboring-Group Interactions for the Self-Selection of a Catalytic Unit. *Angew. Chemie Int. Ed.* **2008**, *47*, 2475. DOI: <https://doi.org/10.1002/anie.200703857>.
- Prins, L. J.; Scrimin, P. Covalent Capture: Merging Covalent and Noncovalent Synthesis. *Angew. Chemie Int. Ed.* **2009**, *48*, 2288. DOI: <https://doi.org/10.1002/anie.200803583>.
- Belowich, M. E.; Valente, C.; Stoddart, J. F. Template-Directed Syntheses of Rigid Oligorotaxanes under Thermodynamic Control. *Angew. Chemie Int. Ed.* **2010**, *49*, 7208. DOI: <https://doi.org/10.1002/anie.201004304>.
- Belowich, M. E.; Valente, C.; Smaldone, R. A.; Friedman, D. C.; Thiel, J.; Cronin, L.; Stoddart, J. F. Positive Cooperativity in the Template-Directed Synthesis of Monodisperse Macromolecules. *J. Am. Chem. Soc.* **2012**, *134*, 5243. DOI: <https://doi.org/10.1021/ja2107564>.
- Chung, M.-K.; White, P. S.; Lee, S. J.; Gagné, M. R. Synthesis of Interlocked 56-Membered Rings by Dynamic Self-Templating. *Angew. Chemie Int. Ed.* **2009**, *48*, 8683. DOI: <https://doi.org/10.1002/anie.200903478>.
- Mal, P.; Breiner, B.; Rissanen, K.; Nitschke, J. R. White Phosphorus Is Air-Stable Within a Self-Assembled Tetrahedral Capsule. *Science* **2009**, *324*, 1697. DOI: <https://doi.org/10.1126/science.1175313>.
- Horiuchi, S.; Murase, T.; Fujita, M. Noncovalent Trapping and Stabilization of Dinuclear Ruthenium Complexes within a Coordination Cage. *J. Am. Chem. Soc.* **2011**, *133*, 12445. DOI: <https://doi.org/10.1021/ja205450a>.
- Pluth, M. D.; Bergman, R. G.; Raymond, K. N. Acid Catalysis in Basic Solution: A Supramolecular Host Promotes Orthoformate Hydrolysis. *Science* **2007**, *316*, 85. DOI: <https://doi.org/10.1126/science.1138748>.
- Sadownik, J. W.; Philp, D. A Simple Synthetic Replicator Amplifies Itself from a Dynamic Reagent Pool. *Angew. Chemie Int. Ed.* **2008**, *47*, 9965. DOI: <https://doi.org/10.1002/anie.200804223>.
- Von Delius, M.; Geertsema, E. M.; Leigh, D. A. A synthetic small molecule that can walk down a track. *Nat. Chem.* **2010**, *2*, 96. DOI: <https://doi.org/10.1038/nchem.481>.
- Chaur, M. N.; Collado, D.; Lehn, J.-M. Configurational and Constitutional Information Storage: Multiple Dynamics in Systems Based on Pyridyl and Acyl Hydrazones. *Chem. A Eur. J.* **2011**, *17*, 248. DOI: <https://doi.org/10.1002/chem.201002308>.

23. Vantomme, G.; Lehn, J.-M. Photo- and Thermoresponsive Supramolecular Assemblies: Reversible Photorelease of K⁺ Ions and Constitutional Dynamics. *Angew. Chem. Int. Ed.* **2013**, *52*, 3940. DOI: <https://doi.org/10.1002/anie.201210334>.
24. Vantomme, G.; Hafezi, N.; Lehn, J.-M. A light-induced reversible phase separation and its coupling to a dynamic library of imines. *Chem. Sci.* **2014**, *5*, 1475. DOI: <https://doi.org/10.1039/c3sc53130a>.
25. Romero, E.; D'Vries, R.; Zuluaga, F.; Chaur, M. Multiple Dynamics of Hydrazone Based Compounds. *J. Braz. Chem. Soc.* **2015**, *26*, 1265. DOI: <https://doi.org/10.5935/0103-5053.20150092>.
26. Chaur, M.N. Aroylhydrazones as potential systems for information storage: photoisomerization and metal complexation. *Rev. Colomb. Quim.* **2012**, *41*, 349-358. DOI: <https://doi.org/10.15446/rev.colomb.quim.v43n1.50540>.
27. Vantomme, G.; Jiang, S.; Lehn, J.-M. Adaptation in Constitutional Dynamic Libraries and Networks, Switching between Orthogonal Metalloselection and Photoselection Processes. *J. Am. Chem. Soc.* **2014**, *136*, 9509. DOI: <https://doi.org/10.1021/ja504813r>.
28. Lehn, J.-M. Conjecture: Imines as Unidirectional Photodriven Molecular Motors—Motional and Constitutional Dynamic Devices. *Chemistry* **2006**, *12*, 5910. DOI: <https://doi.org/10.1002/chem.200600489>.
29. Stadler, A.-M.; Harrowfield, J. Bis-acyl-/aroyl-hydrazones as multidentate ligands. *Inorganica Chim. Acta* **2009**, *362*, 4298. DOI: <https://doi.org/10.1016/j.ica.2009.05.062>.
30. Pouralimardan, O.; Chamayou, A.-C.; Janiak, C.; Hosseini-Monfared, H. Hydrazone Schiff base-manganese(II) complexes: Synthesis, crystal structure and catalytic reactivity. *Inorganica Chim. Acta* **2007**, *360*, 1599. DOI: <https://doi.org/10.1016/j.ica.2006.08.056>.
31. Mangalam, N. A.; Sivakumar, S.; Sheeba, S. R.; Prathapachandra Kurup, M. R.; Tiekkink, E. R. T. Chemistry of molecular and supramolecular structures of vanadium(IV) and dioxygen bridged V (V) complexes incorporating tridentate hydrazone ligands. *Inorganica Chim. Acta* **2009**, *362*, 4191. DOI: <https://doi.org/10.1016/j.ica.2009.06.029>.
32. Bernhardt, P. V; Chin, P.; Sharpe, P. C.; Richardson, D. R. Hydrazone chelators for the treatment of iron overload disorders: iron coordination chemistry and biological activity. *Dalton Trans.* **2007**, *9226*, 3232. DOI: <https://doi.org/10.1039/b704102k>.

Article citation:

Gordillo, M. A.; Zuluaga, F.; Chaur, M. N. Acylhydrazone-based dynamic combinatorial libraries: study of the thermodynamic/kinetic evolution, configurational and coordination dynamics. *Rev. Colomb. Quim.* **2016**, *45* (3), 39-50. DOI: <http://dx.doi.org/10.15446/rev.colomb.quim.v45n3.61408>.

Descripción

La Revista Colombiana de Química (Rev. Colomb. Quim., versión online ISSN 2357-3791, versión impresa ISSN 0120-2804) es una publicación científica arbitrada, del Departamento de Química, Facultad de Ciencias de la Universidad Nacional de Colombia sede Bogotá. Desde su lanzamiento en 1971, y hasta 1980, la Revista Colombiana de Química publicó un volumen por año y su periodicidad cambió a uno o dos volúmenes por año desde 1981 hasta 2006. A partir de 2007 y hasta la fecha publica tres volúmenes por año. Todos sus volúmenes se encuentran disponibles online en el sitio web <http://www.revistas.unal.edu.co/index.php/rkolquim/index>.

La Revista Colombiana de Química se encuentra indexada en las bases de datos SCOPUS, PUBLINDEX, DOAJ, SCIELO, LATINDEX Y REDALYC. Esta publicación cuenta con un Comité Científico y Editorial compuesto por investigadores de reconocida trayectoria en sus áreas de especialidad y acepta contribuciones relevantes en las diversas áreas de la química tales como química analítica, bioquímica, orgánica, fisicoquímica, alimentos, inorgánica, ciencias de materiales, organometálica, enseñanza de la química, entre otras. El público objetivo son profesionales relacionados con cualquier área de la química.

Tipos de artículos

Artículos de investigación

Son artículos que presentan resultados de investigación que no han sido publicados previamente. Los autores deben resaltar la contribución de su trabajo al conocimiento. Se sugiere un máximo de 40 referencias.

Artículos de revisión

Serán solicitados por invitación del Comité Editorial, teniendo en cuenta la experiencia de los autores en un determinado tema. Son artículos que presentan el estado actual del conocimiento sobre un tema. En este tipo de artículos, el autor además de efectuar la revisión, debe establecer su aporte y criterio propios. Debe presentar más de 50 referencias, preferiblemente de los últimos 5 años.

Ética

En la Revista Colombiana de Química se toma como código de conducta ética el propuesto por el Comité de Ética de Publicaciones (COPE): <http://publicationethics.org/> para editores de revistas científicas. En este se sancionan el plagio y la autoría fantasma, la duplicación de resultados o cualquier otro tipo de modificación fraudulenta. De igual modo se promueve y aplica un sistema de evaluación por pares donde se garantiza el anonimato de autores y evaluadores.

Conflictos de intereses

La revista define un conflicto de interés como cualquier asunto que interfiera en: la presentación completa y objetiva, la revisión por pares, la toma de decisiones editoriales, o la publicación de artículos de investigación presentados a la revista. El conflicto de intereses puede ser de naturaleza financiera y no financiera, profesional o personal, y puede surgir en relación a una organización u otra persona.

Envío y esquema de revisión general

Los manuscritos enviados a la Revista Colombiana de Química para su posible publicación deben ser inéditos (**no sometidos al mismo tiempo a ninguna otra revista impresa o digital**). Los autores son responsables por las opiniones e ideas declaradas en el manuscrito. La precisión de la información en los manuscritos, incluyendo figuras y tablas, es responsabilidad completa del autor o de los autores.

Los manuscritos serán recibidos para su evaluación vía correo electrónico (rcolquim_fcbog@unal.edu.co) o a través de la plataforma en línea de la Revista (<http://www.revistas.unal.edu.co/index.php/rkolquim>).

Requisitos generales de envío

1. Para los envíos a través del portal en línea, el autor debe estar registrado en el portal, de no ser el caso debe registrarse siguiendo los pasos necesarios. Antes de comenzar, es importante que compruebe que su envío cumple escrupulosamente todos los requisitos solicitados por la revista (Ver sección Preparación para el envío online).
2. La versión del documento en línea no debe incluir resumen ni datos de autores, estos se incluyen en los metadatos, es decir, en el formulario de envío. Por el contrario, si el artículo es enviado por correo electrónico debe contener todos los datos que se especifican en la sección Formato.

Para las dos formas de envío deben adjuntarse una carta de presentación del artículo, donde se incluyan los aspectos más relevantes del artículo, una lista de tres posibles evaluadores con sus respectivos datos de contacto y firma de todos los autores.

4. Las fotos, diagramas, mapas y gráficas se enumeran como figuras. Las fotos y mapas deben adjuntarse en un archivo aparte, en formato TIFF o JPEG al tamaño en que van a salir, con 300 dpi de resolución, y en escala de grises o en blanco y negro. En caso de que tengan 4 o más ítems, se debe cambiar la escala de grises por diferentes tramas. No se deben insertar en Word ya que pierden la resolución, y en el programa de diseño van a salir pixeladas. Si las gráficas corresponden a archivos trabajados en Excel o Word se deben enviar en dichos programas, pero abiertas, no como imagen para que se puedan editar.

Esquema de revisión

- Después de recibir el artículo y verificar que cumpla con el formato establecido en esta guía, se envía a revisión por pares según el tema tratado.
- Después de recibir las evaluaciones, se envía la decisión del Comité Editorial al autor de correspondencia:
 - Aceptado con cambios mínimos:** Los autores deben enviar una nueva versión a la revista. Una vez el editor verifica que los cambios fueron realizados (los autores deben enviar una lista detallada con los cambios realizados o el porqué de los cambios no realizados), el artículo es aceptado.
 - Cambios mayores:** Los autores deben enviar una nueva versión a la revista, la cual será sometida a evaluación corta (los autores deben enviar una lista detallada con los cambios realizados o el porqué de los cambios no realizados).
 - Rechazado:** Los autores deciden si someten una nueva versión a la revista, la cual será tratada como un artículo nuevo.
- Si el artículo es aceptado aparecerá inicialmente en formato pre impresión en la página Web de la revista (<http://www.revistas.unal.edu.co/index.php/rkolquim/index>). Posteriormente se reemplazará por la versión diagramada.

Formato

El documento se debe presentar en archivo Word .doc o .docx, tamaño carta, interlineado 2,0, con márgenes superior e inferior de 2,5 cm y 3,0 cm en los lados, con letra Times New Roman 12, páginas numeradas de inicio a fin. Se deben usar los títulos: **RESUMEN, ABSTRACT, RESUMO, INTRODUCCIÓN, MATERIALES Y MÉTODOS, RESULTADOS Y DISCUSIÓN, CONCLUSIONES, AGRADECIMIENTOS y REFERENCIAS.**

Idioma

Los manuscritos se aceptan en español, inglés o portugués, sin embargo, siempre **el título, resumen y palabras claves deben presentarse en los tres idiomas**. Como estrategia para aumentar la difusión y visibilidad de los resultados se sugiere presentar los manuscritos en inglés.

Página inicial

Título

El título debe ir en minúscula, a menos que la mayúscula sea mandatoria. Debe ser conciso pero informativo y no debe exceder 120 caracteres incluyendo los espacios. Debe aparecer siempre en español, inglés y portugués. Por ejemplo:

• Oxidación catalítica detolueno y 2-propanol sobre óxidos mixtos de Mn y Co obtenidos por coprecipitación.

• Catalytic oxidation of toluene and 2-propanol over Mn and Co mixed oxides obtained by coprecipitation method.

• A oxidação catalítica de tolueno e 2-propanol em óxidos mistos de Mn e de Co, obtidos por coprecipitação.

Autor(es) y filiación

- Nombres y apellidos completos.
- Último título profesional.
- Institución en la cual trabaja.
- País y ciudad de residencia.
- Correo electrónico (de cada autor).

En los datos de filiación se debe conservar el orden categórico: Laboratorio, instituto, universidad, ciudad, estado, país, e-mail. Cada filiación debe ser enlistada con números en superíndice y referenciada a cada autor. El autor de correspondencia debe ir denotado con asterisco. Por ejemplo:

Mauricio Acelas¹, Elizabeth Gil², Markus Doerr³, Martha Daza³, Juan Manuel Urbina^{1*}

¹Laboratorio de Química Orgánica y Biomolecular - LQOBio, Facultad de Ciencias, Universidad Industrial de Santander, Ciudad Universitaria, AA 678, Bucaramanga, Colombia.

²Facultad de Ciencias, Pontificia Universidad Javeriana, Carrera 7 N° 43-82, Bogotá D.C., Colombia.

³Grupo de Bioquímica Teórica - GBQT, Facultad de Ciencias, Universidad Industrial de Santander, Ciudad Universitaria, AA 678, Bucaramanga, Colombia.

*Autor para correspondencia: jurbina@uis.edu.co

Cuerpo del artículo

Todo el texto debe venir justificado (alineado a izquierda y derecha), con las páginas y líneas numeradas continuamente. Todos los títulos y subtítulos primarios y secundarios deben ir justificados a la izquierda. Los títulos (**RESUMEN, PALABRAS CLAVE, INTRODUCCIÓN, MATERIALES Y MÉTODOS, RESULTADOS Y DISCUSIÓN, AGRADECIMIENTOS, CONCLUSIONES y REFERENCIAS**) deben ir con mayúscula sostenida y negrilla. Los **subtítulos primarios** en minúsculas sostenida y en negrilla. Los **subtítulos secundarios** con minúscula sostenida y en cursiva. Siempre se deben definir los términos estadísticos, abreviaturas y los símbolos la primera vez que se usan en el artículo. Para las unidades de medida se debe usar el sistema métrico internacional.

Cuando no van seguidos de unidades, los números enteros hasta diez se escriben con la palabra (uno, dos, diez) y mayores de diez con números (11, 12, 102). Cuando se utilicen números, estos deben ir seguidos de sus unidades y se mantendrá un espacio entre uno y otro (100 m, 50 mL). Si se trata de porcentaje no deje espacio entre el número y la unidad (80%). En manuscritos escritos en español las cifras decimales irán separadas por coma (,) y en inglés por punto (.). Cite cada figura y tabla en el texto de acuerdo al orden de aparición y en el siguiente formato: Figura 1 o Figuras 1 y 2 o Figuras 1A-1F o Tabla 1.

Resumen

Resumen de máximo 200 palabras. Se sugiere poner una frase introductoria. Deben mencionarse los propósitos de la investigación, los resultados relevantes (proporcionando datos específicos y, de ser posible, su significación estadística), y las conclusiones principales sin incluir citas bibliográficas. Se debe hacer énfasis en los aspectos nuevos e importantes del estudio. Debe evitar presentarse un resumen descriptivo (aquel donde no se presentan datos), en cambio, debe presentarse un resumen analítico (aquel en donde se presentan los datos relevantes obtenidos en la investigación). Debe aparecer siempre en español, inglés y portugués.

Palabras clave

Deben listarse de 3 a 6 palabras claves. No se deben emplear las palabras ya usadas en el título del manuscrito. Deben aparecer siempre en español, inglés y portugués.

Introducción

Deben presentarse los fundamentos lógicos para la realización del trabajo. Solo se dan las referencias estrictamente oportunas y no se deben incluir datos o conclusiones del trabajo que se está publicando. Al final de la introducción, debe presentarse el objetivo del trabajo.

Materiales y métodos

En una subsección deben listarse los reactivos utilizados, la marca y el país. Se deben usar subtítulos en los procedimientos utilizados. Los procedimientos deben tener el detalle suficiente para permitir a otros profesionales reproducir la investigación. Se deben incluir los equipos empleados, incluyendo nombre del fabricante y país, además de las referencias de la metodología y métodos estadísticos. Deben describirse los métodos nuevos o los que han sido sustancialmente modificados, sustentando las razones para utilizarlos y evaluando sus limitaciones.

Los autores que envíen artículos de revisión, deberán describir los métodos empleados para localizar, seleccionar, extraer y sintetizar la información. Siempre que se hagan pruebas estadísticas, debe usarse un subtítulo “Análisis estadístico” para su descripción.

Resultados y discusión

Los resultados deben presentarse en un orden lógico y concordante con el orden de los métodos. Se deben destacar los resultados que contribuyen a la generación de nuevo conocimiento. La información contenida en tablas no debe repetirse en figuras y viceversa.

En la discusión deben destacarse los aspectos nuevos y relevantes del estudio, y evitar repetir información ya facilitada en la sección INTRODUCCIÓN. Se recomienda evaluar posibles relaciones entre los resultados obtenidos, juzgar los resultados en relación con los obtenidos por otros autores, y proponer hipótesis que expliquen los datos obtenidos. En esta sección debe haber una extensión mínima de tres páginas a doble espacio.

Conclusiones

Debe aparecer mínimo un párrafo con las conclusiones, vinculado a los objetivos del estudio, evitando enumerarlas o presentarlas como frases sueltas. Se deben realizar afirmaciones plenamente respaldadas por los datos.

Agradecimientos

Deben mencionarse las fuentes de financiación de los proyectos de investigación y/o apoyos recibidos para la realización del estudio (becas, equipos, reactivos, entre otros). Pueden nombrarse a aquellas personas que hayan prestado su ayuda intelectual al trabajo, pero cuyas contribuciones no justifiquen la autoría, describiendo la contribución llevada a cabo, por ejemplo, “apoyo técnico”, “revisión crítica del escrito”, “recolección de muestras”.

Referencias

El formato está basado en la guía de estilos de la American Chemical Society (ACS).

Referencias en texto: Todas las citas que aparecen en el texto deben coincidir con las presentadas en la sección REFERENCIAS, y viceversa.

Debe evitarse citar como bibliografía:

- Los resúmenes presentados en congresos u otras reuniones.
- Comunicaciones personales.
- Datos no publicados. La citación de un artículo “en prensa” supone que el artículo ya fue aceptado para publicación.

Las citas deben realizarse con números itálicos en paréntesis en la línea del texto, y dentro de la puntuación. Por ejemplo:

- Las condiciones de extracción se encuentran reportadas en otros estudios (1).

Si hay varias citas se separan con coma (,) sin espacios entre los números; si son citas consecutivas, se separan con guión (-). Por ejemplo:

- Los resultados obtenidos fueron similares a los reportados por otros autores (8, 26-30).

Las citas se deben escribir con números naturales acorde a su orden de aparición. Si dentro de la redacción del texto se debe mencionar el autor, entonces la citación debe ser:

- Un autor: Duque (2)
- Dos autores: Duque y Palomeque (3)
- Más de dos autores: Duque *et al.* (4)

Formato de referencias: Las referencias deben ser organizadas en el mismo orden numérico en el que fueron presentadas a lo largo del texto.

Revistas

Se debe anotar el apellido y las iniciales del nombre de todos los autores. Apellidos se separan de las iniciales del nombre con coma. Las iniciales de los nombres de autores se acompañan con punto. Los autores se separan con punto y coma. Luego se escribe el título. El nombre abreviado de la revista en cursiva, de acuerdo al Chemical Abstracts Service Source Index (CASSI, <http://cassi.cas.org/search.jsp>). El año en negrita, el volumen en itálica y las páginas (separadas por guion). De igual manera, si el artículo cuenta con DOI es necesario incluirlo al final de la referencia.

- Hasta seis autores: se incluyen todos los autores.

Da Silva, R.; Nissim, I.; Brosnan, M.; Brosnan, J. Creatine synthesis: Hepatic metabolism of guanidinoacetate and creatine in the rat in vitro and in vivo. *Am. J. Physiol. Endocrinol. Metab.* **2009**, 296, 256-261. DOI: <http://dx.doi.org/10.1152/ajpendo.90547.2008>.

- Más de seis autores: incluir hasta los seis primeros autores y a continuación escribir *et al.*

Libros y otras monografías

- Libros sin editores
 - Stout, J.; Antonio, J.; Kalman, D. *Essentials of creatine in sports and health*. Humana Press Inc.: Totowa, NJ, 2008; pp 30-40. DOI: <http://dx.doi.org/10.1007/978-1-59745-573-2>.
 - Budavari, S.; O'Neil, M. J.; Smith, A.; Heckelman, P. E.; Obenchain, J. R., Jr.; Gallipeau, J. A. R.; D'Arecea, M. A. *The merck index, an encyclopedia of chemicals, drugs, and biologicals*, 13th ed. Merck & Co., Inc.: Whitehouse Station, NJ, 2001; pp 1768-1769.
- Libros con editores
 - Rowe, R. C.; Sheskey, P. J.; Owen, S. C. (eds.). *Handbook of pharmaceutical excipients*, 5th ed. Pharmaceutical Press and American Pharmacists Association: Grayslake, IL, 2006; pp 798-799.
- Capítulo en libro editado
 - McBrien, M. Selecting the Correct pH Value for HPLC. In *HPLC made to measure: A practical handbook for optimization*; Kromidas, S., Ed.; Wiley-VCH: Weinheim, Germany, 2006; pp 89-103.

Libros y otras monografías

- Impreso
 - King, K. J. Development of a pressurized system for oxidation studies of volatile fluids. M.S. Thesis, The Pennsylvania State University, State College, PA, Marzo 1983.
- Electrónico
 - Abrams, N. M. Efficiency enhancement in dye-sensitized solar cells through light manipulation. Ph.D. Dissertation [Online], The Pennsylvania State University, University Park, PA, December 2005. <http://etda.libraries.psu.edu/theses/approved/WorldWideIndex/ETD-1061/index.html> (consultado el 2 de abril de 2014).

Sitios Web

Penn State Department of Chemistry. <http://www.chem.psu.edu/> (consultado el 7 de junio de 2014).

Mallet Chemistry Library, University of Texas Libraries. ThermoDex home page: An index of selected thermodynamic and physical property resources. <http://www.lib.utexas.edu/thermodex/> (consultado el 19 de marzo de 2014).

En prensa

Martínez, F.; Jouyban, A.; Acree, W. E., Jr. Comments on “Solubility and thermodynamic function of a new anticancer drug ibrutinib in 2-(2-ethoxyethoxy)ethanol + water mixtures at different temperatures”. *J. Chem. Thermodyn.* **2015**. In press. DOI: <http://dx.doi.org/10.1016/j.jct.2015.11.031>

Tablas y figuras

Las fotos, diagramas, mapas y gráficas se clasifican como figuras. Deben usarse figuras como alternativa a las tablas; evite redundancia entre tablas, figuras y texto.

Las figuras con sus leyendas deben enviarse individualmente en formato .TIFF, de excelente calidad, con una resolución mínima de 300 dpi y con uno de dos tamaños (9 cm de ancho, que es una columna, o 20 cm que cubre las dos columnas). La impresión a color no genera costos adicionales para los autores, sin embargo, representa un mayor costo para la revista. Teniendo esto en cuenta, se debe utilizar escala de grises o tramas siempre que sea posible. Deben usarse colores cuando sea estrictamente necesario. Figuras que hayan sido creadas en Excel o Word deben ser enviadas en esos programas. Las tablas deben estar en el cuerpo del artículo al final del documento. Tanto las tablas como las figuras deben ser autocontenido (poder interpretarse sin necesidad de recurrir al cuerpo del artículo). En la leyenda de la figura, o en el título o pie de la tabla, deben describirse las claves, abreviaturas y demás explicaciones. Se recomienda proporcionar además de los promedios, las desviaciones estándar y demás información estadística relevante a los datos.

La rotulación de cada tabla debe ir a la cabeza de la misma, mientras que en las figuras debe presentarse al pie. Evite figuras pequeñas aisladas: agrupe figuras con información relacionada en figuras compuestas rotuladas con letras (Figura 1a, Figura 3b, etc.). Si un artículo contiene tablas o figuras reproducidas (así sean del mismo autor), es obligación declarar el origen y presentar permiso para utilizarlas. Es responsabilidad de los autores conseguir el correspondiente permiso. Si tiene dudas al respecto, por favor comunicarse con la revista vía correo electrónico (recolquim_febog@unal.edu.co) o por teléfono (+571 3165000 Ext. 14458).

Preparación para el envío online

Antes de realizar el envío de su manuscrito ya sea por el Portal o por correo electrónico, verifique que cumple con las siguientes condiciones:

- Presenta un título en los 3 idiomas solicitados.
- Proporciona nombres y apellidos completos de los autores (e indica quién es el autor de correspondencia), y de cada autor se menciona:
 - o Último título profesional.
 - o Institución en la cual trabaja.

o País y ciudad de reisdencia.
o Correo electrónico.

- Presenta un resumen analítico, de máximo 200 palabras, en los 3 idiomas solicitados.
- Presenta palabras clave, en los 3 idiomas solicitados.
- El cuerpo del artículo se encuentra en el formato solicitado.
- Las referencias citadas en el cuerpo del artículo aparecen en la sección REFERENCIAS, y viceversa.
- El formato de las referencias sigue las indicaciones estipuladas en esta guía.
- En las referencias se menciona el DOI de los artículos, si es el caso.
- Las figuras están en formato .TIFF con resolución mayor a 300 dpi en archivos diferentes al cuerpo del documento. Si las figuras fueron creadas en Word o Excel entonces se envían en ese formato.
- Las tablas van al final del documento.
- Adjunta la carta de presentación del artículo en el formato dispuesto para tal fin.

Manuscrito aceptado para publicación

Si el Editor le ha notificado que su manuscrito podría ser aceptado para publicación en caso de tener en cuenta las modificaciones sugeridas por los revisores, envíe la nueva versión del artículo acompañada de una carta donde detalle cada uno de los comentarios de los revisores, y justifique en caso de que no tenga en cuenta alguna de las sugerencias. Trabaje la nueva versión del artículo con control de cambios o resalte los cambios en esta nueva versión, para que el Editor pueda identificarlos con facilidad.

Una vez haya finalizado el proceso de revisión por pares, el Editor enviará un correo electrónico al(os) autor(es) del manuscrito manifestando la decisión del Comité Editorial. Si el manuscrito ha sido aceptado para publicación, se adjuntarán al correo las sugerencias, indicaciones y comentarios que cada evaluador efectuó sobre los aspectos de fondo y de forma del artículo. Para continuar con el proceso de publicación el(los) autor(es) deben enviar los siguientes archivos al correo de la revista (recolquim_fcbog@unal.edu.co):

- La nueva versión del documento en donde se trabaje con control de cambios o se resalten las modificaciones trabajadas.
- Una carta en la que se detallen cada uno de los comentarios de los revisores, justificando aquellos casos en los que no se siguió una determinada indicación o sugerencia.
- Las imágenes que se hayan modificado en virtud de los comentarios de los revisores y las necesidades de la nueva versión. Las imágenes deben estar en formato .TIFF con una resolución mayor a 300 dpi.

Costo de la publicación

La publicación de un artículo, con una extensión no mayor a 3 páginas de la revista, tendrá un costo de \$30.000 pesos colombianos. Las páginas adicionales tendrán un costo de \$20.000 pesos colombianos cada una.

Description

Revista Colombiana de Química (Rev. Colomb. Quim. Online version ISSN 2357-3791, printed version ISSN 0120-2804) is a peer-reviewed scientific journal from the Department of Chemistry, Faculty of Sciences of Universidad Nacional de Colombia, Bogotá. Since its launch in 1971 and until 1980 Revista Colombiana de Química published a volume per year, and its frequency changed to one or two volumes per year from 1981 to 2006. From 2007 until the present, this journal has published three volumes per year. All of its volumes are available online at the website: <http://www.revistas.unal.edu.co/index.php/rcoquim/index>.

Revista Colombiana de Química is indexed in databases such as Scopus, Publindex, DOAJ, SciELO, Latindex, and Redalyc. This publication has a Scientific and Editorial Board composed of renowned researchers in each subject, and accepts relevant contributions to the different areas of chemistry such as analytical chemistry, biochemistry, organic and physical chemistry, food chemistry, inorganic chemistry, material sciences, organometallic chemistry, and chemistry teaching, among others. The target audience are professionals of any area of chemistry.

Types of manuscripts

Research articles

They are articles that present results of investigation that have not been published previously. The authors should highlight the contribution of their work to novel knowledge. It is suggested a maximum of 40 references.

Reviews

They will be requested by invitation of the Publishing Board, considering the experience of the authors in a specific subject. They are articles that present the current state of the knowledge on a subject. Additionally, in this type of articles, the authors should clearly establish their contribution and own criterion. It has to present more than 50 references, preferably of the last 5 years.

Ethics

Revista Colombiana de Química follows the ethics policy proposed by COPE: <http://publicationethics.org/> intended for peer-reviewed scientific journals. Please be aware that plagiarism, ghost writing, and duplication of results are considered to go against our ethics policy. This journal uses an evaluation system in which authors and referees are unknown to each other.

Conflicts of interest

The journal defines a conflict of interest as any subject that interfere in: the complete and objective presentation, the review by pairs, the taking of publishing decisions, or the publication of investigation articles presented to the journal. The conflict of interests can be of financial and no financial nature, professional or personal, and can come up in relation to an organization or another person.

Submitting and outline for the general review

Manuscripts submitted to the Revista Colombiana de Química for their possible publication have to be unpublished (**no subjected at the same time to any other journal, either printed or digital**). The authors are responsible for their opinions and ideas declared in the manuscript. The precision of the information in a manuscript, including figures and tables, is complete responsibility of the author(s).

Manuscripts can be submitted for their evaluation via email (rcolquim_fcbog@unal.edu.co) or through the platform on-line of the journal (<http://www.revistas.unal.edu.co/index.php/rcoquim>).

General requirements for submitting

1. Sending through the portal online are possible if the author is registered. If not, the author should register following the necessary steps. Before beginning, it is important to check that the sending meets all the requirements requested by the journal (See section Preparation for on-line sending).
2. Neither abstract nor authors' data should be included in the on-line version of the document. These information should be included in the metadata, that is to say, in the submission form. On the contrary, if the article is sent by e-mail it has to contain all the data that is specify in the Format section.
3. In both cases, on-line submitting or via e-mail, a letter presenting the article must be submitted. This letter should include the most relevant aspects of the manuscript, a list of three possible reviewers, with their respective contact data. The letter should be sign by all the authors.
4. Photos, diagrams, maps, and figures should be named as figures. Photos and maps should be attached in a separated file, in a TIFF or JPEG format. They should have the size at which they have to be published, with a resolution of 300 dpi, and in a grey scale in black and white. If a grey scale is not good enough then different trams should be used. Photos and maps should not be copied in Word because they lose resolution, and therefore there will be problems during the formatting. If the graphic corresponds to archives developed in Excel or Word, then authors should send it in the original program.

Reviewing flow

- After receiving the manuscript and verifying that it fulfills with the format established in this guide, it is sent to peer-reviewers.
- After receiving the evaluations, the decision of the Editorial Board is sent to the correspondence author:
 - **Accepted with minor changes:** Authors should send a new version to the journal. When the editor verifies that the changes were made (the authors have to send a detailed list with the changes made or the reason why they do not make the changes), the article is accepted.
 - **Major changes:** Authors should send a new version to the journal, which will be subjected to a fast evaluation (the authors have to send a detailed list with the changes made or the reason why they do not make the changes).
 - **Rejected:** The authors decide if they subject a new version to the journal, which will be treated as a new article.

- If the article is accepted, it will appear initially in a pre-print format in the web page of the journal (<http://www.revistas.unal.edu.co/index.php/rcoquim/index>). Later on it will be replaced by the diagramed version.

Preparation

The document has to be presented in a Word .doc or .docx file, size letter, 2.0 line spacing, with top and bottom margins of 2.5 cm and 3.0 cm in right and left margins, font Times New Roman, pages consecutively numbered. The titles: **ABSTRACT, RESUMEN, RESUMO, INTRODUCTION, MATERIALS AND METHODS, RESULTS AND DISCUSSION, CONCLUSIONS, ACKNOWLEDGEMENTS, and REFERENCES** should be used.

Language

Manuscripts are accepted in Spanish, English or Portuguese. However, **the title, abstract, and key words should be written in the three languages**. As a strategy to increase the diffusion and visibility of the manuscript, the journal encourage to the authors to present the manuscript in English.

First page

Title

The title has to be in small letter, unless the capital is compulsory. It has to be concise but informative and does not have to exceed 120 characters including spaces. The title has to appear always in Spanish, English, and Portuguese. For example:

- Catalytic oxidation of toluene and 2-propanol over Mn and Co mixed oxides obtained by coprecipitation method.
- Oxidación catalítica de tolueno y 2-propanol sobre óxidos mixtos de Mn y Co obtenidos por coprecipitación.
- A oxidação catalítica de tolueno e 2-propanol em óxidos mistos de Mn e de Co, obtidos por coprecipitação.

Author(s) and their filiations

- Full names.
- Last professional title.
- Working institution.
- Country and city of residence.
- E-mail (for each author).

Filiation data should keep a categorical order as follows: laboratory, institute, university, city, state, country, e-mail. Each filiation should be listed with numbers in superscript and referenced to each author. The author of correspondence has to be denoted with an asterisk. For example:

Mauricio Acelas¹, Elizabeth Gil², Markus Doerr³, Martha Daza³, Juan Manuel Urbina^{1*}

¹Laboratorio de Química Orgánica y Biomolecular - LQOBio, Facultad de Ciencias, Universidad Industrial de Santander, Ciudad Universitaria, AA 678, Bucaramanga, Colombia.

²Facultad de Ciencias, Pontificia Universidad Javeriana, Carrera 7 N° 43-82, Bogotá D.C., Colombia.

³Grupo de Bioquímica Teórica - GBQT, Facultad de Ciencias, Universidad Industrial de Santander, Ciudad Universitaria, AA 678, Bucaramanga, Colombia.

*Author of correspondence: jurbina@uis.edu.co

Body of the manuscript

The manuscript should be justified (aligned to both left and right), with the pages and lines numbered continuously. All titles and primary and secondary subtitles should be justified to the left. The titles (**ABSTRACT, INTRODUCTION, MATERIAL AND METHODS, RESULTS AND DISCUSSION, CONCLUSIONS, ACKNOWLEDGEMENTS, and REFERENCES**) have to go with capital letter and bold type. The primary subtitles have to go with small letter sustained and bold type. The secondary subtitles have to go in italic. Always the statistics terms, abbreviations, and symbols have to be defined the first time they are used in the manuscript. For the measurement units, the International Metric System should be used.

When not followed by units numbers are written up to ten with the word (one, two, three, etc.) and higher than ten with numbers (11, 12, 102). Numbers with units should be followed by the units keeping a space between one and another (100 m, 50 mL). If the number represents a percentage then there should not be any space between the number and the unit (80%). In manuscripts written in Spanish decimals are separated by comma (,) and in English by point (.). Each figure and table in the text must be quoted according to the order of apparition and in the following format: Figure 1 or Figures 1 and 2 or Figures 1A-1F or Table 1.

Abstract

Abstract should have a maximum of 200 words. To write an introductory sentence is suggested. The authors have to mention the aim of the investigation, the notable results (providing specific data and, if possible, its statistical significance), and the main conclusions without bibliographic references. Authors should emphasize towards the new and important aspects of the study. A descriptive abstract should be avoided (where no data is shown), instead, an analytical abstract (where notable data obtained in the investigation is shown) should be presented. The abstract has to appear always in Spanish, English, and Portuguese.

Key words

Between three to six words have to be listed. The words used in the title of the manuscript should not be used in this section. Key words have to appear always in Spanish, English, and Portuguese.

Introduction

The logical foundations for the realization of the work have to be presented. Only strictly timely references should be given. Data or conclusions of the manuscript should not be included in this section. At the end of the introduction, the aim of the work have to be shown.

Materials and methods

In a subsection, the reagents used, trade, and the country have to be listed. The methods used should be listed by subtitles. The procedures have to have the sufficient detail to allow other professionals to reproduce the experiments. This section must include the equipment, including name of the manufacturer and country, in addition, the references of the methodology and statistical methods should be provided. Authors should describe the new methods or those that have been substantially modified, supporting the reasons to use them and evaluating their limitations.

Authors submitting reviews should describe the methods employed to locate, select, extract, and synthesize the information. If statistical tests are done, then a subtitle "Statistical analysis" should be included for their description.

Results and discussion

Results should be presented in a logical order and in accordance to the order presented in the MATERIALS AND METHODS section. Authors should highlight the results that contribute to the generation of new knowledge. The information contained in tables does not have to be repeated in figures, and vice versa.

New and outstanding outcomes of the study should be highlighted. Information presented in the sections INTRODUCTION should not be shown again in this section. It is advised to evaluate possible relations between the obtained results, to judge the results in relation with the ones obtained by other authors, and to propose hypotheses to explain the obtained data. The sections should have a minimum extension of three pages written in double space.

Conclusions

Minimum one paragraph should be presented as conclusion (s). Conclusions should be in accordance to the aim of the study, avoiding to enumerate them or to present them as loose sentences. Author should present the conclusions well supported by the data.

Acknowledgements

Funding sources should be mentioned in this section. Support received for the realization of the study (e.g., scholarships, equipment, reagents) should also be included. Authors can appoint those people that contributed to the work, but whose contributions do not justify the authorship, describing the contribution carried out, for example, "technical support", "critical review of the writing", "collecting samples".

References

The format is based in the guide of styles of the American Chemical Society (ACS).

References in text: All the appointments that appear in the text have to coincide with those presented in the section REFERENCES, and vice versa.

Authors must avoid referencing as bibliography:

- The summaries presented in congresses or other meetings.
- Personal communications.
- Unpublished data. The citation of a manuscript as "in press" supposes that it was already accepted for publication.

The references should appear with italic numbers in parentheses in the line of the text, and inside the punctuation. For example:

- The conditions of extraction are reported in other studies (1).

If there is more than one reference there must be separated by comma (,) without spaces between numbers. If they are consecutive references they are separated by hyphen. For example:

- The results obtained were similar to those reported by other authors (8, 26-30).

The references should be written with natural numbers in accordance to their order of apparition. If within the text the author(s) are to be mentioned, then the citation has to be as:

- An author: Duque (2)
- Two authors: Duque y Palomeque (3)
- More than two authors: Duque *et al.* (4)

Format of references: The references have to be organized in the same numerical order in which they were presented along the text.

Journals

The surname and the initials of the name of all the authors have to be included. Surnames should be separated of the initials of the name by comma. The initials of the names of authors should be accompanied with point. Authors should be separated with semicolon. After the authors information the title should be written. The name abbreviated of the journal in italic, according to the Chemical Abstracts Service Source Index (CASSI, <http://cassi.cas.org/search.jsp>). The year in bold type, the volume with italic type and the pages (separated with hyphen). If available the DOI should be included.

- Up to six authors: all the authors should be included.

Da Silva, R.; Nissim, I.; Brosnan, M.; Brosnan, J. Creatine synthesis: Hepatic metabolism of guanidinoacetate and creatine in the rat in vitro and in vivo. *Am. J. Physiol. Endocrinol. Metab.* **2009**, 296, 256-261. DOI: <http://dx.doi.org/10.1152/ajpendo.90547.2008>.

- More than six authors: include until the sixth author and then write *et al.*

Books and other monographs

- Books without editors
 - Stout, J.; Antonio, J.; Kalman, D. *Essentials of creatine in sports and health*. Humana Press Inc.: Totowa, NJ, 2008; pp 30-40. DOI: <http://dx.doi.org/10.1007/978-1-59745-573-2>.
 - Budavari, S.; O'Neil, M. J.; Smith, A.; Heckelman, P. E.; Obenchain, J. R., Jr.; Gallipeau, J. A. R.; D'Areca, M. A. *The merck index, an encyclopedia of chemicals, drugs, and biologicals*, 13th ed. Merck & Co., Inc.: Whitehouse Station, NJ, 2001; pp 1768-1769.
- Books with editors
 - Rowe, R. C.; Sheskey, P. J.; Owen, S. C. (eds.). *Handbook of pharmaceutical excipients*, 5th ed. Pharmaceutical Press and American Pharmacists Association: Grayslake, IL, 2006; pp 798-799.
- Chapter in edited book
 - McBrien, M. Selecting the Correct pH Value for HPLC. In *HPLC made to measure: A practical handbook for optimization*; Kromidas, S., Ed.; Wiley-VCH: Weinheim, Germany, 2006; pp 89-103.

Doctoral Thesis (or similar)

- Printed
 - King, K. J. Development of a pressurized system for oxidation studies of volatile fluids. M.S. Thesis, The Pennsylvania State University, State College, PA, March 1983.
- Online
 - Abrams, N. M. Efficiency enhancement in dye-sensitized solar cells through light manipulation. Ph.D. Dissertation [Online], The Pennsylvania State University, University Park, PA, December 2005. <http://etda.libraries.psu.edu/theses/approved/WorldWideIndex/ETD-1061/index.html> (consulted on the 2nd April 2014).

Web sites

Penn State Department of Chemistry. <http://www.chem.psu.edu/> (consulted on the 7th june 2014).

Mallet Chemistry Library, University of Texas Libraries. ThermoDex home page: An index of selected thermodynamic and physical property resources. <http://www.lib.utexas.edu/thermodex/> (consultado el 19 de marzo de 2014).

In press

Martínez, F.; Jouyban, A.; Acree, W. E., Jr. Comments on "Solubility and thermodynamic function of a new anticancer drug ibrutinib in 2-(2-ethoxyethoxy)ethanol + water mixtures at different temperatures". *J. Chem. Thermodyn.* **2015**. In press. DOI: <http://dx.doi.org/10.1016/j.jct.2015.11.031>

Tables and figures

Photos, diagrams, maps, and graphics should be mentioned as figures. We encourage authors to present data in figures instead to tables. In any case, redundancy among tables, figures, and text should be avoided.

Figures with legends have to be sent individually in format .TIFF, of excellent quality, with a minimum resolution of 300 dpi and with one of two sizes (9 cm of width, that is a column, or 20 cm that covers the two columns). The color impression does not generate additional costs for the authors, however, it represents a greater cost for the journal. With this in mind, a scale of grey or trams should be used whenever possible. The use of color might be considered when it is strictly necessary. Figures originally created in Microsoft Word or Excel should be sent in that program.

Tables should be included in the body of the manuscript at the end of the document. Both tables and figures have to be self-contained (They should be interpreted without needing information from the body of the manuscript). Keys and abbreviations should be described in the legend of the figure and in the title or foot of the table. It is advised to provide in addition to the average, the standard deviation, and other notable statistical information.

The labels of each table have to be at the top of it, whereas in figures the labels have to be presented at their foot. Small figures should be avoided: group figures with information related in compound figures entitled with letters (Figure 1a, Figure 3b, etc.). If a manuscript contains tables or figures reproduced (even if they are from the author (s) submitting the manuscript) it is compulsory to the authors to declare the origin and to present permission to use them. It is responsibility of the authors to achieve the corresponding permission. In case of any doubt in this regard, please contact the journal via e-mail (rcolquim_febog@unal.edu.co) or by telephone (+571 3165000 Ext. 14458).

Preparation for on-line submiting

Before sending your manuscript, by the Portal or by email, verify that it fulfils with the following conditions:

- It has a title in the 3 languages requested.
- It provides full names of the authors, and for each one it is mentioned:
 - Last professional title.
 - Institution in which the author works.

- o Country and city of residence.
- o E-mail.
- It presents an analytical abstract, of maximum 200 words, in the three languages requested.
- It presents keywords, in the 3 languages requested.
- The body of the article follows the format requested.
- The cited references in the body of the article appear in the section REFERENCES and vice versa.
- The format of the references follows the indications stipulated in this guide.
- In the references the DOI of the articles are presented, if it is the case.
- The figures are in format .TIFF with resolution greater than 300 dpi. (in separated files). If a figure was created in Word or Excel then sent it in that format.
- The tables are placed at the end of the document.
- A letter presenting the manuscript in a format as suggested above is included. Available in <http://www.revistas.unal.edu.co/index.php/rcolquim>

Manuscript accepted for publication

If the Editor has notified the correspondence author that his (her) manuscript could be accepted for publication in case the modifications suggested by the referees are taken into account, the author should send the new version of the manuscript accompanied of a letter detailing the response to each one of the comments. In the case a comment is not taken into account the author should justify the reason. The new version of the manuscript should be created with the “track changes” option or highlighting in yellow the changes, so that the Editor can identify them easily.

Once the process of reviewing is completed, the Editor will send an email to the correspondence author manifesting the decision of the Editorial Board. If the manuscript is accepted for publication, an e-mail attaching the suggestions, indications, and comments of each reviewer will be sent to the correspondence author. To continue with the process of publication, the author should send the following archives to the email of the journal (rcolquim_fcbog@unal.edu.co):

- The new version of the manuscript in which the author uses the option “track changes” or highlight in yellow the modifications performed.
- A letter detailing the response to each one of the comments. In the case a comment is not taken into account the author should justify the reason.
- In the case that a reviewer suggest that a figure should be modified, then be aware that it should be in format .TIFF with a resolution greater than 300 dpi.

Cost of the publication

The publication of a manuscript with an extension up to three pages of the journal will have a cost \$30,000 Colombian pesos. Additional pages will cost of \$20,000 Colombian pesos each one.

Contenido

Carta del editor
Editor's letter

Química Orgánica y Bioquímica

Anti-pepsin activity of silicon dioxide nanoparticles
Actividad antipepsina de nanopartículas de dióxido de silicio
Atividade antipepsina de nanopartículas de dióxido de silício
Hussein Kadhem Al-Hakeim, Khlowd Mohammed Jasem, Shatha Rouf Moustafa

1-4

5-11

12-21

22-27

28-32

33-38

39-50

51-60

Fisicoquímica y Química Inorgánica

A DFT study on Dichloro $\{(E)$ -4-dimethylamino-N'-[(pyridin-2 yl)methylidene- κ N]benzohydrazide- κ O $\}M^{2+}$ ($M=Zn$, Cu , Ni , Fe , Mn , Ca and Co) complexes: Effect of the metal over association energy and complex geometry
Un estudio DFT en complejos Dicloro $\{(E)$ -4-dimetilamino-N'-[(piridin-2 il)metilideno- κ N] benzohidrazida- κ O $\} M^{2+}$ ($M = Zn$, Cu , Ni , Fe , Mn , Ca y Co): efecto del metal sobre la energía de asociación y la geometría del complejo
Um estudo DFT nos complexos Dicloro $\{(E)$ -4-dimetilamino-N'-[(piridin-2 il) metilideno- κ N] benzohidrazida- κ O $\} M^{2+}$ ($M = Zn$, Cu , Ni , Fe , Mn , Ca y Co): efeito do metal sobre a energia de associação e a geometria do complexo
Gustavo Gutiérrez, Mónica A. Gordillo, Manuel N. Chaur

Síntesis y caracterización estructural de hidrotalcitas de Cu-Zn-Al
Synthesis and structural characterization of Zn-Al-Cu hydrotalcites
Síntese e caracterização estrutural de hidrotalcitas de Cu-Zn-Al
Johana Rodríguez Ruiz, Adolfo Pájaro Payares, Edgardo Meza Fuentes

Acylhydrazone-based dynamic combinatorial libraries: study of the thermodynamic/kinetic evolution, configurational and coordination dynamics
Librerías combinatorias dinámicas basadas en acil-hidrazone: estudio del desarrollo termodinámico/cinético, dinámicas de configuración y de coordinación
Livrarias combinatórias dinâmicas baseadas na acil-hidrazone: estudo da evolução cinética/termodinâmica, dinâmicas de configuração e da coordenação
Mónica A. Gordillo, Fabio Zuluaga, Manuel N. Chaur

Guía para autores
Guide for authors



La Revista Colombiana de Química (Rev.Colomb.Quim) se encuentra indexada y referenciada en: Publindex-Índice Bibliográfico Nacional (categoría A2 - dic 2013); Chemical Abstracts; SciELO Colombia; Scopus Q4 (SJR/2013: 0,112); Latindex; Redalyc y Directory of Open Access Journals (DOAJ).

Es publicada cuatrimestralmente por el Departamento de Química de la Universidad Nacional de Colombia. Se orienta a la divulgación científica de contribuciones provenientes de la investigación en las diversas áreas de la química.

Open Acces Journal: full contents available on-line at:
<http://www.revistas.unal.edu.co/index.php/rcolquim>
http://www.scielo.org.co/scielo.php?script=sci_serial&pid=0120-2804&lng=es&nrm=iso